
STABLE, MISSING AND WILD INFLATION: THE CASE OF THE EURO AREA *

CLEMENTE PINILLA-TORREMOCHA[†]

FIRST DRAFT 10.04.2022

CURRENT VERSION 10.11.2023

Abstract

This paper analyses why Euro area inflation has reached a 40-year high, after the economic reopening following COVID-19. To do so, it introduces a novel framework that captures in a single set-up: 1. The anatomy of an economy, characterized long-term and business-cycle variables (e.g. potential GDP, trend inflation, and output-gap, inflation-gap). 2. Time-varying volatilities, which are specifically incorporated to accommodate extreme observations that can have strong influence on parameter estimates. 3. To diagnose the structural shocks at play, focusing on their nature (transitory and permanent) and channels (global and domestic -from a supply and demand side-, and energy supply shocks). The results show that in 2022, trend inflation has risen sharply to 3-4% due to a reduction in production capacity - negative supply shocks from a global and domestic side. The inflation-gap (transitory part) is at 6-7%, explaining around 85% of the total increase in headline inflation, which is mainly driven by energy supply shocks and global-domestic demand. With these results, in the short-term, Euro area headline inflation is expected to rapidly decrease; while, in the medium-term, it is anticipated to stay above the ECB's inflation target. Overall, this paper offers new insights on what drivers have fueled Euro area inflation post-COVID19.

JEL CLASSIFICATION: E32, E44.

KEYWORDS: LONG-TERM INFLATION EXPECTATIONS, EURO AREA, PERMANENT AND TRANSITORY SHOCKS, UNOBSERVED COMPONENTS, TRENDS AND CYCLES, STOCHASTIC VOLATILITY, DOMESTIC-GLOBAL, DEMAND-SUPPLY.

*Universidad de Alicante. Email: clemente.pinilla@ua.es.

[†]I am very grateful to Prof. Gabriel Pérez-Quirós for his guidance and advice. I thank all the professors at the Alicante Macroeconomic PhD Workshop, and participants at ASSET 2023, and 48th Simposio Spanish Economic Association. Financial support from Universidad de Alicante is greatly appreciated. I acknowledge receipt of a full fee waiver at the 48th Simposio SAEe.

1. INTRODUCTION

Inflation was not a concern for many years, but since the COVID economic reopening worldwide inflation has reached a 40-year high. This study emerges in the context of the multifaceted crisis instigated by the COVID-19 pandemic, with sources on both the global and the domestic side. The public health crisis, exacerbated by an initial supply shock brought the global economy to an abrupt standstill, leading to huge economic dislocations (e.g., in production). Subsequently, a demand shock intensified its effects, largely due to the COVID economic reopening, and was later accompanied by an energy supply shock following the Russian invasion of Ukraine. This paper investigates the nature of these shocks, transitory and permanent effects, driving Euro area inflation.

This paper aims to examine the different driving factors behind Euro area (EA) headline inflation across three different periods: (i) The stable period of anchored inflation at 2%, (ii) the missing inflation of 2012-17, and (iii) the current environment of high inflation since the COVID economic reopening. Moreover, it can shed light on the reviving hypothesis of ‘de-anchoring of inflation expectations’ from below 2% level in 2012-2017 and from above 2% level after 2020.¹

The paper builds on and seeks to integrate two main methodologies employed in the study of inflation fluctuations. One is to determine the underlying drivers that caused the previous three periods. Recently, [Ciccarelli and García \(2021\)](#) highlight the role of a global inflation channel in transmitting spillovers from US to Euro area inflation.² However, they do not distinct on whether this channel has permanent or temporally effects. The other approach is to use an unobserved component trend-cycle model. For example, [Jarociński and Lenza \(2018\)](#) find that trend inflation in the Euro area remained pretty stable at 2% level from 2000 to 2016. In other words, the missing disinflation was primarily caused by negative transitory developments in inflation (i.e., inflation gap). Nevertheless, they do not identify the potential factors that drove the inflation gap or trend inflation.

Under the lens of a hierarchical multivariate model of unobserved components, variables are first decomposed into slow and fast-moving variables (i.e., trends and cycles). Second, permanent and transitory shocks are estimated featuring stochastic volatility - with fat-tailed errors as in [Jacquier, Polson and Rossi \(2004\)](#) - to handle extreme realizations such as the COVID-19 outliers.^{3,4} I identify the following structural shocks (i) domestic supply, (ii) domestic demand, (iii) global supply, (iv) global demand, and (v) energy supply shocks from a cyclical and a permanent view. The identification of shocks relies on

¹This debate started years ago, in academic and policy circles, when inflation was expected to be higher after 2012, on the back of the ongoing recovery, but it was persistently below target - the average of headline inflation from 2012Q1 to 2018Q4 was 1.28. Nowadays, there seems to be a paradigm shift with the current inflation dynamics, where EA headline inflation has reached a 40-year high.

²In the spirit of recent theoretical and empirical papers that analyze inflation dynamics from an open economy perspective, this paper also includes global activity measures. See [Martínez-García and Wynne \(2010\)](#); [Kabukçuoglu and Martínez-García \(2018\)](#); [Duncan and Martínez-García \(2023\)](#).

³My model is essentially an extension of the Vector Autoregressive (VAR) model with common trends of [Del Negro, Giannone, Giannoni and Tambalotti \(2017, 2019\)](#), taking into account stochastic volatility. Stochastic volatility is specifically included for handling COVID-19 outliers, given that these extreme realizations can have strong effects on parameter estimates and forecasts generated by conventional constant-parameter VAR. See these papers for addressing COVID-19 outliers in standard VAR models: [Carriero et al. \(2021\)](#); [Lenza and Primiceri \(2022\)](#); [Schorfheide and Song \(2021\)](#).

⁴Excluding stochastic volatility can compromise the accurate decomposition of variables. Specifically, the pronounced decline in real GDP during the COVID-19 period is offset between potential GDP and the output gap, leading to a notable reduction in potential GDP.

general sign-restrictions. To identify demand-side and supply-side factors, I follow that supply-side forces move output and inflation in opposite directions, while demand-side forces imply a positive comovement. In order to distinguish between domestic and global shocks I follow [Corsetti, Dedola and Leduc \(2014\)](#), this implies that global shocks affect global variables more than domestic ones, and viceversa for domestic shocks. Finally, to identify an energy supply shock I follow the lessons from [Kilian \(2008, 2009\)](#). To summarize, this model allows me to explore the time-varying channel of shocks, and whether shocks hitting the economy have permanent/temporal effects on EA headline inflation (and other macroeconomic variables) from the early 1990s to 2022Q2.

I document the following findings. First, there is significant fluctuation in the EA trend inflation revealing two substantial declines. Over the decade of the 90s, inflation trend declined from 4% to 2%; and stayed anchored at 2% for almost two decades. Inflation trend slowdown over 100 basis points, going from 2% in 2012Q3 to 1% in 2016Q1.⁵ The timing of the decline in trend inflation, between 2012-2016, pairs well with the demand-side view - both domestic and global - of [Ciccarelli et al. \(2017\)](#). However, I find it from a permanent nature instead of transitory one. Second, after the strong ‘COVID economic reopening’, trend inflation has risen above the 2% level, around 3 to 4% in 2022Q2, characterized by a combination of global and domestic shocks from a supply side. These permanent supply factors, identified by the model, could perfectly resemble the recent persistent supply chain bottlenecks of non-energy industrial goods (i.e., shortage of shipping containers, or the microchip crisis). The fact that trend inflation is above 2%, suggests that EA inflation is expected to be persistently higher than ECB’s target in the medium-term.⁶ Though the recent dynamics of trend inflation are not documented in the literature yet, they pair well with the ECB’s expected disinflation path and change in monetary policy strategy. At the end of 2022, the ECB changed its view about inflation. The message changed from *‘the current inflation spike is temporary and driven largely by transitory factors’* in 2021Q4, to *‘[...] inflation is expected to decline from an average of 8.4% in 2022, 6.3% in 2023, 3.4% in 2024 and to 2.3% in 2025. [...] Headline inflation is expected to fall to the ECB’s medium-term inflation target of 2% in the second half of 2025’* in 2022Q4. Nevertheless, the current highs that inflation is making, since the ‘COVID economic reopening’, are mainly driven by transitory factors (such as domestic and global excess demand and energy supply shock)- around 85% of total inflation. Third, the model captures positive and negative hysteresis effects on potential GDP.⁷ There is a significant slowdown of EA potential GDP growth (i.e., from the early 90s to 2005-06 average quarter-on-quarter growth trend is 0.54%, and from 2006 onwards it decreases to 0.24%).⁸ This version of ‘secular stagnation’ hypothesis is captured in the model by permanent global factors (demand-supply) that contributed significantly to the slowdown of

⁵This paper favors a gradual de-anchoring that starts in 2012, as documented in [Gimeno and Ortega \(2016\)](#); [Lyziak and Paloviita \(2017\)](#); [Corsello, Neri and Tagliabracci \(2021\)](#) and [Hilscher, Raviv and Reis \(2022\)](#). Moreover, my results show evidence against a strong version of anchored inflation expectations in the Euro area around the mid-2010s (see [Strohsal and Winkelmann \(2015\)](#); [Jarociński and Lenza \(2018\)](#); [Dovern et al. \(2020\)](#)).

⁶This result is in line with the new analysis of [Hilscher, Raviv and Reis \(2022\)](#). They find that a high risk of persistent high Eurozone inflation 2022. Moreover, [Reis \(2022\)](#) explores different channels to explain the sudden rise in inflation, and points to similar aspects as the ones of this paper.

⁷In the absence of permanent shocks, potential GDP grows at a constant factor \bar{c} (see Equation 2 in Section 3).

⁸This result is related to the findings made for the slowdown of U.S. trend GDP growth by [Antolin-Diaz et al. \(2017\)](#) and [Maffei-Faccioli \(2021\)](#). They document a significant decline in long-run output growth in the early 2000s. In particular, [Maffei-Faccioli \(2021\)](#) identifies that mainly permanent demand-side shocks affected the slowdown in trend GDP growth after 2000.

EA potential GDP.⁹ The last result is about the slope of the Phillips curve. I find that an apparent flat Phillips curve from a reduced-form point of view is mainly due to a flat demand curve, calling for a stable supply curve. This result is fully consistent with a strict inflation targeting.¹⁰

Related Literature. The primary contribution of this paper is to introduce a model that captures in a single framework: 1. The anatomy of an economy, characterized long-term and business-cycle variables. 2. Time-varying volatilities and covariances, which are specifically incorporated to accommodate extreme observations, such as COVID-19 outliers, which can have strong influence on parameter estimates. 3. To diagnose the most common structural channels of shocks (e.g. supply and demand), in terms of their nature, whether these shocks have permanent or transitory effects on variables.

The price inflation literature is vast. In this subsection, I present three characteristic literature branches in understanding price inflation, with a particular focus on the Euro area.

The first approach to understand inflation dynamics is through the lens of reduced form decomposition models of trend and cycle.¹¹ Within this framework, the literature has focused on analyzing the hypothesis of de-anchoring inflation expectations, often referred to as medium to long-term, or trend, inflation. Specifically, the focus has been on elucidating the 'missing inflation' phase and the recent surges in inflation. The standard challenge in these models, and also in my model, is how to estimate the medium / long-term inflation expectations. The literature in the U.S. and Euro area take different approaches. For example, [Gimeno and Ortega \(2016\)](#) rely on EA investors' inflation swaps, [Jarociński and Lenza \(2018\)](#) use professional long-term EA inflation expectations, and [Hasenzagl et al. \(2018\)](#) make use of one-year-ahead inflation expectations for US consumers and professional forecasters.¹² For the case of the Euro area, the results are significantly different. While [Gimeno and Ortega \(2016\)](#) find evidence for a slowdown in long-run inflation expectations, which is estimated to have fallen from the 2% level since late 2014; [Jarociński and Lenza \(2018\)](#) find the opposite, a remarkable stable trend inflation at 2% level from 2000 to 2016. Because of this discrepancy in results, I define what are medium / long-term inflation expectations in order to avoid confusion in the rest of the paper. Following [Clark and Davig \(2009\)](#), medium / long-term inflation expectations are simply the rate at which people - consumers, and businesses - expect prices to rise in the medium long-term future. Hence, with respect to these papers, I model trend inflation using time series that contain information about households' and firms' perceived inflation.

The second view seeks to identify the fundamental drivers that may have influenced both historical

⁹This result is in line with the theory that poses permanent change in globalization after the synchronised world trade collapse in late 2008. The collapse was caused by the sudden, severe and globally postponement of purchases, especially of durable consumer and investment goods. See [Baldwin and Taglioni \(2009\)](#), [Abiad et al. \(2014\)](#) and [Chen et al. \(2019\)](#).

¹⁰To identify the Phillips curve, this paper uses the proposed methodology by [Bergholt, Furlanetto and Vaccaro-Grange \(2023\)](#). These insights are consistent with the conclusions found by these authors regarding the US economy.

¹¹Seminal contributions to the literature were initially made through the univariate models presented by [Beveridge and Nelson \(1981\)](#); [Harvey \(1985\)](#); [Watson \(1986\)](#); [Clark \(1987\)](#). Subsequently, in the 2000s, [Stock and Watson \(2007\)](#) extended a version of the univariate unobserved component trend-cycle model to incorporate stochastic volatility.

¹²Recent empirical evidence for the Euro area (e.g. [Álvarez and Correa-López \(2020\)](#)) shows that time series that could contain information about households' and firms' perceived inflation are better at predicting inflation than professional forecasters or financial markets - in the context of open economy Phillips curves. Similar results are obtained for the U.S. by [Coibion and Gorodnichenko \(2015\)](#), where they conclude that the inflation puzzles after the 2008 disappears when using households' inflation expectations instead of professional forecasters' ones. Moreover, they conclude that firms have similar expectations as households, as opposed to professional forecasters.

and the recent dynamics of inflation. To do so, the literature relies on structural models - typically Vector Autoregressive (VAR) models - that lack the previous decomposition features. Meaning that, under the lens of these models, it is impossible to distinguish between a permanent and a transitory perspective. The following four papers use a VAR model to understand the potential drivers of the missing inflation period. (i) [Ferroni and Mojon \(2014\)](#) put the emphasis on global demand shocks, where these shocks explain a large part of the increase in inflation in 2008 and the subsequent decline in the following years. (ii) [Conti et al. \(2017\)](#) record a combination of negative effects of energy supply, and domestic aggregate demand shocks. (iii) [Ciccarelli et al. \(2017\)](#) mark the importance of a first stage of domestic shocks and a second stage of global shocks, constraining headline inflation for a prolonged period. (iv) Finally, [Bobeica and Jarociński \(2019\)](#) emphasize the role of domestic shocks to explain the missing inflation episode. More recently, [Ciccarelli and García \(2021\)](#) explore whether rises in U.S. inflation, in mid 2021, could signal a return of inflation worldwide. They find a global inflation channel that operates through inflation compensation markets and reinforces international spillovers from U.S. to Euro area inflation. Moreover, all the recent *ECB Economic Bulletins* reports have a common denominator; current surges in inflation are heavily influenced by global supply-demand mismatches and energy pressures.¹³

Finally, to understand price inflation, the third approach relies on the Phillips Curve. In particular, whether the slope of this curve has flattened. In other words, inflation fails to respond to changes in the level of economic slack (i.e., output-gap) or to the unemployment gap in the way that is predicted by a conventional Phillips curve. This hypothesis points to a break down in the relationship between inflation and level of economic slack. Indeed, the literature presents a wide range of conflicting findings, including on the existence, stability, steepness of the slope of the Phillips curve, and underlying measures. Nevertheless, a survey of the extensive empirical literature on the Phillips Curve is beyond the scope of this paper. Using the proposed methodology by [Bergholt, Furlanetto and Vaccaro-Grange \(2023\)](#), this paper finds a stable supply curve, combined with a substantially flat demand curve. These findings are clearly at odds with a decline in the Phillips curve slope, advocated by a large and yet growing literature. But fully consistent with a strict inflation targeting. Thus, these results show evidence against a string of papers that poses that taking into account trend inflation can flatten the Phillips curve ([Ascari and Sbordone \(2014\)](#); [Gemma et al. \(2023\)](#); [Ball et al. \(1988\)](#); [Shirota \(2015\)](#)).

Relative to the aforementioned research, from the econometric point of view, this paper has a number of attractive features: it does not rely on arbitrary inflation proxies or preliminary de-trending of the data which may create distortions.¹⁴ In addition, the model contains a rich lag structure to capture dynamic heterogeneity within the cycle components - which captures multivariate and lagged commonalities in real, nominal (including energy prices) and labor market variables at business cycle frequencies. Cycles in the model connect the output gap to prices and their expectations via a global Phillips curve relationship and to unemployment via Okun's law. The model features stochastic volatility in order to handle extreme observations, such as COVID-19 outliers, and finally, it allows to perform decomposition analysis and

¹³See [O'Brien et al. \(2021\)](#); [Koester et al. \(2021\)](#); [De Santis et al. \(2022\)](#); [Koester et al. \(2022\)](#); [Staff \(2022\)](#).

¹⁴For example, in order to take into account a 'stochastic' inflation trend some papers rely on exogenous exponentially weighted moving averages of headline inflation. Others use ad-hoc de-trending filters like the Hodrick-Prescott (HP) filter. See the critique of [Hamilton \(2018\)](#) with respect to HP filter.

historical decompositions of variables into permanent and cyclical *structural drivers*.

The paper is structured as follows, in the next section I introduce the data, its sources and transformations. Section 3, I describe the econometric methodology, and the shocks identification framework. In Section 4, I present the empirical findings. Section 5 provides a battery of extensions and robustness tests; and Section 6 provides some concluding comments.

2. DATA: SOURCES, TRANSFORMATION AND DESCRIPTION

Sources. Data are gathered from two main institutions EuroStat and OECD, and back-dated using the Area Wide Model (AWM) database of [Fagan, Henry and Mestre \(2005\)](#). The frequency of the data are quarterly and spans the period 1970Q1-2022Q2. My dataset consists of two blocks, Euro area and whole world. From EuroStat’s database, I collect for the Euro area the following variables: real GDP, unemployment, consumer confidence indicator, Harmonised Index of Consumer Prices (HICP), price perception of households over the next 12 months, unit labor cost index, and energy price index. From OECD’s database, I collect the following variables: OCDE’s real GDP and HICP - as proxy of the whole world.¹⁵ Finally, my database is characterized by a ‘ragged edge’, i.e., it has missing values.

Transformations. The series that are not already available in seasonal adjusted form are seasonally adjusted using JDemetra+ 2.2 - this software uses the following algorithm X-13ARIMA-SEATS. Table 1 reports for each variable the name (column 1), mnemonic (column 2), transformation (column 3), and the data span including the back-dated period. A brief comment is needed for variables y^8 and y^9 , that represent the GDP and HICP of the world, respectively. These two variables are defined as the ratio between the analogous Euro area variable and OCDE. This transformation becomes relevant, in Section 3, to implement the sign restrictions identification proposed by [Corsetti, Dedola and Leduc \(2014\)](#).

Variable name	Symbol	Transformation	Data span
Real GDP	y^1	log	1970.Q1 - 2022Q2
Unemployment Rate	y^2	Δ Q-Q	1970.Q1 - 2022Q2
Consumer Confidence	y^3	none	1985.Q1 - 2022Q2
HICP	y^4	Δ log Q-Q	1970.Q1 - 2022Q2
Price Perception HH	y^5	none	1985.Q1 - 2022Q2
Unit Labor Cost Index	y^6	Δ log Q-Q	1970.Q1 - 2022Q2
Energy Price Index	y^7	log	1987.Q4 - 2022Q2
World Real GDP (WRG)	y^8	$\log(y^1) - \log(\text{WRG})$	1970.Q1 - 2022Q1
World HICP (WH)	y^9	$\Delta (\log(y^4) - \log(\text{WH}))$ Q-Q	1970.Q1 - 2022Q2

Table 1. Description of the variables

3. ECONOMETRIC METHODOLOGY

The model described in this section is the Vector Autoregressive (VAR) model with common trends of [Del Negro, Giannone, Giannoni and Tambalotti \(2017, 2019\)](#) featuring stochastic volatility (in a similar

¹⁵The consumer confidence and price perception of households over the next 12 months indicators are qualitative surveys, that are reported as aggregated diffusion time series for the Euro area. The frequency of these diffusion series is monthly, so I transform them taking quarterly averages.

spirit as [Primiceri \(2005\)](#)). Hence, it is a standard decomposition model of multivariate time series that embeds two hierarchical levels of latent variables. First, series are jointly decomposed into trends and cycles (the first hierarchical level of unobserved components). Second, the variance covariance matrices of both, trends and cycles, are allowed to change over time (adding the second hierarchical level of unobserved components). In addition, the transparency and structural character of the method allows me to easily separate the nature of a set of shocks - energy, global and domestic factors - into permanent and transitory structural shocks, and assess potential changes in terms of volatility overtime. Finally, underlying structural drivers are identified using sign restrictions.

3.A. THE MODEL: A VAR WITH COMMON TRENDS FEATURING STOCHASTIC VOLATILITY

The model is given by the measurement equation

$$y_t = \Lambda \bar{y}_t + \tilde{y}_t, \quad (1)$$

where y_t is an $n \times 1$ vector of observables, \bar{y}_t is a $q \times 1$ vector of trends, $q \leq n$, $\Lambda(\lambda)$ is an $n \times q$ matrix of loadings that is restricted and depends on the vector of free parameters λ , and \tilde{y}_t is an $n \times 1$ vector of stationary components. The rank of Λ , which is equal to q , determines the number of common trends, and the number of cointegrating relationships is therefore $n - q$. Hence, $\Lambda(\lambda)$ maps the trend component \bar{y}_t to the dependent variable y_t . Both \bar{y}_t and \tilde{y}_t are latent variables and evolve according to the following transition equations, a random walk with drift

$$\bar{y}_t = \bar{c} + \bar{y}_{t-1} + \epsilon_t, \text{ with } \epsilon_t \sim \mathcal{N}(0, \Sigma_t^\epsilon), \quad (2)$$

and a VAR

$$\tilde{y}_t = \sum_{j=1}^P A_j \tilde{y}_{t-j} + u_t, \text{ with } u_t \sim \mathcal{N}(0, \Sigma_t^u) \quad (3)$$

respectively, where the A_j s are $n \times n$ matrices.

The covariance matrices of the error terms ϵ_t and u_t i.e., Σ_t^ϵ and Σ_t^u have time-varying elements. The modelization of time-varying innovations follows [Primiceri \(2005\)](#), [Benati and Mumtaz \(2007\)](#) and [Gali and Gambetti \(2009\)](#). The structure of the heteroscedastic unobservable shocks is very similar for the permanent and stationary shocks, with the only difference that the dimension of the latter one is a $n \times n$ matrix, and the former one is a $q \times q$ matrix. I consider the following structure for the error terms,

$$\Sigma_t^z = \Phi_{z,t}^{-1} H_{z,t} (\Phi_{z,t}^{-1})', \quad (4)$$

where $z = \{ \epsilon, u \}$, $\Phi_{z,t}$ is a lower triangular matrix with elements $\phi_{ij,t}^z$ and $H_{z,t}$ is a diagonal matrix

with diagonal elements $h_{i,t}^z$. The structure of Φ_t^z and H_t^z is

$$\Phi_{z,t} = \begin{pmatrix} 1 & 0 & \dots & 0 \\ \phi_{21,t}^z & 1 & \ddots & \vdots \\ \vdots & \ddots & \ddots & 0 \\ \phi_{k1,t}^z & \dots & \phi_{kk-1,t}^z & 1 \end{pmatrix}, H_{z,t} = \begin{bmatrix} h_{1,t}^z & 0 & \dots & 0 \\ 0 & h_{2,t}^z & \ddots & \vdots \\ \vdots & \ddots & \ddots & 0 \\ 0 & \dots & 0 & h_{k,t}^z \end{bmatrix},$$

where

$$\phi_{i,t}^z = \phi_{i,t-1}^z + V_{i,t}^z, \text{Var}(V_{i,t}^z) = D_i^z, \quad (5)$$

and

$$\ln h_{i,t}^z = \ln h_{i,t-1}^z + Z_{i,t}^z, \text{Var}(Z_{i,t}^z) = g_i^z \quad (6)$$

for $i = 1 \dots k$, where $k = \{q, n\}$. Therefore, this model has two sets of time varying ‘coefficients’ $\phi_{ij,t}^\epsilon$ and $\phi_{ij,t}^u$ - for the permanent and transitory parts - and two stochastic volatility models for the diagonal elements of each component, $h_{i,t}^\epsilon$ and $h_{i,t}^u$. It is worth noting the following relationships

$$\begin{aligned} \Phi_{\epsilon,t}(H_{\epsilon,t})^{-1/2}\epsilon_t &= w_t^p, \text{Var}(w_t^p) = I_q, \\ \Phi_{u,t}(H_{u,t})^{-1/2}u_t &= w_t^t, \text{Var}(w_t^t) = I_n. \end{aligned}$$

All the innovations in the model are assumed to be distributed according to

$$\begin{bmatrix} w_t^p \\ w_t^t \\ V_t^\epsilon \\ Z_t^\epsilon \\ V_t^u \\ Z_t^u \end{bmatrix} \sim \text{i.d.d. } \mathcal{N} \left(\begin{bmatrix} 0_q \\ 0_n \\ 0_{\frac{q^2-q}{2}} \\ 0_q \\ 0_n \\ 0_{\frac{n^2-n}{2}} \end{bmatrix}, \begin{bmatrix} I_q & 0 & 0 & 0 & 0 & 0 \\ 0 & I_n & 0 & 0 & 0 & 0 \\ 0 & 0 & D^\epsilon & 0 & 0 & 0 \\ 0 & 0 & 0 & G^\epsilon & 0 & 0 \\ 0 & 0 & 0 & 0 & D^u & 0 \\ 0 & 0 & 0 & 0 & 0 & G^u \end{bmatrix} \right), \quad (7)$$

with

$$G^z = \begin{bmatrix} g_1^z & 0 & 0 & 0 \\ 0 & g_2^z & 0 & 0 \\ 0 & 0 & \ddots & 0 \\ 0 & 0 & 0 & g_k^z \end{bmatrix},$$

and

$$D^z = \begin{bmatrix} D_1^z & 0_{1 \times 2} & \dots & 0_{1 \times (k-1)} & 0_{1 \times k} \\ 0_{2 \times 1} & D_2^z & \ddots & 0_{2 \times k-1} & 0_{2 \times k} \\ \vdots & \ddots & \ddots & \ddots & \vdots \\ 0_{(k-1) \times 1} & 0_{k-1 \times 2} & \ddots & D_{k-1}^z & 0_{(k-1) \times k} \\ 0_{k \times 1} & 0_{k \times 2} & \ddots & 0_{k \times (k-1)} & D_k^z \end{bmatrix},$$

where with $D_1^z \equiv \text{Var}(V_{21,t}^z)$, $D_2^z \equiv \text{Var}([V_{31,t}^z, V_{32,t}^z]')$, \dots , and $D_k^z \equiv \text{Var}([V_{k1,t}^z, \dots, V_{k(k-1),t}^z]')$, implying that the non-zero and non-one elements of $\Phi_{z,t}$ belonging to different rows evolve independently. Moreover, all matrices are conforming positive definite matrices, and $\mathcal{N}(\cdot, \cdot)$ denotes the multivariate Gaussian distribution.¹⁶ This structure also implies that trend and cycles are orthogonal (i.e., the model is an “independent trend/cycle decomposition”).

Baseline specification. In the baseline specification, y_t contains nine macroeconomic variables, see table 2. The model features trend components in levels and growth rates. Column two and three of table 2 describes the macroeconomic trends ($q = 5$), and cycles ($n=9$) characterizing the set of variables in the system.

Variable name	Trend	Cycle
Real GDP	Potential GDP	Output Gap
Unemployment Rate	none	Unemployment Cycle
Consumer Confidence	none	Consumer Confidence Cycle
HICP	Trend Inflation	Inflation Gap
Price Trends next 12 m	Trend Inflation	Price Expectation Cycle
Unit Labor Cost Index	Trend Inflation	Labor Cost Cycle
Energy Price Index	Trend Energy	Energy Price Cycle
World GDP	Potential W GDP	World Output Gap
World HICP	Trend W Inflation	World Inflation Gap

Table 2. Description of the variables

In this sense, my analysis combines in the same framework, (i) slow-moving variables (trends) that are different from typical business cycle fluctuations (e.g potential GDP, trend inflation), and (ii) fast-moving variables (cycles) that are the typical business cycle fluctuations (e.g output-gap, energy price cycle). The estimation sample spans the period 1990Q1-2022Q2.¹⁷ Hence, the main assumptions that describe the macroeconomic trends are:

Slow-moving variables: 1. The EA output trend - i.e., EA potential GDP - is restricted to be common across only real EA GDP.¹⁸

2. The medium / long-term inflation (trend inflation) is extracted using the information in inflation, households’ perceived inflation, and the unit labor cost (a proxy for firms’ inflation expectations).¹⁹ The use of unit labor costs (defined as the growth of nominal wage adjusted per employee) play a role in shaping firms’ inflation expectations by influencing future firms’ pricing decisions. In theoretical models, the unit labor cost and price inflation are closely interrelated in the medium / long-run. This is due

¹⁶As discussed in Primiceri (2005), there are mainly two justifications for assuming a block-diagonal structure for the joint set of innovations in the model. First, parsimony, as the model is already quite heavily parameterized. Second, ‘allowing for a completely generic correlation structure among different sources of uncertainty would preclude any structural interpretation of the innovations’. See Primiceri (2005, pp. 6-7).

¹⁷The series used in the baseline specification are available, some of them, from 1970Q1 - see table 1 The period 1970Q1-1989Q4 is used as presample to inform the priors on the initial conditions of the trend and the cycle, which I discuss in the next section. In the robustness section, the baseline sample is extended to 1970Q1.

¹⁸The drift coefficient in the unit root process, that constantly accumulates over time, can be thought as an average effect of technological innovation.

¹⁹The use of households’ and firms’ inflation expectations to track the long-term inflation trend is motivated by the extensive work of Coibion, Gorodnichenko and coauthors. Recently, Candia, Coibion and Gorodnichenko (2021) show that firms’ inflation expectations exhibit many of the characteristics of households’ inflation expectations and dramatically depart from the inflation expectations of professional forecasters. In another work, Coibion and Gorodnichenko (2015) present new econometric and survey evidence consistent with firms having similar expectations as households. Moreover, they show evidence that inflation expectation of professional forecasters do not proxy well the expectations of households.

to prices and nominal wages must adjust relative to each other to be consistent with the fact that, in the long-run, the real wage is determined by slow-moving factors such as productivity, wage demands or bargaining power.²⁰²¹

3. The energy trend which is restricted to be common to EA energy prices. This assumption is inspired by the concluding remarks of the seminal paper of Kilian (2008), where it is highlighted the important influence of energy prices on economic performance. In particular, Kilian highlights the role of energy price fluctuations. In principle, permanent disturbances coming from energy prices should be very low, since the major movements in energy prices should come from the cycle part (which have a temporary influence on the economy).

4. The fourth and fifth trends denote the world potential output and world trend inflation. These two trends are of core use if one seeks to understand the importance of global supply and demand shocks. In particular, to address whether global demand–supply imbalances have potential permanent effects after the pandemic shock.

The main reason for estimating five trends is to identify the following permanent shocks: domestic demand and supply-side factors, energy supply factors, and global demand and supply-side factors. The identification scheme is presented in the next section.²²

Fast-moving variables: The macroeconomic cycles are characterized for the same number of variables in the system, 9, see column three in table 2. Notice that changes in unemployment and the consumer confidence indicator are left trendless.²³ Finally, the information gathered within the interrelation of these macroeconomy cycles - output gap (\tilde{y}^1), unemployment cycle (\tilde{y}^2), consumer confidence (\tilde{y}^3), inflation gap (\tilde{y}^4), price expectation cycle (\tilde{y}^5), labor cost cycle (\tilde{y}^6), energy price cycle (\tilde{y}^7), world output gap (\tilde{y}^8), and world inflation cycle (\tilde{y}^9) - can be compared to a fully specified Dynamic Stochastic General Equilibrium (DSGE) model. To be more precise, the cycle VAR structure nests several structural models, for example: (i) a range of Phillips curve models, since inflation can be a purely forward-looking process, driven by expectations on inflation (price expectation cycle) or expectations of future real economic activity (consumer confidence). Moreover, it integrates ‘the triangle model of inflation’, where potential fluctuations of inflation in response to the temporary influence of movements in energy prices

²⁰In my model, changes in the long-run labor cost inflation are gradual and not affected by short-term fluctuations of the economy. Short-term fluctuations are captured by the labor cost cycle. Hence, any change in the long-run labor cost inflation is mapped to the long-term inflation trend.

²¹From an empirical side, Mehra (1991) - for the U.S.- shows that long-run movements in price inflation are related to long-run movements in productivity-adjusted wage inflation, i.e., these variables are cointegrated. However, the presence of the common stochastic trend runs from the rate of change in prices to the rate of change in wages, and not vice versa as suggested by the "price markup" view. For the case of the Euro area, in a recent paper of Bobeica et al. (2019), they find that there is a clear link between the rate of change in labor cost and the rate of change in prices. Moreover, they find that this link becomes stronger when inflation is high. However, in this paper I do not explore that this link could depend on an inflation regime, given that it would make the second part of structural analysis too difficult and cumbersome.

²²The eigenvalues of the variance-covariance matrix of the trend components are in absolute value close to zero when additional trends are introduced, suggesting the presence of five trends across the variables included in the system. In the robustness section, the rate of unemployment enters in levels, instead of Q-Q differences, to estimate a natural rate of unemployment and unemployment-gap. Hence, including an additional trend in the system, and leaving unchanged the number of cycles.

²³The inclusion of unemployment and consumer confidence are particularly important for proper estimation of the stationary component of GDP- i.e., the output gap. In fact, core now-casting models, used in many Central Banks, rely on these two core variables. See Laxton and Tetlow (1992); Kamber et al. (2018) and Barbarino et al. (2020), for a more recent view.

(energy price cycle), the degree of resource utilization in the economy (output-gap and unemployment cycle).²⁴ To understand inflation dynamics from an open economy perspective, it also takes into account a global Phillips curve part.²⁵ (ii) From the perspective of the EA output-gap, it features the inverse relation of the Okun's law since output is linked to unemployment fluctuations. Moreover, it captures how slack in real output is affected when potential international political events arise – as is the case for oil price, food and beverages, and the recent global supply bottlenecks. Hence, my model accounts for a wide variety of sources that can modify the interrelation of these macroeconomy cycles.

3.B. PRIORS AND ESTIMATION PROCEDURE

Priors. First, I need to specify a distribution for the initial conditions \bar{y}_0 and $\tilde{y}_{0:-p+1} = (\tilde{y}'_0, \dots, \tilde{y}'_{-p+1})'$ are distributed according to $\bar{y}_0 \sim \mathcal{N}(\underline{y}_0, I_q)$ and $\tilde{y}_{0:-p+1} \sim \mathcal{N}(0, \underline{\Sigma}_0^A)$, where \underline{y}_0 and $\underline{\Sigma}_0^A$ are computed using pre-sample data.

Starting with the prior for $\Lambda(\lambda)$ is given by $p(\lambda) = N(1, 0.5^2)$, the product of independent Gaussian distributions for each element λ of the matrix $\Lambda(\lambda)$. The priors for the VAR coefficients $\mathcal{A} = (A_1, \dots, A_p)$ have a normal posterior distribution with mean $\bar{\mathcal{A}}$ and variance $\bar{\Sigma}^A$, based on prior mean $\underline{\mathcal{A}}$ and $\underline{\Sigma}_0^A$, where:

$$(\bar{\Sigma}^A)^{-1} = (\underline{\Sigma}_0^A)^{-1} + \sum_{t=1}^T \left((\Sigma_t^u)^{-1} \otimes \tilde{x}_t \tilde{x}_t' \right),$$

$$\text{vec}(\bar{\mathcal{A}}) = \bar{\Sigma}^A \left\{ \text{vec} \left(\sum_{t=1}^T (\Sigma_t^u)^{-1} \tilde{y}_t \tilde{x}_t' \right) + (\underline{\Sigma}_0^A)^{-1} \text{vec}(\underline{\mathcal{A}}) \right\} I(\text{vec}(\underline{\mathcal{A}})),$$

\tilde{x}_t contains the lags of \tilde{y}_t and $I(\text{vec}(\underline{\mathcal{A}}))$ is an indicator function that is equal to 0 if the VAR is explosive - some of the eigenvalues of $\mathcal{A}(L)$ are greater than 1 - and to 1 otherwise. Hence, I am enforcing a stationarity constraint on the VAR. Moreover, the prior for the VAR parameters $\text{vec}(\underline{\mathcal{A}})$, describing the components \tilde{y}_t , is a standard Minnesota prior with the hyperparameter for the overall tightness equal to the commonly used value of 0.2 (see [Giannone, Lenza and Primiceri \(2015\)](#)), and centered at zero rather than one, since I am dealing with stationary processes. Finally, the VAR uses four lags ($p = 4$).

The priors for the variance-covariance time-varying elements follows [Benati and Mumtaz \(2007\)](#), with some minor modifications to take into account the important differences between the permanent (Σ_t^e) and transitory (Σ_t^u) matrices governing each process. Prior distributions for the time-varying elements in the permanent side are going to be scaled down by a factor of one hundred. Such a choice is clearly arbitrary, but motivated by my goal of informing to the model that the former elements should have much lower volatility than its counter part (the transitory elements). In other words, the elements belonging to the slow-moving variables should resemble two features: (i) low volatility in magnitude and (ii) expected changed in the volatility should also be low. This approach helps me to deal with the problem of label

²⁴See [Gordon \(1981, 1988\)](#). Moreover, it reflects the view of [Yellen \(2016\)](#) which is widely shared by policy makers and central bankers. See also the work of [Hasenzagl, Pellegrino, Reichlin and Ricco \(2018\)](#) that emphasizes the inclusion of an energy price cycle.

²⁵The importance of including cyclical global activity measures is suggested in [Martínez-García and Wynne \(2010\)](#); [Kabukçuoğlu and Martínez-García \(2018\)](#); [Duncan and Martínez-García \(2023\)](#).

switching in mixture models in order to reliably recover the entire posterior distribution.²⁶

In order to calibrate the prior distributions for $\phi_{ij,0}^z$ and $h_{i,0}^z$, I ‘estimate’ a time-invariant version of $\mathbf{1}$ based on an unbalanced dataset, from 1970 Q1 to 1989 Q4.²⁷ Let Σ_0^z be the estimated variance-covariance matrices from the time-invariant decomposition model. Let L^z be the lower-triangular Choleski factor of Σ_0^z - i.e., $L^z L^{z'} = \Sigma_0^z$. The initial conditions for the stochastic volatility process, $\ln h_0^u$ and $\ln h_0^\epsilon$, are set to follow a $\mathcal{N}(\ln \mu_0^u, 10 \times I_n)$ and $\mathcal{N}(\ln \mu_0^\epsilon, 0.1 \times I_q)$, respectively. The prior means, $\mu_0^z = \{\mu_0^\epsilon, \mu_0^u\}$ is a vector collecting the logarithms of the squared elements on the diagonal of L^z . Then each column of L^z is divided by the corresponding element on its diagonal - i.e., \tilde{L}^z are the rescaled matrices - and set the initial conditions of the elements below the diagonal, $\phi_{ij,0}^u$ and $\phi_{ij,0}^\epsilon$, to follow a $\mathcal{N}(\tilde{\phi}_{ij,0}^u, 100 \times \tilde{V}(\tilde{\phi}_{ij,0}^u))$ and $\mathcal{N}(\tilde{\phi}_{ij,0}^\epsilon, \tilde{V}(\tilde{\phi}_{ij,0}^\epsilon))$, respectively. The prior means of $\tilde{\phi}_{ij,0}^z$ are the non-zero and non-one elements of \tilde{L}^z (i.e., the elements below the diagonal). The variance-covariance matrices, $\tilde{V}(\tilde{\phi}_{ij,0}^u)$, are postulated to be diagonal with each individual (i,i) element equal to the absolute value of the corresponding $\tilde{\phi}_{ij,0}^z$.

The matrices in D^z are also calibrated following [Benati and Mumtaz \(2007\)](#). D^z follow a diffuse inverse Wishart - $p(D_i^z) = IW(\kappa, \kappa(\eta_z D_i^z))$ - with just enough prior degrees of freedom, κ , set equal to the number of rows in D_i^z plus two to have a well-defined prior mode. The mode D_i^z is scaled by the number of degrees of freedom and $\eta_{u,\epsilon} = \{10^{-3}, 10^{-5}\}$. Each D_i^z is composed of the row elements below the diagonal in \tilde{L}^z .

Finally, as for the variances of the stochastic volatility innovations (i.e., the elements of G^z), I follow [Cogley and Sargent \(2001, 2005\)](#) and [Benati and Mumtaz \(2007\)](#). They postulate an inverse-Gamma distribution, $g_j^z \sim IG\left(\frac{\kappa}{2}, \frac{g_j^z}{2}\right)$, for the elements of G^z with κ degrees of freedom and prior mode g_i^z . I apply some modifications to take into account the important differences between the permanent (G^u) and transitory (G^ϵ) volatility innovations. In this way, I am enforcing that the model does not mix permanent with transitory parts. For the stochastic volatility innovations from the transitory part, I use the same specifications as the former papers, $g_j^u \sim IG\left(\frac{1}{2}, \frac{10^{-4}}{2}\right)$. The choice of for the stochastic volatility innovations belonging to the permanent part are chosen accordingly to represent specific features. In this sense, I set the mode of diagonal elements of the matrix $G^\epsilon = \{g_1^\epsilon, g_2^\epsilon, g_3^\epsilon, g_4^\epsilon, g_5^\epsilon\}$ to $G^\epsilon = \{8.3 * 10^{-6}, 3.3 * 10^{-5}, 8.6 * 10^{-5}, 8.3 * 10^{-6}, 3.3 * 10^{-5}\}$. A priori, it implies that the expected change over a period of a hundred years in the volatility of potential GDP, inflation trend, energy trend, potential world GDP, and world inflation trend is 0.33, 1.33, 3.33, 0.33, 1.33 percentage points, respectively.²⁸ In addition, these priors are quite tight, as I set the degrees of freedom equal to one hundred (i.e., $\kappa = 100$) as in [Del Negro et al. \(2017, 2019\)](#). Therefore, I am feeding the system with rather strong priors on the potential movement of all trend components. There are two intrinsic reasons for the selection of these priors: (i) to ensure these do not reflect business cycle fluctuations; and (ii) to a priori prevent scenarios such as de-anchoring of long-term inflation trend. Nevertheless, if data spoke loudly in favor of

²⁶See [Geweke \(2007\)](#) and [Stephens \(2000\)](#).

²⁷This is not a real estimation. I run just a few iterations MCMC to decompose the pre-sample data into trends and cycles, and obtain the matrices of interest. Notice that this procedure yields ‘stupid’ elements (i.e., $\phi_{ij,0}^\epsilon, \phi_{ij,0}^u, h_{i,0}^\epsilon$ and $h_{i,0}^u$).

²⁸Relative to the previous prior mean values for the stochastic volatilities imposed on the cycle component, the current prior mean values exhibit reductions by factors of 12 for GDP trends, 3 for inflation trends, and 1.2 for energy trends.

relevant movements in the low-frequency components of the system, it would push away from the prior assumptions.²⁹

Estimation. The state-space model, given by equations 1 through 7, is efficiently estimated with Bayesian methods - Gibbs Sampling and Metropolis Hastings algorithm - using Kalman Filter, in conjunction with modern simulation smoothing techniques (Carter and Kohn (1994)) that easily help me to accommodate missing observations, and draw the latent states. All results are based on 150,000 simulations, of which I discard the first 100,000 as burn-in draws and save every 200th draw in order to reduce the autocorrelation across draws.³⁰ Section A of the appendix describes the Gibbs sampler, which accommodates the hierarchical decomposition model to different modeling choices.

3.C. SHOCK IDENTIFICATION STRATEGY

In this paper, I identify the shocks that are mostly emphasized in the inflation literature. These structural factors are energy supply, global and domestic from a demand and supply side. All of them are identified from a permanent and transitory perspective to properly understand inflation dynamics.

In order for me to make economically meaningful statements with respect the channels of shocks, I need to impose restrictions on the variance-covariance matrices ($\Sigma_t^\epsilon, \Sigma_t^u$). These restrictions help me to map the economically meaningful structural shocks from the estimated reduced-form residuals. In this sense, I first introduce the mapping between reduced-form and structural trend residuals be $\epsilon_t = B_t w_t^P$, where B_t is a non-singular matrix such that $B_t B_t' = \Sigma_t^\epsilon$ and $w_t^P \sim N(0_{q,1}, I_{q,q})$ are the structural permanent shocks with unit variance. Last, the mapping between reduced-form and transitory structural residuals be $u_t = C_t w_t^T$, where C_t is a non-singular matrix such that $C_t C_t' = \Sigma_t^u$ and $w_t^T \sim N(0_{n,1}, I_{n,n})$ are the structural transitory shocks with unit variance.

Notice that the latent variables - i.e., trends and cycles - in equation 1 can be rewritten as follows,

$$\begin{aligned}
y_t &= \Lambda \left(\bar{y}_0 + \sum_{h=1}^t h\bar{c} + \sum_{j=0}^{t-1} \epsilon_{t-j} \right) + \sum_{j=0}^{t-1} \tilde{A}_j u_{t-j} \\
&= \Lambda \left(\bar{y}_0 + \sum_{h=1}^t h\bar{c} + \sum_{j=0}^{t-1} B_{t-j} B_{t-j}^{-1} \epsilon_{t-j} \right) + \sum_{j=0}^{t-1} \tilde{A}_j C_{t-j} C_{t-j}^{-1} u_{t-j} \\
&= \Lambda \left(\bar{y}_0 + \sum_{h=1}^t h\bar{c} \right) + \underbrace{\Lambda \sum_{j=0}^{t-1} B_{t-j} w_{t-j}^P}_{\text{Permanent Shocks}} + \underbrace{\sum_{j=0}^{t-1} \tilde{A}_j C_{t-j} w_{t-j}^T}_{\text{Transitory Shocks}}
\end{aligned}$$

by just applying successive substitution for \bar{y}_{t-j} and \tilde{y}_{t-j} , where \tilde{A}_j is the companion form matrix at the power of horizon j , and applying the mapping between reduced-form and structural residuals. Then

²⁹While in the baseline specification I specify the same prior on the variance-covariance matrix of the trend components for the Euro area and the world, this could be in principle different for the two region components. The robustness section shows that with ‘looser’ trend priors, I simply let \bar{y}_t capture some higher-frequency movements, with not much impact on the substantive results. In addition to alternative prior specifications on the trend components, I also test different lag specifications for the transitory component.

³⁰I assess the convergence of the Markov chain by inspecting the autocorrelation properties of the ergodic distribution’s draws. Moreover, I follow the diagnostic for monitoring the convergence of multiple Metropolis Hastings chains of Geweke et al. (1991). The inefficiency factors for all posterior elements are represented in Figure 11 of Appendix B.

ΛB_t is interpreted as $d\bar{y}_t/dw_t^P$ and $\tilde{A}_j C_{t+j}$ is interpreted as $d\tilde{y}_{t+j}/dw_t^T$. Both represent the effects on the low and high-frequency components, respectively.

The structural identification relies on sign-restrictions. First, in order to identify demand-side and supply-side factors, my set of sign restrictions rests on the following argument that supply-side forces move output and inflation in opposite directions, while demand-side forces imply a positive comovement. Second, to distinguish between domestic and global shocks I follow the comovements proposed by [Corsetti et al. \(2014\)](#), this implies that global shocks affect global variables more than domestic ones, and viceversa for domestic shocks.³¹ To satisfactorily implement this restriction, world GDP and inflation need to be expressed as the ratio of EA to world, as described in Section 2. For instance, if a shock results in an increase in real EA GDP, and concurrently leads to an increase in the EA's share of global GDP, it can be inferred that the shock had a greater impact on the domestic economy than on the rest of the world, and thus, can be classified as a domestic shock. Conversely, if the shock results in a decline in the EA economy's share of global GDP, it can be deduced that the shock had a greater impact on the rest of the world, and thus, can be classified as a global shock. For example, a global supply shock would affect positively to EA GDP, negatively to world GDP (+/(++)) (i.e., the denominator grows more than the numerator and EA's share of global GDP is reduced), negatively to EA inflation and positively to world inflation (-/(-)) (i.e., the EA's share of global inflation increases due to the denominator is more negative than the numerator). Energy supply shocks increase the price of energy, have a negative impact on EA real activity, and rise EA inflation on impact. These restrictions reflect the lessons from the literature that identifies various types of energy-related shocks. See, for example, [Kilian \(2009\)](#) that models the global crude oil market and then, investigates the impact of these shocks on the key macroeconomic variables. Moreover, I assume that energy supply shocks have a greater impact on the Euro area, due to its high energy dependence with respect to the world.³² Finally, permanent domestic supply shocks do not exert an influence on the long-term trend of energy. Additionally, the transitory component of these shocks has no contemporaneous impact on the energy cycle.

Tables 3 and 4 present the set of sign restrictions applied to the permanent and transitory shocks, respectively. The restrictions are consistent across both types of shocks, with a few minor variations. Specifically, for permanent shocks, it is assumed that positive domestic supply-demand shocks have an unrestricted effect on energy price trend. The reason, for not imposing any restriction, is that the Euro area is not a energy producer, hence it is very unlikely that the Euro area could permanently affect energy prices. Whereas the rest of the world is an energy producer and it can affect it. Finally, on the transitory side four shocks are left unidentified. These shocks could be masking structural shocks such as labor-market shocks, consumption shocks, uncertainty shocks or expectation shocks, among others. Nevertheless, I find that the total explained share by these four unidentified shocks is around 10% on a historical basis.

The identification algorithm is based on the sign restrictions approach proposed by [Canova and](#)

³¹Other empirical papers that also aim at identifying global and domestic shocks, using similar techniques, are [Bobeica and Jarczyński \(2019\)](#) and [Conti et al. \(2017\)](#).

³²Currently, the Euro area has an energy import dependency rate that stands around 60%.

	Domestic Supply	Domestic Demand	Energy Supply	Global Supply	Global Demand
EA Potential GDP	+	+	-	+	+
EA Inflation Trend	-	+	+	-	+
Energy Price Trend	≈ 0	•	+	-	+
W Potential GDP	+	+	-	-	-
W Inflation Trend	-	+	+	+	-

Table 3. Sign restrictions on trends

	Domestic Supply	Domestic Demand	Energy Supply	Global Supply	Global Demand
Output Gap	+	+	-	+	+
Unemployment Cycle	•	•	•	•	•
Consumer Confidence Cycle	+	•	•	•	•
Inflation Gap	-	+	+	-	+
Price Expectation Cycle	-	+	+	•	•
Labor Cost Cycle	•	•	•	•	•
Energy Price Cycle	≈ 0	+	+	-	+
World Output Gap	+	+	-	-	-
World Inflation Gap	-	+	+	+	-

Table 4. Sign restrictions on cycles

De Nicolo (2002) and Uhlig (2005) and refined by Rubio-Ramirez, Waggoner and Zha (2010).³³ This approach is implemented in the same way as for traditional SVARs with sign restrictions. The key difference with respect to standard SVARs is that the structural analysis is not only focus on business cycle fluctuations, but also on low-frequency movements. I focus on the same set of structural shocks that are likely to be relevant for quantifying their role in driving inflation’s trend and gap.

4. RESULTS: DYNAMICS AND DRIVERS OF THE EA INFLATION TREND AND CYCLE

This section documents my main empirical results obtained from the estimated model. First, I show the dynamics of the hidden states of the model; in other words, I plot the evolution of the potential GDP, inflation trend, output and inflation gap for the Euro area since 1990. Second, I quantify the nature - permanent and transitory - of the structural shocks at play to explain the past and recent dynamics of EA inflation. To do so, I construct a historical decomposition with the effect at time t of each structural shock. Finally, I test whether the Phillips Curve, in the Euro area, is flat. This exercise separates the variation in inflation-gap and output-gap into the components driven by demand and supply disturbances.

4.A. HIDDEN COMPONENTS, IT IS THE TREND NOT THE CYCLE

Figures 1 and 2 show the estimated low and high-frequency components of inflation and GDP together with the actual data. Trends components are plotted first, and cycles in the second row. The red solid lines correspond to the actual data, while the thick black lines represent the point-wise median estimates

³³Additional details on the sign restrictions algorithm are provided in Appendix A.2

of the trend and cycle components, with the associated 68% credible bands.

The trend-cycle components capture accurately the slow and high-moving behavior with relatively small uncertainty. Focusing on the trend components, there are substantial fluctuations in the trend components of both inflation and GDP over the sample, despite the tight priors imposed on the time-varying variance-covariance matrix. The data thus speaks loudly in favor of significant low-frequency variation.

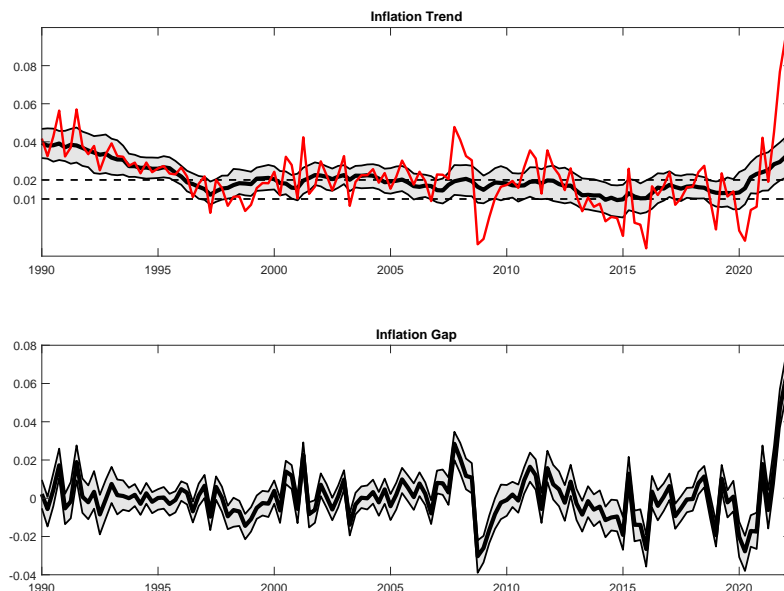


Figure 1. Actual data and estimated trends and cycles of HICP inflation

Note: Point-wise median (solid black line) with 68% credible bands are based on 150000 draws. HICP is defined in annualized quarter-on-quarter terms.

Inflation (Trend Inflation & Inflation-Gap). There is significant fluctuation in the point-wise median of trend inflation over the sample considered, which can be divided in five different time windows. First, trend inflation appreciably declined above 200 basic points, at the beginning of the 1990s, from 4% to 2% level, in 1995. Second, trend inflation stayed anchored around the 2% level for almost two decades until 2012Q3. Moreover, this period features very low fluctuations in trend inflation, reinforcing the concept of anchored expectations. Third, during the European sovereign debt crisis, median trend inflation slowdown over 100 basic points reaching an all time low at 1% in 2015Q1. Fourth, after the sovereign debt crisis it re-anchors close to the 2% level. Fifth, after the strong ‘COVID economic reopening’, trend inflation rises above the 2% level. I would like to highlight that my measure of trend inflation exhibits a robust correlation with three medium-long term market expectation metrics (i.e., Euro area inflation swaps of five, ten and twenty years ahead). This correlation is statistically significant and distinct from zero, as detailed in Figure 11 within Appendix B.

The first two findings are well in line with the narrative that inflation expectations were fully anchored at 2% level thanks to a strong credibility of price stability (see [Altissimo et al. \(2006\)](#); [Bowles et al. \(2007\)](#); [Gorter et al. \(2008\)](#)). But, the recent decline between 2012 and 2016, however, is more controversial. Some studies place that EA trend inflation show little signs of de-anchoring around the mid-2010s (see

Strohsal and Winkelmann (2015); Jarociński and Lenza (2018); Dovern et al. (2020)), while this paper favors a gradual de-anchoring that starts in 2012, as documented in Gimeno and Ortega (2016); Lyziak and Paloviita (2017) and Corsello et al. (2021). In addition, the recent dynamics of trend inflation are not documented in the literature yet. This result suggest that inflation is expected to be persistently higher than ECB’s target in the medium-term. Moreover, it seems to be well in line with the change in ECB’s monetary policy strategy. The message changed from ‘*The current inflation spike is temporary and driven largely by transitory factors.*’ in 2021Q4, to ‘*[...] inflation is expected to decline from an average of 8.4% in 2022, 6.3% in 2023, 3.4% in 2024 and to 2.3% in 2025. [...] Headline inflation is expected to fall to the ECB’s medium-term inflation target of 2% in the second half of 2025.*’ in 2022Q4.³⁴ On the other hand, when focusing on the current dynamics of the inflation-gap (bottom figure), the model displays values around 6-7%. This means that around 85% of the current increase in headline inflation, is mainly explained by transitory factors.

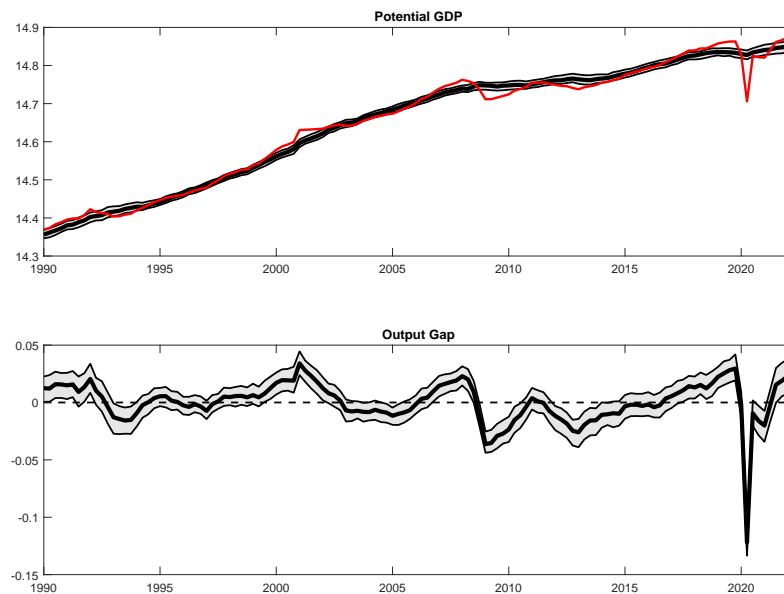


Figure 2. Actual data and estimated trends and cycles of real GDP

Note: Point-wise median (solid black line) with 68% credible bands are based on 150000 draws. Real GDP is defined in log terms.

GDP (Potential GDP & Output-Gap). The point-wise median dynamics of potential GDP shows two different patterns along the studied period.³⁵ (i) The period between the early 90s to 2005-06 shows a strong average growth trend of 0.54% quarter-on-quarter (Q-Q). (ii) From 2006 onwards, the model displays a version of ‘secular stagnation’ hypothesis according to which the Euro area faced a persistent slow-down of trend growth 0.24% Q-Q. This result is in line with the view of Gordon (2014), where he highlights a version of slow growth in potential output after 2006. This persistent slow growth can still be found even if I exclude the Great Financial Crisis, the European Sovereign Debt Crisis and the

³⁴See Staff (2021, 2022).

³⁵Figure 13 in Appendix C plots the average quarterly growth rate of EA Potential GDP (point-wise median) over five-year rolling windows. It can be easily seen than after 2003-04 the growth rate of EA Potential GDP starts declining abruptly and stays low thereafter.

COVID pandemic, with an average growth trend of 0.3% Q-Q.³⁶ Moreover, these reduced-form results favor the interpretation that, during the COVID-19 pandemic, available factors of production were not heavily affected by the lockdown and the related containment measures.³⁷ Hence, the degree of full capacity remains almost unchanged during the lockdown.³⁸ This result implies a very negative output gap during the lockdown period (-13.9%), as it can be seen by the bottom subfigure. Finally, to assess whether the COVID-19 shock have resulted in long lasting adverse effects on Potential GDP growth rate, it is necessary to carry out a structural analysis.

4.B. HISTORICAL DECOMPOSITION OF EURO AREA INFLATION

This subsection analyzes, from a historical perspective, the contribution of different structural channels driving EA trend inflation (permanent shocks) and EA inflation-gap (transitory shocks).

Permanent factors driving trend inflation. Figure 3 plots the estimated historical decomposition of permanent shocks for the point-wise median of trend inflation. Colored bars represent the estimated cumulative contribution of each structural shocks - domestic (demand and supply-side), global (demand and supply-side) and energy supply - from 1990Q2 to 2022Q2.

Global and domestic factors explain the bulk of trend inflation long-run fluctuations over the entire sample, but energy supply shocks play a minimal role. Nevertheless, the importance of these five factors explaining trend inflation movements changes across the sample. Domestic (supply and demand) and global supply-driven factors play a key role in driving trend inflation downwards in the early and late 1990s. According to the common view that potential gdp - both in the Euro area and world - are growing at a strong path due to the large increases in the supply-side. The accumulation of negative domestic demand shocks seems to be also in line with the short crisis of the early-mid 1990s.

Centering my attention on the early 2000s, domestic and global demand-driven forces are compensated by domestic and global supply-driven factors leading to a decade of stable trend around the 2% level. After the 2008 financial crisis, a sequence of negative shocks arises from the domestic and global side. The contribution of domestic and global demand-driven forces start to de-accumulate, putting downward pressures on trend inflation. On the other hand, downward pressures from the demand side are mainly compensated by a sequence of negative global supply shocks (i.e., notice that negative supply shocks translate into higher trend inflation).

³⁶This result is related to the recent findings of [Antolin-Diaz et al. \(2017\)](#) and [Maffei-Faccioli \(2021\)](#), who document a significant decline in long-run output growth in the United States. In particular, [Maffei-Faccioli \(2021\)](#) is able to identify the drivers of the ‘secular stagnation’ in the U.S. He finds that mainly permanent demand-side shocks affected the slowdown in gdp growth after 2000.

³⁷In Appendix C, Figure 14 presents the decomposition of real GDP into its potential GDP and output-gap components, utilizing a model variant that excludes stochastic volatility on both the permanent and transitory dimensions. This illustration underscores that, when stochastic volatility is not included, the pronounced downturn in real GDP, witnessed during the COVID-19 period, is compensated between the potential GDP and the output-gap. Moreover, I compare in Figure 15 the model estimates with the ones provided by the European Commission (both Potential GDP and Output-gap). This comparison highlights the use of stochastic volatility in decomposition models.

³⁸Probably, one of the main factors that prevented Potential GDP from collapsing was the rapid implementation of policies to support the households and in particular firms. [Bodnár et al. \(2020\)](#) assess that liquidity policies, aimed at reducing firms’ wage bill by temporarily transferring part of the labour costs to governments, have significantly reduced the share of firms under stress as a result of the lockdowns.

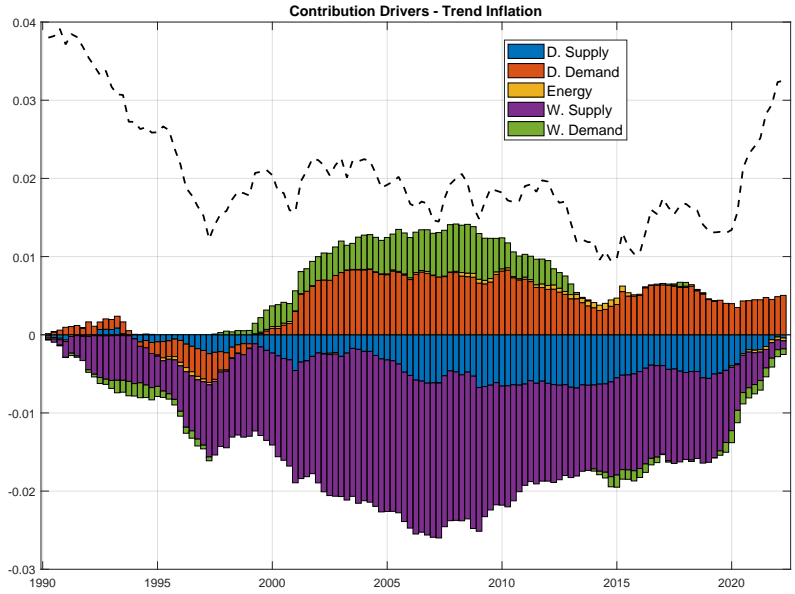


Figure 3. Estimated historical decomposition of the point-wise median of trend inflation from 1990Q2 to 2022Q2

Note: The black line is the point-wise median of trend inflation. The colored bars represent the contribution of each structural shock - domestic (demand and supply-side), global (demand and supply-side) and energy supply - at time t .

The event of the missing inflation in the Euro area seems to favor explanations that are related to the demand-side of the economy, both domestic and global.³⁹ To better understand the importance of demand shocks behind the missing inflation, Figure 4 plots the cumulative contribution of shocks starting on 2008, on the left image, and the share of the variance decomposition of each shock, on the right.

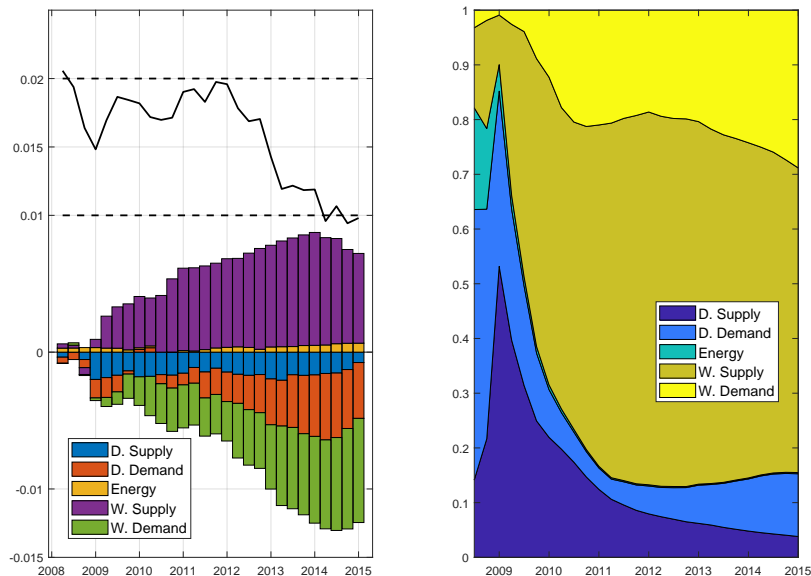


Figure 4. Estimated historical decomposition of median trend inflation from 2008 to 2015

Note: The black line is the point-wise median of trend inflation. The colored bars (areas) represent the contribution (share of the variance decomposition) of each structural shock - domestic (demand and supply-side), global (demand and supply-side) and energy supply - at time t .

³⁹See IMF (2016, 2017).

On the left image, trend inflation starts decreasing from the 2% level after 2012 due to the increasing contribution of negative demand shocks (domestic-global). These shocks explain around 40% of the fluctuations of trend inflation in this period. Consequently, the drivers identified in this study to explain the period of the missing inflation align with those presented in existing literature (Ferroni and Mojon (2014); Conti et al. (2017); Ciccarelli et al. (2017); Bobeica et al. (2019)). Nevertheless, my findings underscore the permanent nature of shocks, contrasting with the transitory effects suggested by the literature.

The recent period of the ‘COVID economic reopening’ is marked by a pronounced surge in trend inflation, attributable to a confluence of both global and domestic supply-side shocks. Figure 5 displays the cumulative impact of shocks starting on 2019Q4, as illustrated on the left, and the historical variance decomposition of each shock, depicted on the right. The importance of adverse global-domestic supply shocks is evident. Indeed, these shocks can be attributed to recent supply chain disruptions at the global and domestic level. The economic disruptions stemming from the pandemic appears to have long-lasting damage on the real economy. Indeed, the observed disequilibrium between supply and demand may have arisen from a reduction in the economy’s supply capacity, coupled with a robust, albeit seemingly transient, resurgence in demand, as illustrated in Figure 6.

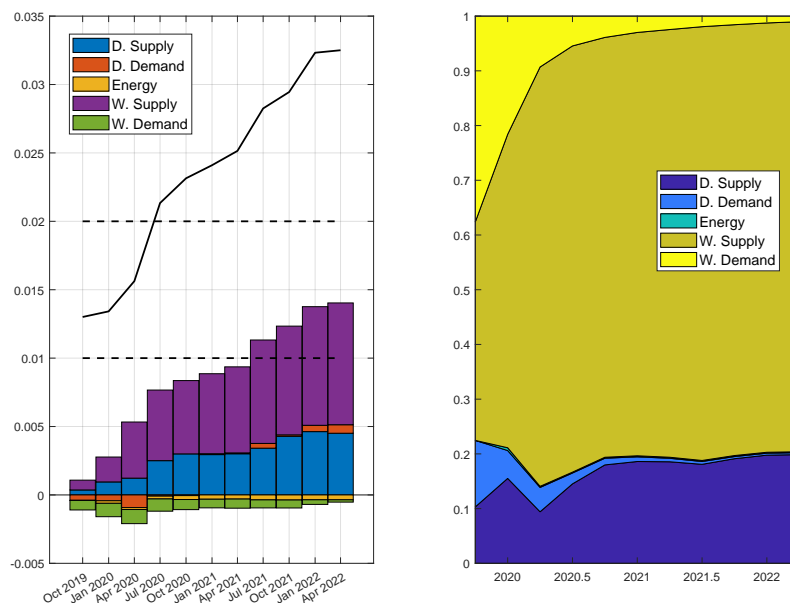


Figure 5. Estimated historical decomposition of median trend inflation from 2019 to 2022

Note: The black line is the point-wise median of trend inflation. The colored bars (areas) represent the contribution (share of the variance decomposition) of each structural shock - domestic (demand and supply-side), global (demand and supply-side) and energy supply - at time t .

Transitory factors driving inflation-gap. Figure 6 plots the estimated historical decomposition of transitory shocks for the point-wise median of inflation-gap - the dashed black line. In colored bars are presented the estimated contribution of each structural shocks at each moment in time - domestic (demand and supply-side), global (demand and supply-side), energy supply and the sum of the four unidentified shocks- from 1990Q2 to 2022Q2. The sum of the four unidentified shocks could be masking

structural shocks such as labor supply shocks, consumption shocks, uncertainty shocks or expectation shocks, among others.

The recent inflationary episodes have been mainly caused by a confluence of transitory factors (around 85% of the total inflation surge can be explained by transitory forces). The inflation-gap has been influenced by both domestic and global demand shocks, as well as perturbations in energy supply. During this period, the trio of shocks account for approximately 70% of the total variance observed in the inflation-gap, see Figure 16 in Appendix C. In particular, from the second quarter of 2021 onwards, as economies reopened and pandemic-induced restrictions were relaxed, demand shocks began to exert pressure on the economic landscape. This surge in domestic demand can be potentially traced back to the elevated savings accumulated during the lockdown phase. Within the Euro area, a combination of pandemic-induced constraints and supportive fiscal measures, such as job retention schemes, culminated in an unprecedented increase in household savings, peaking at 25% of disposable income in the second quarter of 2020. Subsequent to the economic revival, while the savings ratio has receded considerably from its peak, it remained elevated compared to pre-pandemic benchmarks as of the fourth quarter of 2022.⁴⁰ Following the economic resurgence, the United States and several other nations experienced a marked augmentation in their import activities, with a pronounced emphasis on consumer goods (i.e., this increase is 24% relative to 2019 levels in U.S.).⁴¹ Additionally, the recent surges have been exacerbated by the Russian invasion of Ukraine that caused enormous cuts in energy supply, making energy prices to skyrocket.

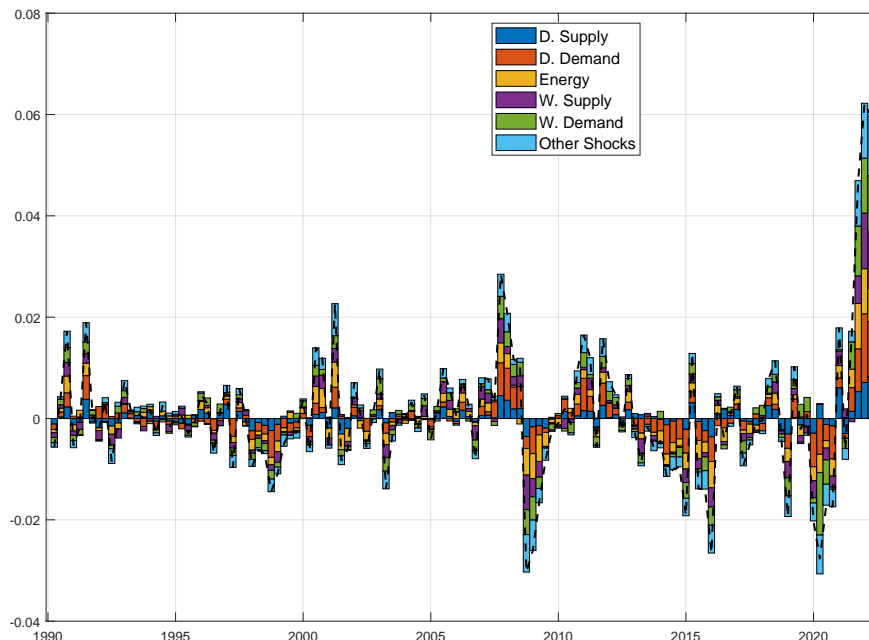


Figure 6. Estimated historical decomposition of the point-wise median of inflation-gap from 1990Q2 to 2022Q2

Note: The black line is the point-wise median of inflation-gap. The colored bars represent the contribution of each structural shock - domestic (demand and supply-side), global (demand and supply-side), energy supply and the sum of the four unidentified shocks - at time t .

⁴⁰See De Santis and Stoevsky (2023); Bańkowski et al. (2023).

⁴¹See Higgins et al. (2021).

From a historical perspective, Figure 17 in Appendix C plots the asymptotic variance decomposition of inflation-gap (point-wise median). Notably, throughout the entire sample, domestic shocks explain around 40% of the historical variance in inflation-gap. Global shocks contribute to around 30%, while energy supply shocks constitute 10%. A 20% remains unexplained, stemming from the unidentified shocks. A particularly salient observation is the augmented contribution of global demand shocks to the asymptotic share, witnessing an increase of 5-7% in the aftermath of the COVID-19 pandemic.

4.C. HISTORICAL DECOMPOSITION OF EURO AREA GDP

This subsection analyzes the contribution of different structural channels driving EA potential GDP (permanent shocks) and EA output-gap (transitory shocks).

Permanent factors driving potential GDP. Figure 7 shows the historical decomposition of permanent shocks for the point-wise median of potential GDP. It is important to notice that in the absence of shocks, potential GDP grows at a constant factor \bar{c} (see Equation 2). Hence, permanent shocks affecting potential GDP generate positive and negative hysteresis effects. In other words, potential GDP growth, given by \bar{c} , can be boosted or slowed down at time t .⁴²

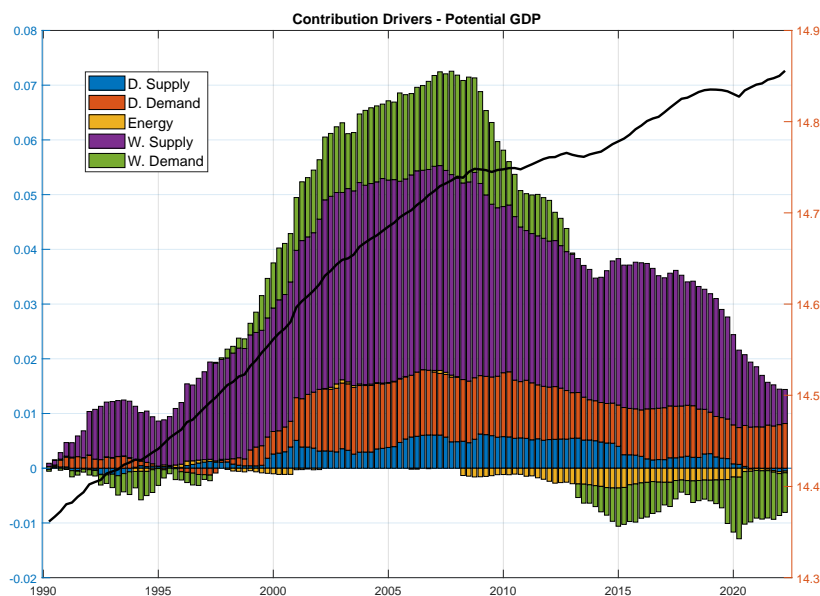


Figure 7. Estimated historical decomposition of the point-wise median of potential GDP from 1990.Q2 to 2022.Q2

Note: The black line is the point-wise median of potential GDP. The colored bars represent the contribution of each structural shock - domestic (demand and supply-side), global (demand and supply-side) and energy supply - at time t .

In the first part of the sample, shocks positively contribute potential gdp growth, in which global factors play a major role explaining the long-run fluctuations of potential GDP, up to 2007. Second, there is a surprising de-accumulation of the contribution of shocks after the 2008 financial crisis. Indeed, after

⁴²For example, [Bluedorn and Leigh \(2019\)](#) provide evidence, for 34 advanced economies, of positive hysteresis where permanent decreases in unemployment are associated with protracted expansions. On the other hand, [Furlanetto et al. \(2021\)](#) find evidence of negative hysteresis. They find that negative permanent demand shocks are quantitatively important for the United States, leading to a permanent decline in employment and investment.

2008, potential gdp growth seems to be entirely driven by the cumulative effect of the drift coefficient \bar{c} . This result can perfectly explain why potential gdp growth is much stronger between 1990-2007 (0.54% Q-Q growth) than after 2008 (0.30% Q-Q growth, excluding the events of the Great Financial Crisis, the European Sovereign Debt Crisis and the Covid pandemic).

These results are suggesting a structural change, after the 2008 financial crisis, with respect to the underlying forces driving potential GDP in the Euro area. The period prior 2008 is characterized by positive hysteresis, where potential GDP is primarily driven by global factors plus the idiosyncratic cumulative effect of the drift coefficient. The period after 2008 is characterized by negative hysteresis, the contribution of global shocks starts de-accumulating putting downward pressure on potential gdp growth. However, domestic shocks hold in terms of total contribution. This result poses a permanent change in globalization, which is in line with the theory of ‘the great trade collapse’. This theory poses that the synchronized world trade collapse in late 2008 (i.e., the collapse was caused by the sudden, severe and globally synchronised postponement of purchases, especially of durable consumer and investment goods) created permanent losses globally.⁴³ Another interesting force driving potential GDP growth down is the negative effects of energy supply shocks between 2007-08, which created negative permanent effects. After the first quarter of 2020, the contribution of global shocks dramatically decreases with the start of the COVID-19 pandemic, while domestic demand shocks hold.

Transitory factors driving output-gap. Figure 8 plots the estimated historical decomposition of transitory shocks for the point-wise median of output-gap - the dashed black line. In colored bars are presented the estimated contribution of each structural shocks at each moment in time - domestic (demand and supply-side), global (demand and supply-side), energy supply and the sum of the four unidentified shocks- from 1990Q2 to 2022Q2.

The Financial Crisis and the European Sovereign Debt Crisis mainly differ in the major factors explaining each period. While the sharp contraction in economic activity during the period of 2008-09 is explained by around 50% by global factors, the economic downturn during 2010-15 seems to be explain by domestic demand factor (around 60-70%). The huge negative output-gap originated due to the COVID-19 lockdown seems to be explained around 50% by global factors. Finally, the rebound in economic activity after the economic reopening is completely explained by demand factors, both domestic and global. In particular, global demand factors explain 60%. This result backs the idea that several nations, including the United States, have experienced a marked augmentation in their import activities, with a pronounced emphasis on consumer goods. See Figure 18 in Appendix C plots the short-term variance decomposition of output-gap (point-wise median) from a historical perspective.

Figure 17 in Appendix C plots the asymptotic variance decomposition of output-gap (point-wise median). Over all the period, the asymptotic shares of each shock explaining EA output-gap are relatively similar to the ones explaining EA inflation-gap. The main difference stems that the asymptotic contribution of global demand shocks, in the aftermath of the COVID-19 pandemic, increases from an average of explaining 10% to 20%. Reducing the explained share of domestic demand, global supply and energy

⁴³See Baldwin and Taglioni (2009), Abiad et al. (2014) and Chen et al. (2019).

supply shocks.

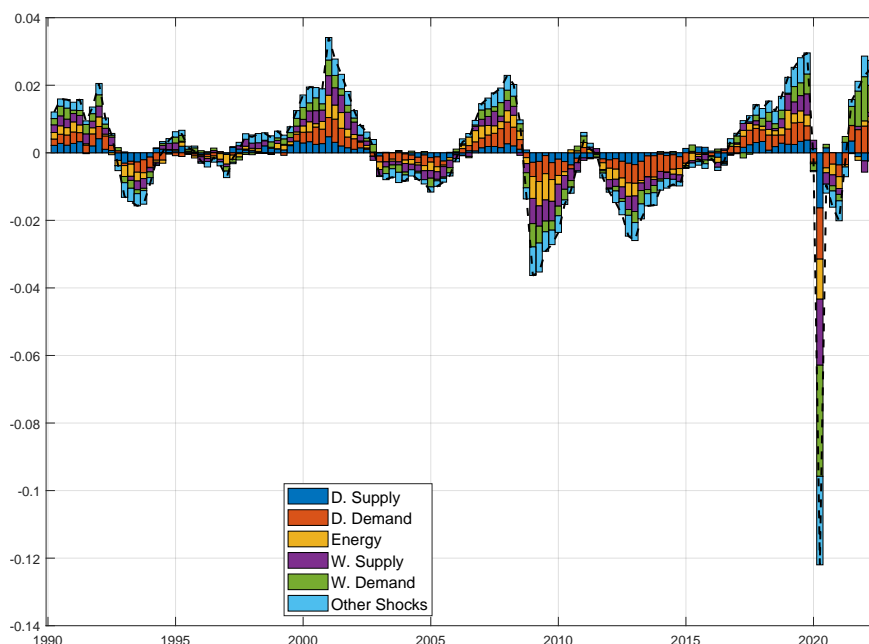


Figure 8. Estimated historical decomposition of the point-wise median of output-gap from 1990.Q2 to 2022.Q2

Note: The black line is the point-wise median of output-gap. The colored bars represent the contribution of each structural shock - domestic (demand and supply-side), global (demand and supply-side), energy supply and the sum of the four unidentified shocks - at time t .

4.D. IDENTIFICATION OF THE PHILLIPS CURVE

In this analysis, I address the notable disconnect between the inflation-gap and output-gap that has been evident since the 1990s, as it is emphasized by a large and yet growing literature. Drawing upon the methodology proposed by [Bergholt et al. \(2023\)](#), I aim to understand this disconnect by examining the structural dynamics of supply and demand.

The Phillips curve, traditionally viewed as an upward-sloping supply curve, is identified when data are purged for supply-side shocks. A low positive regression slope suggests a flattened aggregate supply, with demand dynamics remaining constant. Conversely, the Investment-Saving curve, which is typically downward-sloping, is identified when data are adjusted for demand-side shocks. A less pronounced negative regression slope indicates a stricter central bank commitment to inflation stability, leading to subdued inflationary fluctuations and a flat demand curve, while supply dynamics remain unchanged.

Utilizing the cycle model, I isolate historical data variations attributable to supply and demand shocks. Based on these decompositions, I focus on the median contribution of each shock to fluctuations in the inflation-gap and output-gap. Supply shocks encompass both domestic and global supply dynamics, while demand shocks aggregate domestic and global demand variations.

Figure 9 presents outcomes conditioned on identified demand shocks, revealing a positive correlation between output and inflation. The slope is notably steep at 0.524, with significant statistical relevance.

In contrast, Figure 10, conditioned on supply shocks, shows a negative correlation between output and inflation, with a notably flat slope.

These findings suggest a consistent supply curve contrasting against a notably flat demand curve. Such observations challenge the widely accepted narrative of a declining Phillips curve slope but align with the principles of strict inflation targeting. These insights are consistent with the conclusions of [Bergholt et al. \(2023\)](#) regarding the US economic landscape.

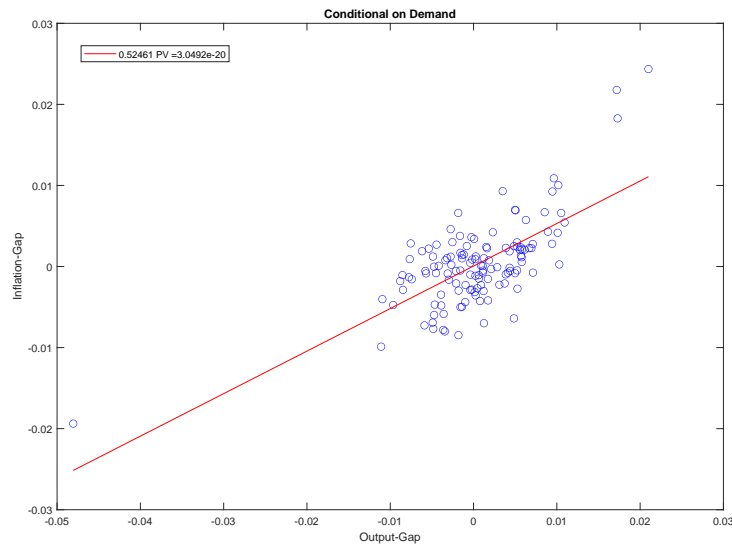


Figure 9. Conditional on demand

Note: Conditional data obtained from the estimated cycle model part. Corresponding slope estimate is 0.524 with a P-value of 0.

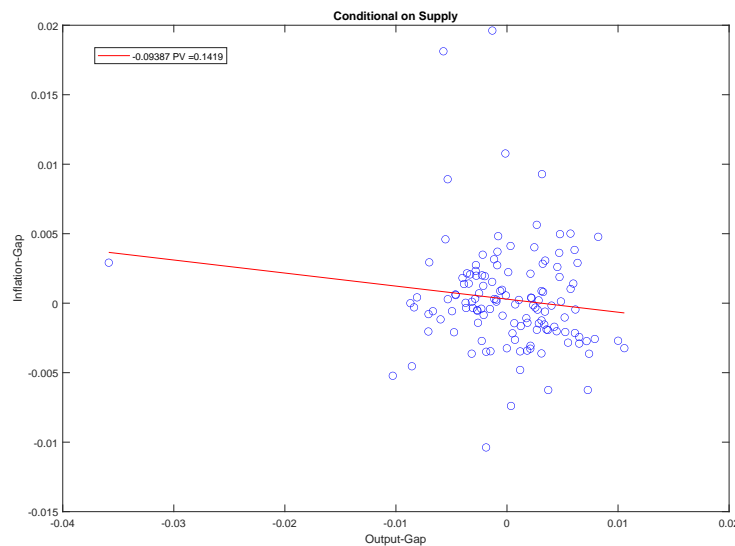


Figure 10. Conditional on supply

Note: Conditional data obtained from the estimated cycle model part. Corresponding slope estimate is -0.09387 with a P-value of 0.14.

5. ROBUSTNESS

This section discusses the robustness of the baseline findings to a battery of sensitivity checks. First, I assess whether alternative specifications of the model produce different results. For every alternative specification, I plot - in the following order - the estimated trends and cycles of HICP inflation and GDP, the complete estimated historical decomposition of the point-wise median of both trends (inflation trend and potential GDP), the estimated historical decomposition of median trend inflation during 2012-2015 and 2019-2022, the complete estimated historical decomposition of the point-wise median of both cycles (inflation and output-gap), the historical variance decomposition at short and long horizon, and the correlation between inflation and output-gap when data are purged from supply and demand shocks. The figures of this section are presented in section D of the Appendix.

The baseline model is changed along the priors on the trend components, given that these are the more controversial ones. I choose less conservative priors in terms of mode and degrees of freedom. To be more specific, I now choose that the priors governing the stochastic volatility of trends are 10 times larger. This implies that, in relative terms with respect to the cycle part (permanent/transitory), the current mean values exhibit ratios of 1.2 for GDP trends, 0.3 for inflation trends, and 0.12 for energy trends. This means that for the baseline case, prior means for the permanent part are, for example, 12 times smaller for the potential GDP than output-gap. With respect to the degrees of freedom, I change them to 50, 25 and 15. This implies that priors are more loose, potentially capturing more business cycle fluctuations.

From Figure D 25 to Figure D 48, it can be seen that changing the priors on the trend components is largely inconsequential for the main findings related to inflation. However, it can be seen that as priors get loosen the reduced-form dynamics in potential GDP become closer to the ones depicted in Figure 14 - where stochastic volatility is not modeled. This points to acknowledging that the tight priors on the trends components should not be seen as simple priors if not as identification devices, at least for modeling potential GDP and output-gap.

Second, I check the sensitivity of the main findings to a extension of the baseline sample from 1970Q1, given that one could argue that one potential concern with the empirical analysis could be that the sample used is driving the main conclusions of this paper. For instance, the estimated latent components (trends and cycles) could be affected by the fact that the baseline sample does not include the pre-Great Moderation period. Figure D 49 to 54 show the results. The main findings are robust to this alternative sample specification.

6. CONCLUSIONS

Since the COVID economic reopening, Euro area inflation has reached a 40-year high. Due to this recent concern, this paper poses two main questions: 1) What are the channels driving inflation? 2) What is the nature (permanent or transitory) of shocks? To do so, this paper proposes a model that diagnoses the structural channels of shocks, discerning whether these shocks have permanent or transitory

effects on variables. Moreover, it is specifically designed to accommodate extreme observations, such as COVID-19 outliers. The shocks at play are global and domestic shocks from a supply-demand side and energy supply shocks, identified by sign-restrictions.

This paper shows evidence in favor of the hypothesis of ‘de-anchoring of inflation expectations’ from below 2% level in 2012-2017 and from above 2% level after the ‘COVID economic reopening’. Trend inflation started to fall below 2% during the European Sovereign Debt Crisis mostly due to (permanent) demand factors (both global and domestic). Along the recent period, trend inflation has risen above the 2% level, around 3 to 4% in 2022Q2, characterized by a combination of global and domestic shocks from a supply side. These permanent supply factors, identified by the model, could perfectly resemble the recent persistent supply chain bottlenecks of non-energy industrial goods. The fact that trend inflation is above 2%, suggest that EA inflation is expected to be persistently higher than ECB’s target in the medium-term. Finally, current inflation is mainly driven by transitory factors, around 85%, such excess demand and energy supply shocks.

While this paper offers a benchmark, jointly disentangling permanent and transitory shocks, I acknowledge that this is done at the cost of imposing an “independent trend/cycle decomposition”. Hence, more work needs to be done on the econometric framework of model decomposition and shock identification. In fact, allowing for the transmission of transitory shocks to the permanent side, seems a fruitful area for future research. For example, allowing a transitory shock to become more persistent or even permanent, if it triggers specific mechanisms in the model that allow to create persistent sources of economic disruption. Moreover, it can help us to shed light in the controversial questions related to hysteresis effects, self-reinforcing expectations and path dependence that are resurfacing since the Great Financial Crisis.

A GIBBS SAMPLER FOR A VAR WITH COMMON TRENDS FEATURING STOCHASTIC VOLATILITY

First, let me use the notation $z_{i:j}$ to denote the sequence $\{z_i, \dots, z_j\}$ for a generic variable z_t . The VAR with Common Trends and SV specified in equations 1 through 6 is estimated using a Gibbs sampler and Metropolis hasting, which involves the following blocks:

1. The first step requires to set up starting values, $\phi_{ij,t}^z, h_{i,t}^z$, to form the history of $\Sigma_{1:T}^\epsilon, \Sigma_{1:T}^u, y_{1:T}$. Draws from the joint distribution $\bar{y}_{0:T}, \tilde{y}_{-p+1:T}, \lambda \mid \text{vec}(\mathcal{A}), \Sigma_{1:T}^\epsilon, \Sigma_{1:T}^u, y_{1:T}, \text{vec}(\mathcal{V})$, are obtained, which is given by the product of the marginal posterior of $\lambda \mid \text{vec}(\mathcal{A}), \Sigma_{1:T}^\epsilon, \Sigma_{1:T}^u, y_{1:T}, \text{vec}(\mathcal{V})$ times the distribution of the initial observations $\bar{y}_{0:T}, \tilde{y}_{-p+1:T} \mid \lambda, \text{vec}(\mathcal{A}), \Sigma_{1:T}^\epsilon, \Sigma_{1:T}^u, y_{1:T}, \text{vec}(\mathcal{V})$. Where $\text{vec}(\mathcal{V}) = \text{vec}(D^u, D^\epsilon, G^u, G^\epsilon)$. The marginal posterior of $\lambda \mid \text{vec}(\mathcal{A}), \Sigma_{1:T}^\epsilon, \Sigma_{1:T}^u, y_{1:T}, \text{vec}(\mathcal{V})$ is given by:

$$p(\lambda \mid \text{vec}(\mathcal{A}), \Sigma_{1:T}^\epsilon, \Sigma_{1:T}^u, y_{1:T}, \text{vec}(\mathcal{V})) \propto \mathcal{L}(y_{1:T} \mid \lambda, \text{vec}(\mathcal{A}), \Sigma_{1:T}^\epsilon, \Sigma_{1:T}^u, \text{vec}(\mathcal{V})) p(\lambda)$$

where $\mathcal{L}(y_{1:T} \mid \lambda, \text{vec}(\mathcal{A}), \Sigma_{1:T}^\epsilon, \Sigma_{1:T}^u, \text{vec}(\mathcal{V}))$ is the likelihood obtained by using the Kalman Filter in the state-space model specified in equation (1). Since $p(\lambda \mid \text{vec}(\mathcal{A}), \Sigma_{1:T}^\epsilon, \Sigma_{1:T}^u, y_{1:T}, \text{vec}(\mathcal{V}))$ could feature an unknown form, this step involves a Metropolis-Hastings algorithm. Then, \bar{c} of the trend components is updated using the median unbiased estimator of [Stock and Watson \(1998\)](#), this step also involves a Metropolis-Hasting algorithm. Finally, in step 1, I use [Carter and Kohn \(1994\)](#) and [Durbin and Koopman \(2002\)](#)'s simulation smoother to obtain draws for the trend and cycle components $\bar{y}_{0:T}, \tilde{y}_{-p+1:T}$, for given λ, \bar{c} and $\text{vec}(\mathcal{A}), \Sigma_{1:T}^\epsilon, \Sigma_{1:T}^u, y_{1:T}, \text{vec}(\mathcal{V})$.

2. The second step is standard to the time-series literature because $\bar{y}_{0:T}, \tilde{y}_{-p+1:T}$ are given. Starting with the transitory component equation, the posterior distribution of $\text{vec}(\bar{\mathcal{A}})$ is given by

$$\begin{aligned} (\bar{\Sigma}^{\mathcal{A}})^{-1} &= (\underline{\Sigma}_0^{\mathcal{A}})^{-1} + \sum_{t=1}^T \left((\Sigma_t^u)^{-1} \otimes \tilde{x}_t \tilde{x}_t' \right), \\ \text{vec}(\bar{\mathcal{A}}) &= \bar{\Sigma}^{\mathcal{A}} \left\{ \text{vec} \left(\sum_{t=1}^T (\Sigma_t^u)^{-1} \tilde{y}_t \tilde{x}_t' \right) + (\underline{\Sigma}_0^{\mathcal{A}})^{-1} \text{vec}(\underline{\mathcal{A}}) \right\} I(\text{vec}(\underline{\mathcal{A}})), \end{aligned}$$

where $\tilde{x}_t = (\tilde{y}_1', \dots, \tilde{y}_T')'$.

3. To obtain the time-varying elements of $\Sigma_{1:T}^u$, $p(\Sigma_{1:T}^u \mid \tilde{y}_{1:T}, \bar{y}_{1:T}, \lambda, \bar{c}, \text{vec}(\mathcal{A}), \Sigma_{1:T}^\epsilon, y_{1:T}, \text{vec}(\mathcal{V}))$, I follow the algorithm described in [Primiceri \(2005\)](#) and [Benati and Mumtaz \(2007\)](#). (i) Compute the VAR residuals, $\hat{u}_t = \tilde{y}_t - \bar{\mathcal{A}}' \tilde{x}_t$. Draw the time-varying, $\phi_{ij,t}^u$, elements of Φ_t^u using the Carter and Kohn algorithm (conditional on $\bar{\mathcal{A}}, H_t^u, D_{1:n}^u$). Then the state space formulation for $\phi_{ij,t}^u$ is derived from the

following relationship

$$\begin{pmatrix} 1 & 0 & \dots & 0 \\ \phi_{21,t}^u & 1 & \ddots & \vdots \\ \vdots & \ddots & \ddots & 0 \\ \phi_{k1,t}^u & \dots & \phi_{kk-1,t}^u & 1 \end{pmatrix} \begin{pmatrix} u_{1,t} \\ u_{2,t} \\ \vdots \\ u_{k,t} \end{pmatrix} = \begin{pmatrix} o_{1,t} \\ o_{2,t} \\ \vdots \\ o_{k,t} \end{pmatrix},$$

where, $\text{VAR}(o_t) = H_t^u$. The state space formulation for $\phi_{21,t}^u$ is

$$\begin{aligned} u_{2,t}^u &= -a_{21,t}^u u_{1,t} + o_{2,t}, \quad \text{VAR}(o_{2,t}) = h_{2,t}^u \\ a_{21,t}^u &= a_{21,t-1}^u + V_{1t}, \quad \text{VAR}(V_{1t}) = D_1^u. \end{aligned}$$

The state space formulation for $a_{31,t}^u$ and $a_{32,t}^u$ is

$$\begin{aligned} u_{3,t} &= -a_{31,t}^u u_{1,t} - a_{32,t}^u u_{2,t} + o_{3,t}, \quad \text{VAR}(o_{3,t}) = h_{3,t}^u \\ \begin{pmatrix} a_{31,t}^u \\ a_{32,t}^u \end{pmatrix} &= \begin{pmatrix} a_{31,t-1}^u \\ a_{32,t-1}^u \end{pmatrix} + \begin{pmatrix} V_{2t} \\ V_{3t} \end{pmatrix}, \quad \text{VAR} \begin{pmatrix} V_{2t} \\ V_{3t} \end{pmatrix} = D_2^u. \end{aligned}$$

The same procedure is applied to obtain the rest of the state space formulations. (ii) Conditional on a draw for $(a_{21,t}), (a_{31,t}$ and $a_{32,t}), \dots, (a_{81,t}, \dots,$ and $a_{87,t})$ calculate the residuals $(V_{1,t}^u, V_{2,t}^u, \dots, V_{8,t}^u)$. Draw each of D_i^u from the inverse Wishart distribution with scale matrix $V_{i,t}' V_{i,t} + (\kappa + i + 1) D_{i,0}^u$ and degrees of freedom $T + \kappa$, where $i = 1, \dots, (n-1)$. (iii) Using the draw of Φ_t^u calculate $o_t = \Phi_t^u u_t$. Notice that, o_t are contemporaneously uncorrelated then drawing $h_{i,t}^u$ can be done separately by simply applying the independence Metropolis-Hastings algorithm conditional on a draw for g_i^u . This is done using the univariate algorithm by [Jacquier et al. \(2004\)](#). Conditional on a draw for $h_{i,t}^u$ draw g_i^u (i.e., each diagonal element of G^u) from inverse Gamma distribution with scale parameter

$$\frac{(\ln h_{i,t}^u - \ln h_{i,t-1}^u)' (\ln h_{i,t}^u - \ln h_{i,t-1}^u) + g_{i,0}^u}{2}$$

and degrees of freedom $\frac{T+v_0}{2}$.

4. To obtain the time-varying elements of $\Sigma_{1:T}^\epsilon$, $p(\Sigma_{1:T}^\epsilon \mid \bar{y}_{1:T}, \tilde{y}_{1:T}, \lambda, \bar{c}, \text{vec}(\mathcal{A}), \Sigma_{1:T}^u, y_{1:T}, \text{vec}(\mathcal{V}))$, of the trend component equation, where the coefficients (\bar{c}) and latent trends (\tilde{y}_t) are known. Now the number of variables is q instead of n . Compute the residuals, $\hat{\epsilon}_t = \bar{y}_t - c - \tilde{y}_{t-1}$. Repeat sub-steps (i)-(iii) to obtain the time-varying elements of $\Sigma_{1:T}^\epsilon$. Repeat steps 1 and 4 M times. The last L draws provide an approximation to the marginal posterior distributions of the model parameters.

Identification procedure. The identification procedure described in subsection 3.C is performed using the algorithm of [Rubio-Ramirez et al. \(2010\)](#), which consists of the following steps, for each given draw from the posterior of the reduced-form parameters (permanent side):

Step one. Draw a $q \times q$ matrix W from $N(0_n, I_q)$ and perform a QR decomposition of W , with the diagonal of R normalized to be positive and $Q^\epsilon Q^{\epsilon'} = I_q$.

Step two. Let S_t^ϵ be the lower triangular Cholesky decomposition of Σ_t^ϵ and define $B_t = S_t^\epsilon Q^{\epsilon'}$. Compute the candidate (permanent) responses are given by B_t . Check the set of permanent responses, if it satisfies all the sign restrictions, store them. If not, discard them and go back to the first step.

Step three. Repeat steps 1 and 2 until M impulse responses that satisfy the sign restrictions are obtained. The resulting set characterizes the set of structural VAR models that satisfy the sign restrictions.

The identification procedure for the transitory side is as follows:

Step one. Draw a $n \times n$ matrix W from $N(0_n, I_n)$ and perform a QR decomposition of W , with the diagonal of R normalized to be positive and $Q^u Q^{u'} = I_n$.

Step two. Let S_t^u be the lower triangular Cholesky decomposition of Σ_t^u and define $C_t^u = S_t^u Q^{u'}$. Compute the candidate impulse responses as $IRF_{j,t} = A_j C_t^u$, where A_j are the reduced form impulse responses from the Wold representation, for $j = 0, \dots, J$. If the set of impulse responses satisfies all the sign restrictions, store them. If not, discard them and go back to the first step.

Step three. Repeat steps 1 and 2 until M impulse responses that satisfy the sign restrictions are obtained. The resulting set characterizes the set of structural VAR models that satisfy the sign restrictions.

B CONVERGENCE OF THE MARKOV CHAIN MONTE CARLO ALGORITHM

This appendix assesses convergence of the Markov chain Monte Carlo algorithm in the baseline application to the Euro area data. Following [Primiceri \(2005\)](#), I assess the convergence of the Markov chain by inspecting the autocorrelation properties of the ergodic distribution's draws. In order to judge how well the chain mixes, common practice is to look at the draws' inefficiency factors (IF) for the posterior estimates of the parameters. Specifically, that is the inverse of the relative numerical efficiency measure of [Geweke et al. \(1991\)](#), i.e., the IF is an estimate of $(1 + 2\sum_{i=1}^{\infty} \rho_i)$, where ρ_i is the i -th autocorrelation of the chain. In this application the estimate is performed using a Parzen window.⁴⁴ Figure 11 plots a complete description of the characteristics of the chain is provided for the different sets of parameters. $D^\epsilon, D^u, G^\epsilon, G^u$: elements of the covariance matrix of the model's innovations; $H_{\epsilon,t}, H_{u,t}$: time varying volatilities from the permanent and transitory side; $\Phi_{\epsilon,t}, \Phi_{u,t}$: time varying simultaneous relations; \mathcal{A} : time-invariant coefficients. As stressed by, [Primiceri \(2005\)](#) values of the IFs below or around twenty are regarded as satisfactory. Again, except for a few cases (i.e., elements in $H_{\epsilon,t}$), the IFs are below 20.

⁴⁴For inefficiency factors, see Section 6.1 of [Giordani et al. \(2011\)](#).

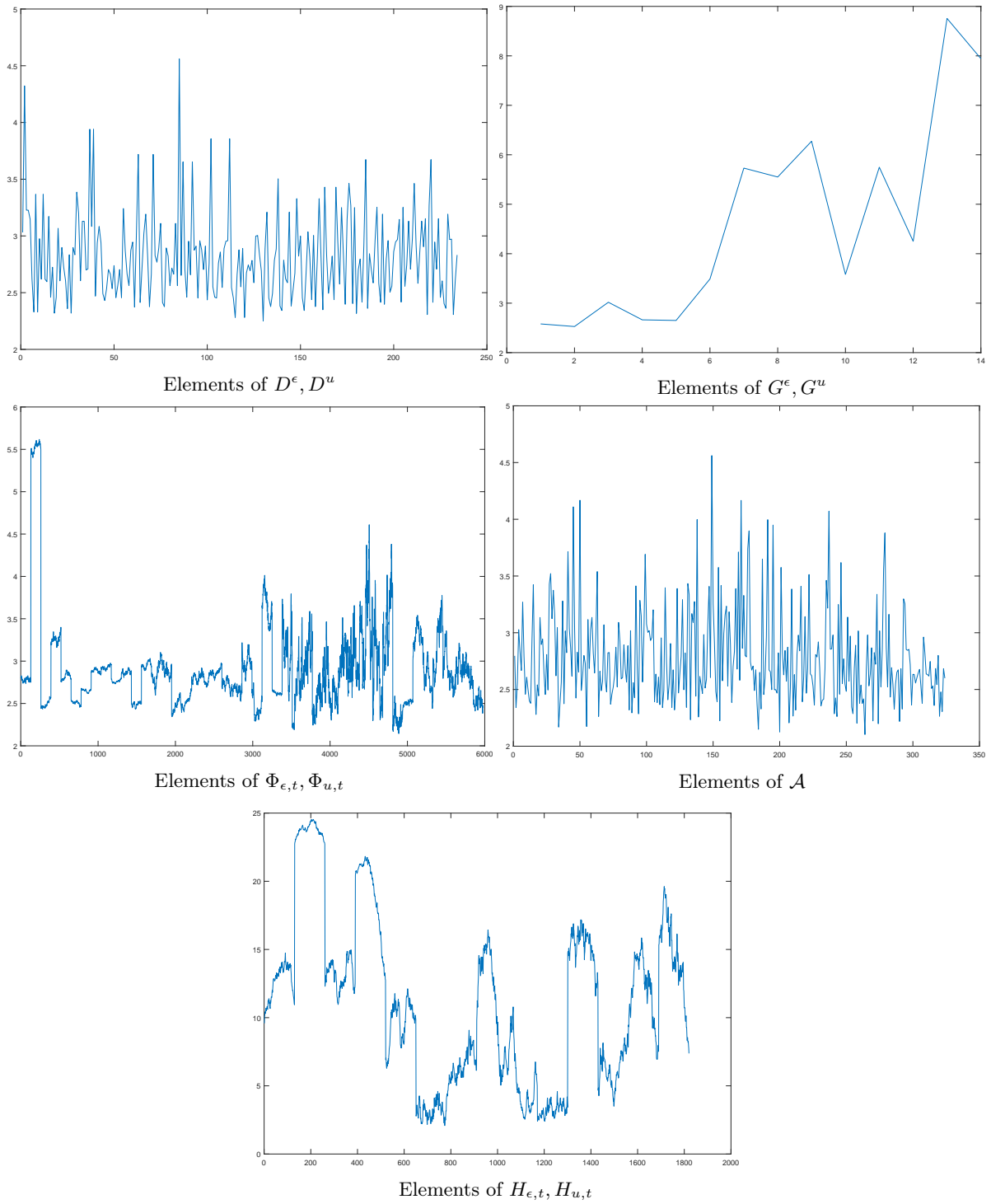


Figure 11. Summary of the distribution of the Inefficiency Factors for different sets of parameters

C FIGURES

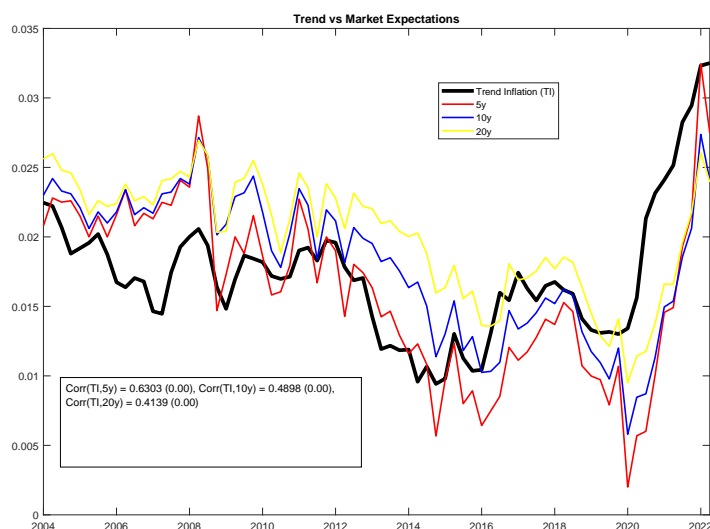


Figure 12. Market inflation swaps: 5, 10 and 20 year and median trend inflation

Note: Source of inflation swaps: Refinitiv. Table in the graph shows the correlation between each market inflation swap and the median trend inflation. In parenthesis, it is shown the p-value significance of each correlation.

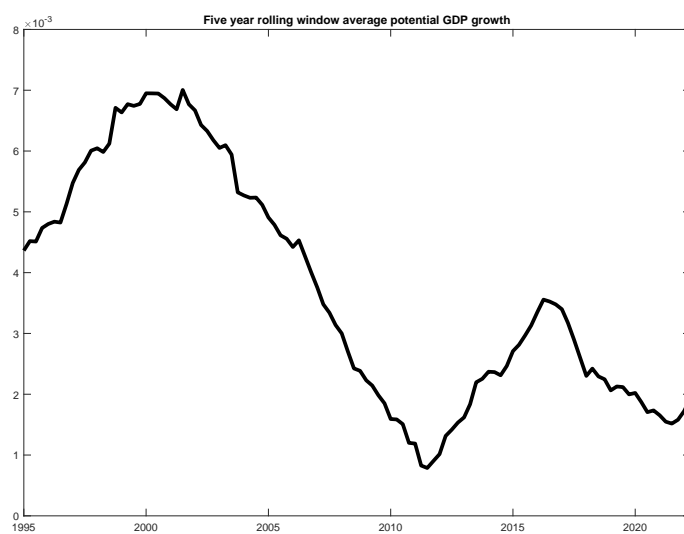


Figure 13. Average quarterly growth rate over five-year rolling windows

Note: Average quarterly growth rate of EA Potential GDP Point-wise median over five-year rolling windows.

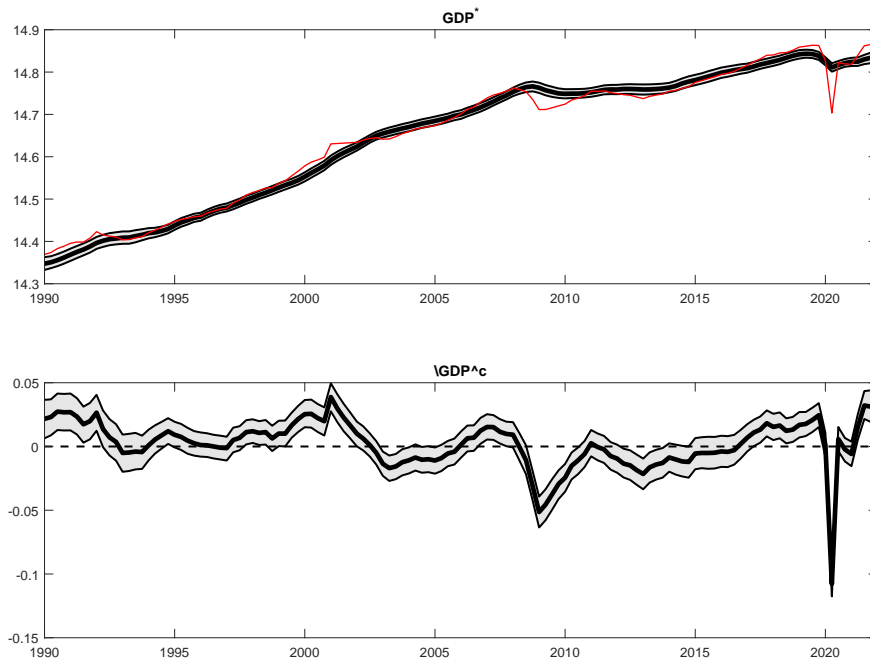


Figure 14. Actual data and estimated trends and cycles of real GDP in a model without Stochastic Volatility

Note: Point-wise median (solid black line) with 68% credible bands. Real GDP is defined in log terms. The model is estimated using the same priors but without the feature of Stochastic Volatility in both the permanent and transitory sides.

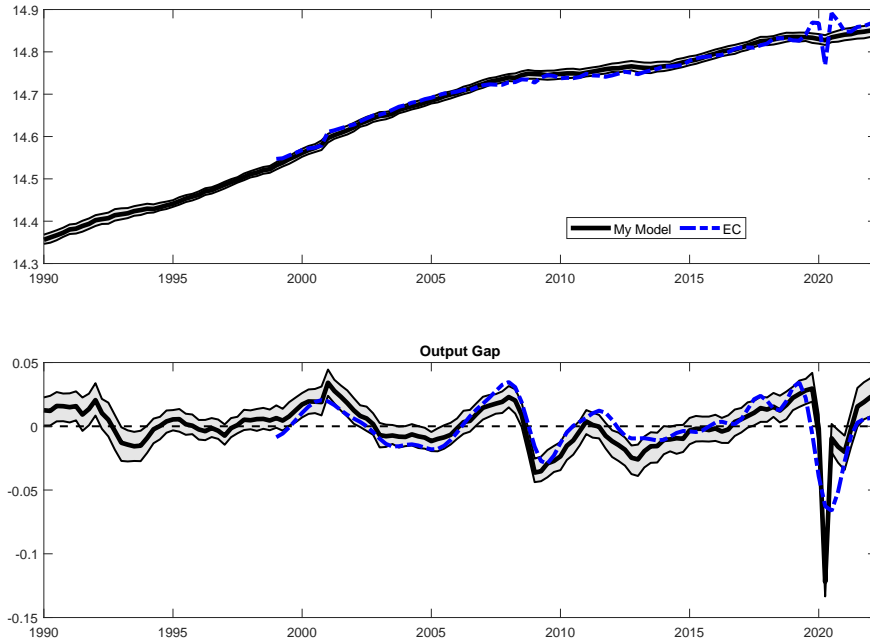


Figure 15. EA Potential GDP and Output-gap from the European Commission compared to the estimated trends and cycles of real GDP in the baseline model.

Note: The dash-dotted blue line represents the official estimates of EA Potential GDP and Output-gap from the European Commission. The model estimates of EA Potential GDP and Output-gap are represented by the point-wise median (solid black line) with 68% credible bands.

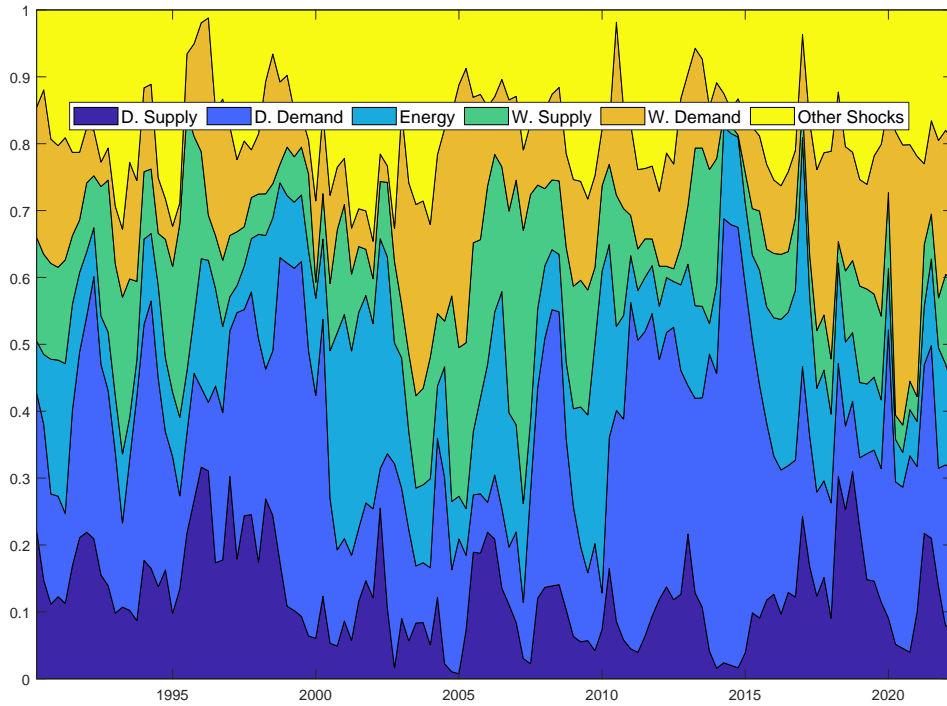


Figure 16. Estimated variance decomposition for the historical decomposition of inflation-gap (point-wise median) from 1990Q2 to 2022Q2. Short term horizon of 1 year

Note: The colored areas represent the share of the variance decomposition of each structural shock - domestic (demand and supply-side), global (demand and supply-side) and energy supply. The variance decomposition is computed over a one year rolling window, allowing the researcher to represent the explained share of each structural shock over a short horizon. The shorter the horizon the more variability there would be in the variance decomposition for the historical decomposition.

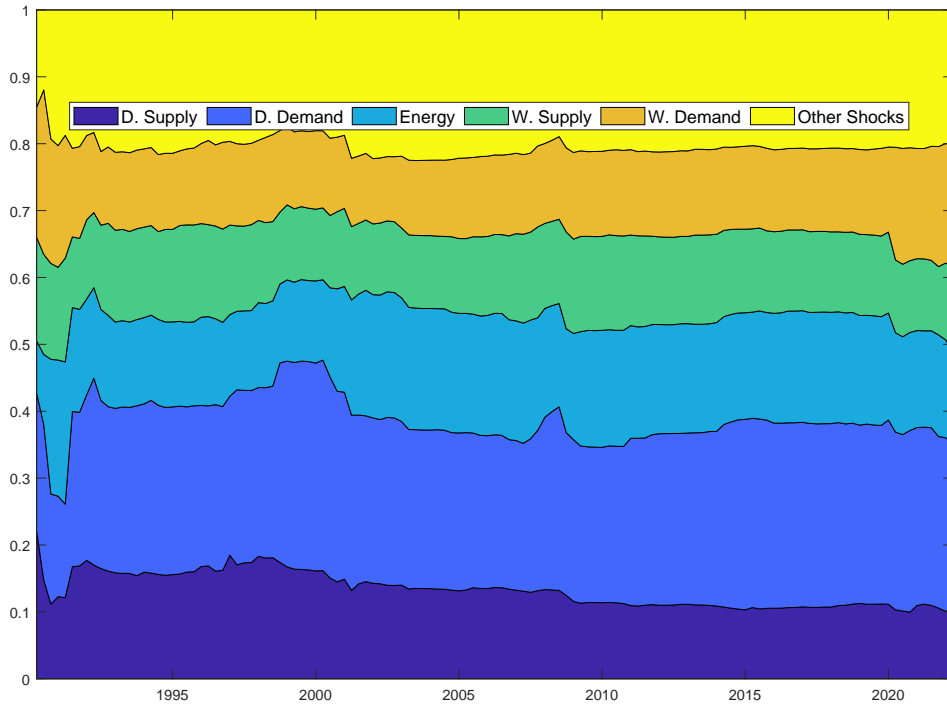


Figure 17. Estimated variance decomposition for the historical decomposition of inflation-gap (point-wise median) from 1990Q2 to 2022Q2. Long term horizon

Note: The colored areas represent the share of the variance decomposition of each structural shock - domestic (demand and supply-side), global (demand and supply-side) and energy supply. The variance decomposition is computed over a long horizon accumulating the shocks over the entire sample. This allows the researcher to represent the asymptotic explained share of each structural shock. The longer the horizon the less variability there would be in the variance decomposition for the historical decomposition.

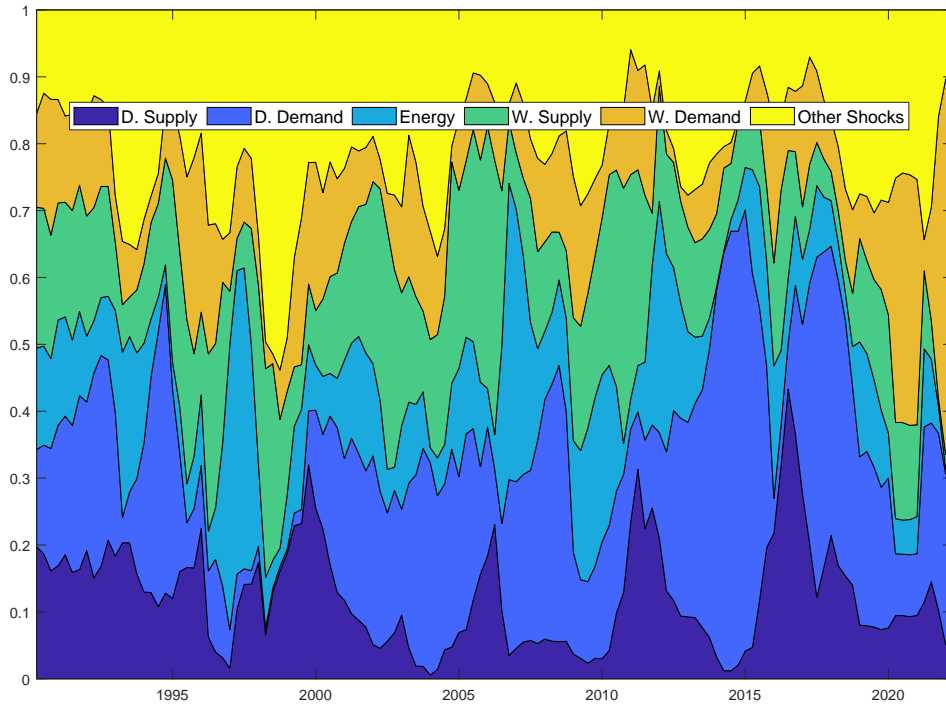


Figure 18. Estimated variance decomposition for the historical decomposition of output-gap (point-wise median) from 1990Q2 to 2022Q2. Short term horizon of 1 year

Note: The colored areas represent the share of the variance decomposition of each structural shock - domestic (demand and supply-side), global (demand and supply-side) and energy supply. The variance decomposition is computed over a one year rolling window, allowing the researcher to represent the explained share of each structural shock over a short horizon. The shorter the horizon the more variability there would be in the variance decomposition for the historical decomposition.

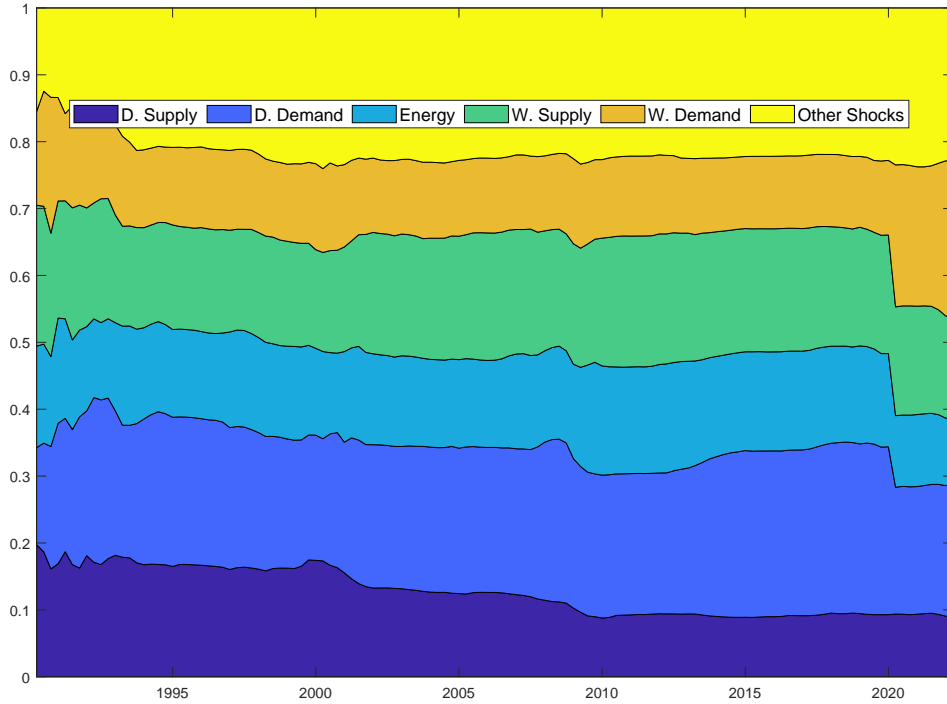


Figure 19. Estimated variance decomposition for the historical decomposition of inflation-gap (point-wise median) from 1990Q2 to 2022Q2. Long term horizon

Note: The colored areas represent the share of the variance decomposition of each structural shock - domestic (demand and supply-side), global (demand and supply-side) and energy supply. The variance decomposition is computed over a long horizon accumulating the shocks over the entire sample. This allows the researcher to represent the asymptotic explained share of each structural shock. The longer the horizon the less variability there would be in the variance decomposition for the historical decomposition.

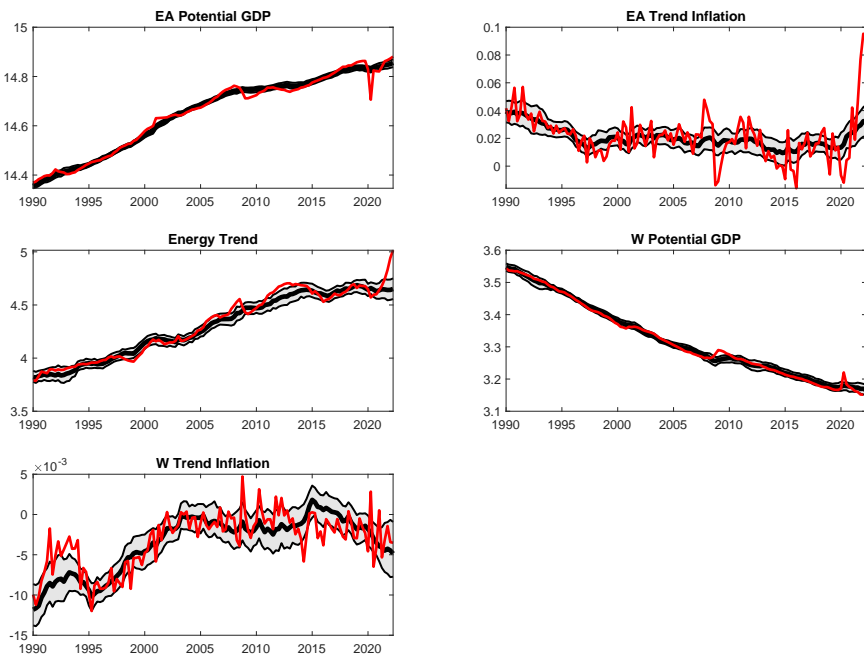


Figure 20. Actual data and estimated trends

Note: Point-wise median (solid black line) with 68% credible bands are based on 150000 draws. Variables are defined as in Table 1 and 2.

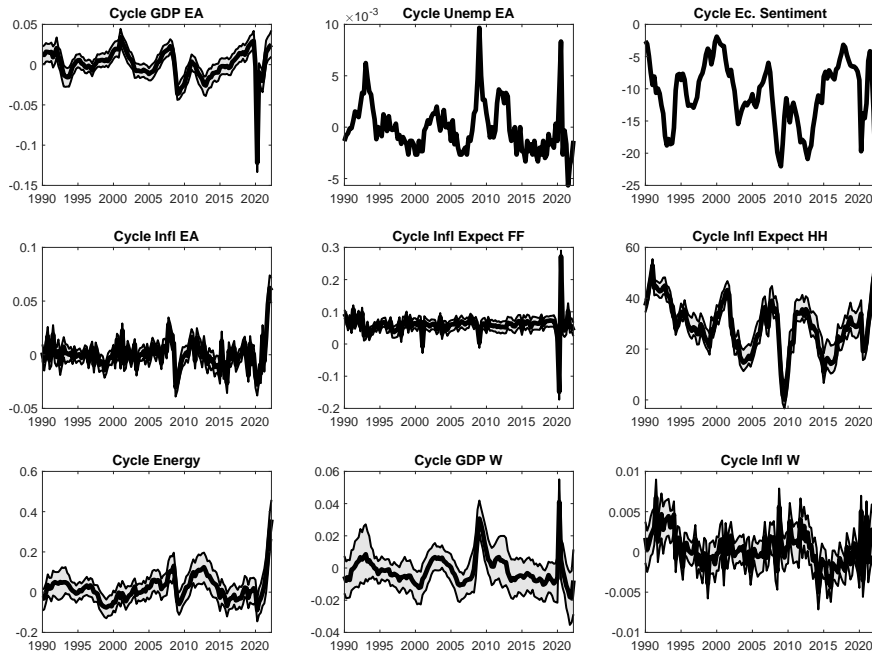


Figure 21. Actual data and estimated cycles

Note: Point-wise median (solid black line) with 68% credible bands are based on 150000 draws. Variables are defined as in Table 1 and 2.

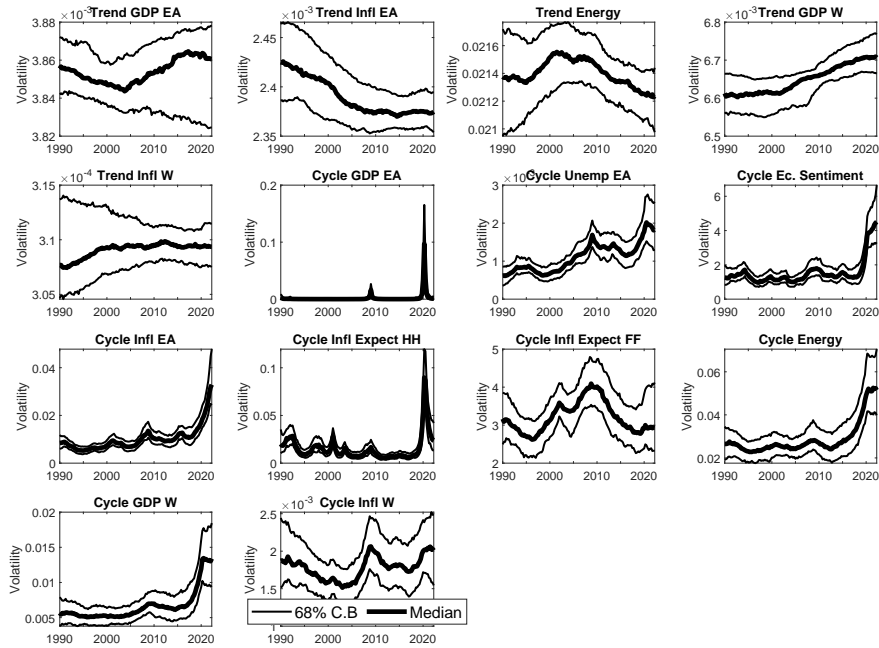


Figure 22. Stochastic volatility. The solid black lines are the posterior medians of the residual time-varying variances permanent (first five) and transitory (last nine), with 68% credible bands

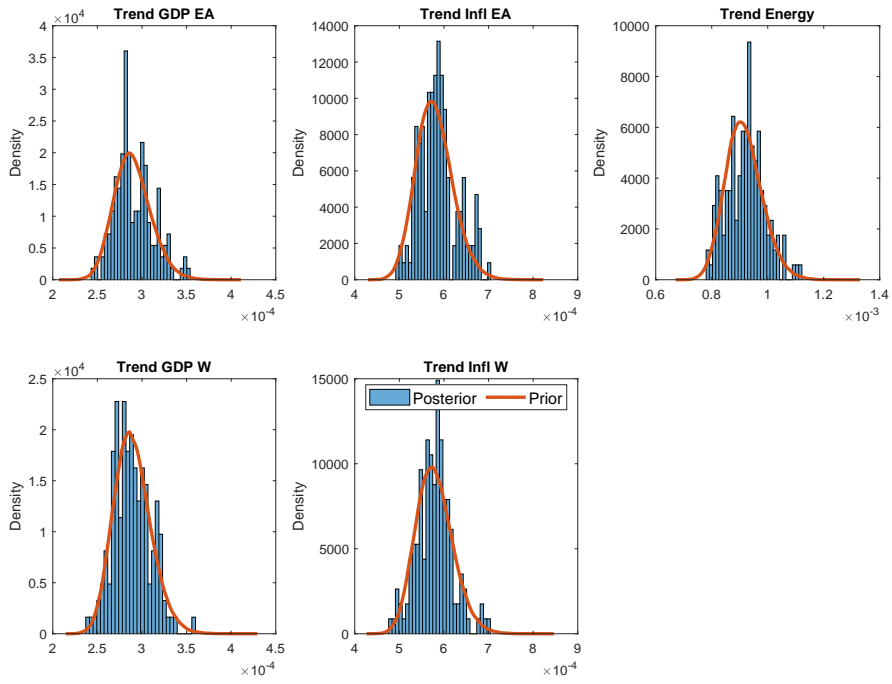


Figure 23. Prior and Posterior Densities of the Coefficients of G^ϵ

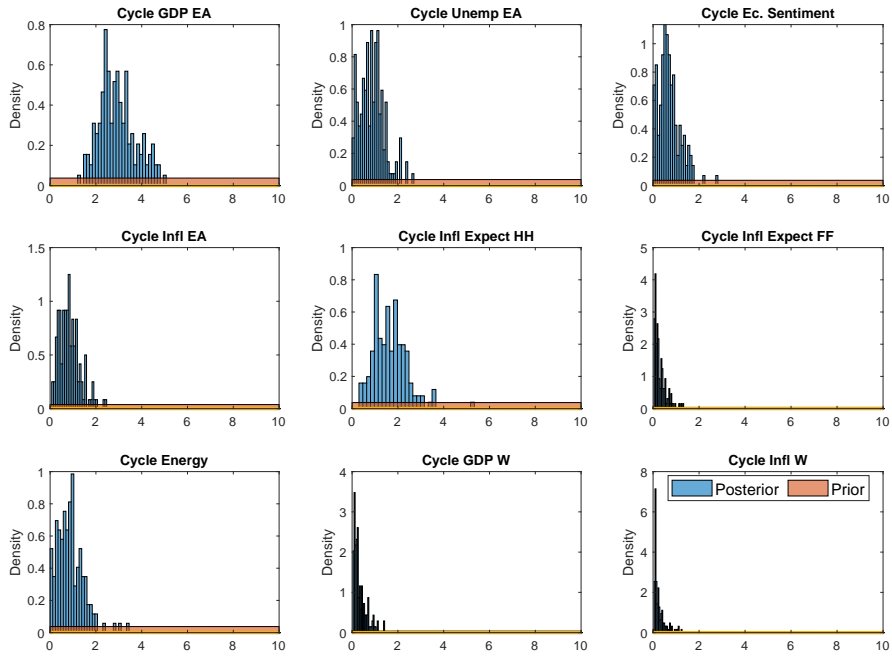


Figure 24. Prior and Posterior Densities of the Coefficients of G^u

D FIGURES ROBUSTNESS TESTS

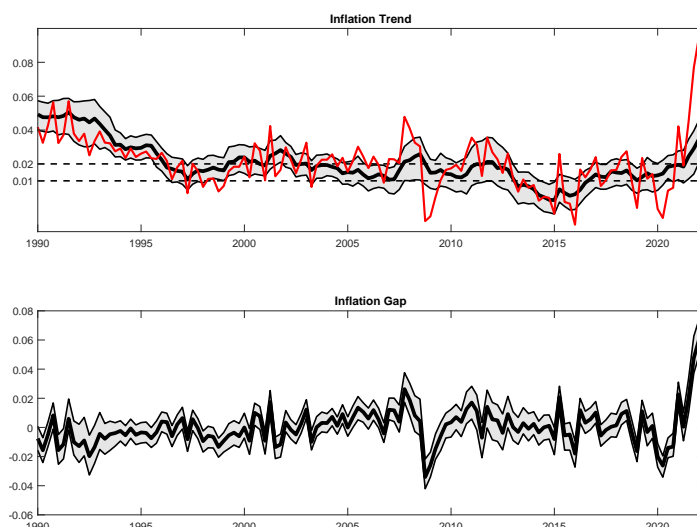


Figure 25. Actual data and estimated trends and cycles of HICP inflation

Note: Priors governing the stochastic volatility of trends are 10 times larger. This implies that the current prior mean values exhibit reductions/increases by factors of 1.2 for GDP trends, 0.3 for inflation trends, and 0.12 for energy trends with respect to the prior mean imposed on the stochastic volatilities of the cycle part. Degrees of freedom are kept at 100. Point-wise median (solid black line) with 68% credible bands. HICP is defined in annualized quarter-on-quarter terms.

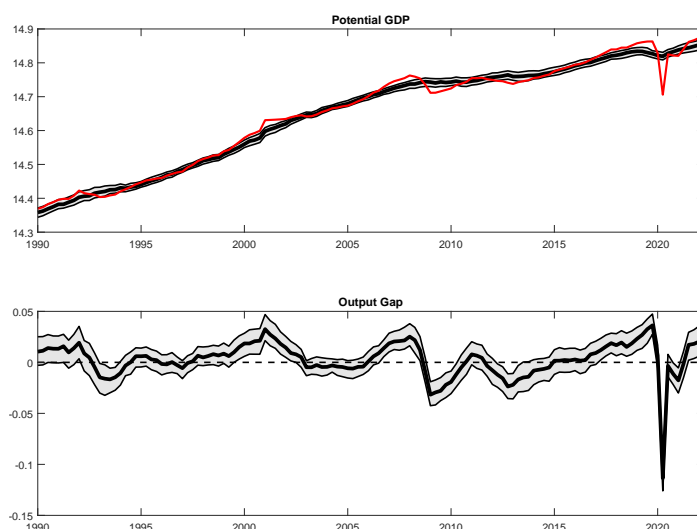


Figure 26. Actual data and estimated trends and cycles of real GDP

Note: Priors governing the stochastic volatility of trends are 10 times larger. This implies that the current prior mean values exhibit reductions/increases by factors of 1.2 for GDP trends, 0.3 for inflation trends, and 0.12 for energy trends with respect to the prior mean imposed on the stochastic volatilities of the cycle part. Degrees of freedom are kept at 100. Point-wise median (solid black line) with 68% credible bands. Real GDP is defined in log terms.

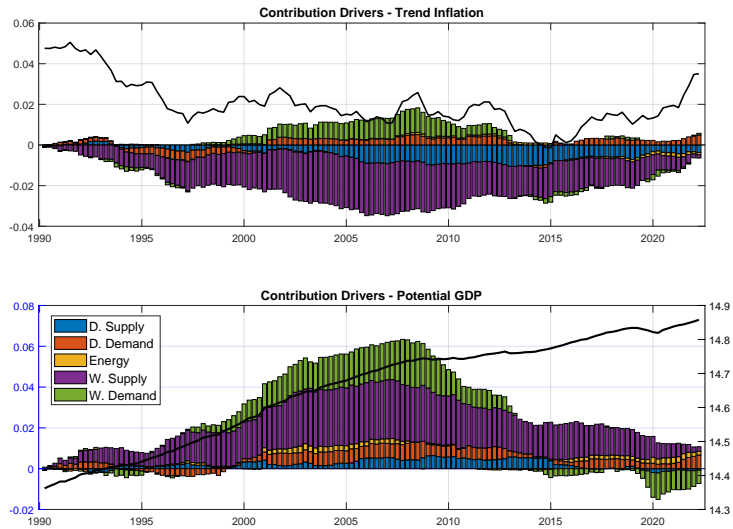


Figure 27. Estimated historical decomposition of the point-wise median of trend inflation (top) and potential GDP (bottom) from 1990.Q2 to 2022.Q2

Note: Priors governing the stochastic volatility of trends are 10 times larger. This implies that the current prior mean values exhibit reductions/increases by factors of 1.2 for GDP trends, 0.3 for inflation trends, and 0.12 for energy trends with respect to the prior mean imposed on the stochastic volatilities of the cycle part. Degrees of freedom are kept at 100. The black line is the point-wise median of trend inflation (top) and potential GDP (bottom). The colored bars represent the contribution of each structural shock - domestic (demand and supply-side), global (demand and supply-side) and energy supply - at time t .

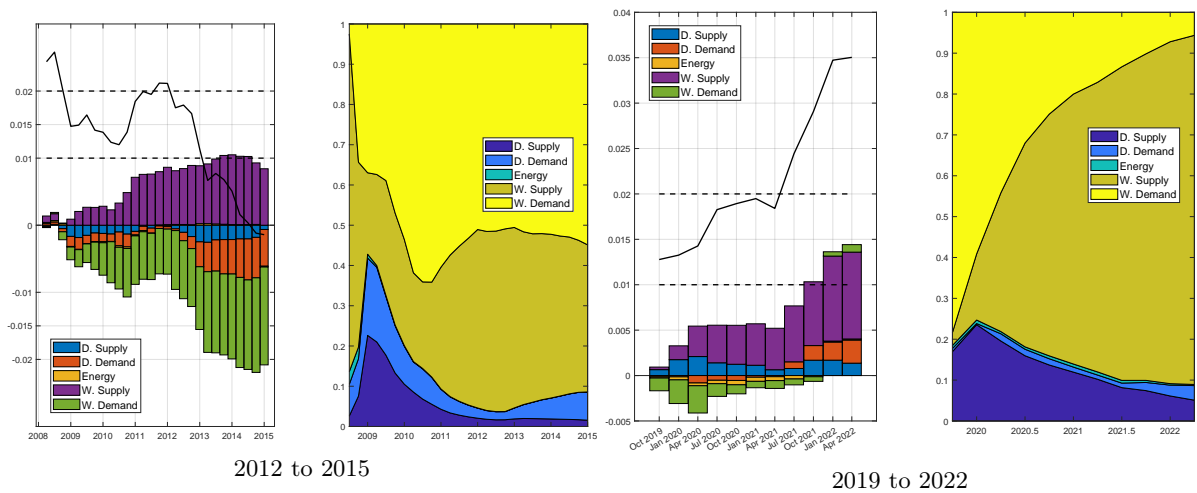


Figure 28. Estimated historical decomposition of median trend inflation

Note: Priors governing the stochastic volatility of trends are 10 times larger. This implies that the current prior mean values exhibit reductions/increases by factors of 1.2 for GDP trends, 0.3 for inflation trends, and 0.12 for energy trends with respect to the prior mean imposed on the stochastic volatilities of the cycle part. Degrees of freedom are kept at 100. The black line is the point-wise median of trend inflation. The colored bars (areas) represent the contribution (share of the variance decomposition) of each structural shock - domestic (demand and supply-side), global (demand and supply-side) and energy supply - at time t .

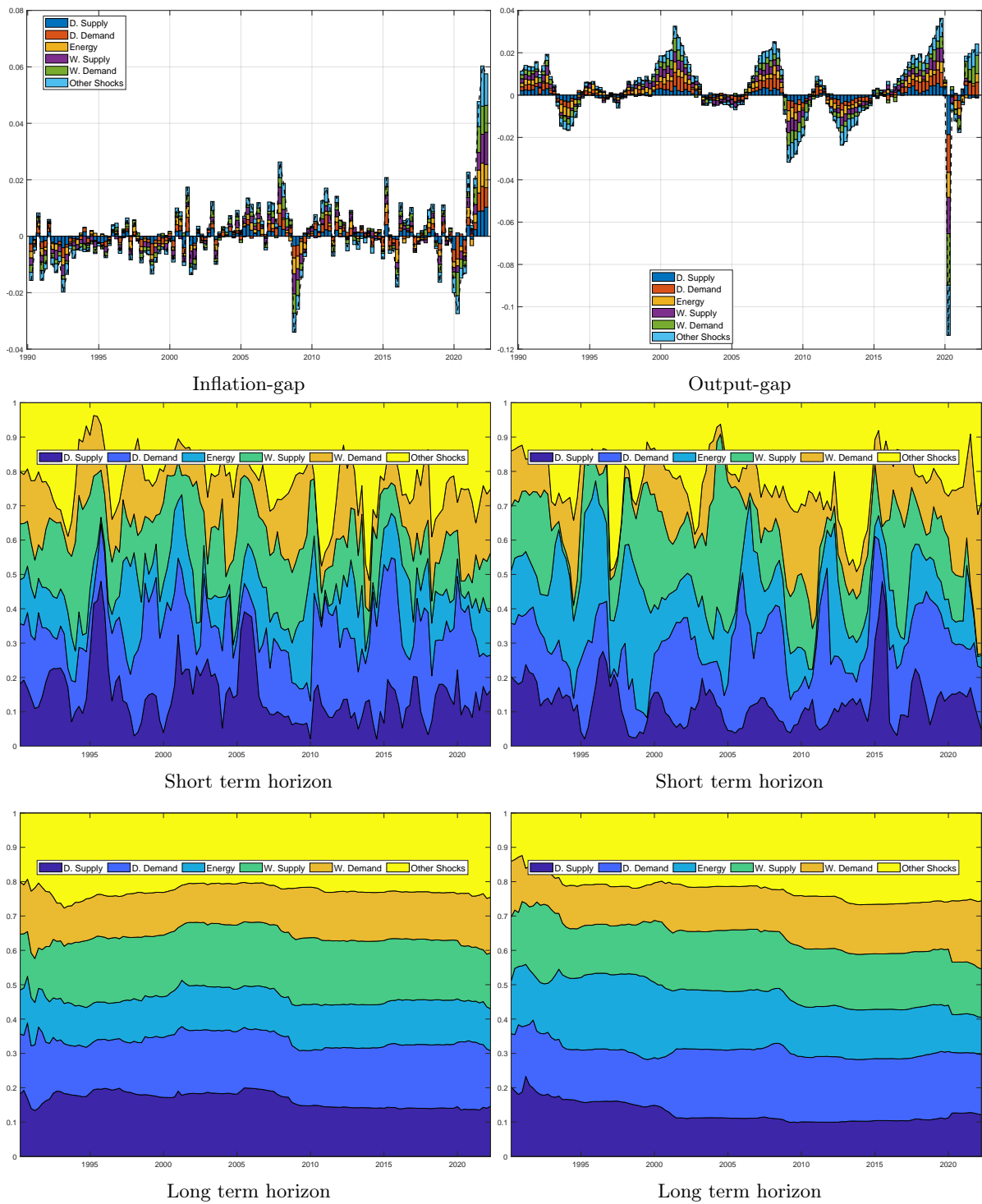


Figure 29. Estimated historical decomposition and variance decomposition

Note: Priors governing the stochastic volatility of trends are 10 times larger. This implies that the current prior mean values exhibit reductions/increases by factors of 1.2 for GDP trends, 0.3 for inflation trends, and 0.12 for energy trends with respect to the prior mean imposed on the stochastic volatilities of the cycle part. The black line is the point-wise median of inflation (left) and output-gap (right). The colored bars (areas) represent the contribution (share of the variance decomposition) of each structural shock - domestic (demand and supply-side), global (demand and supply-side) and energy supply.

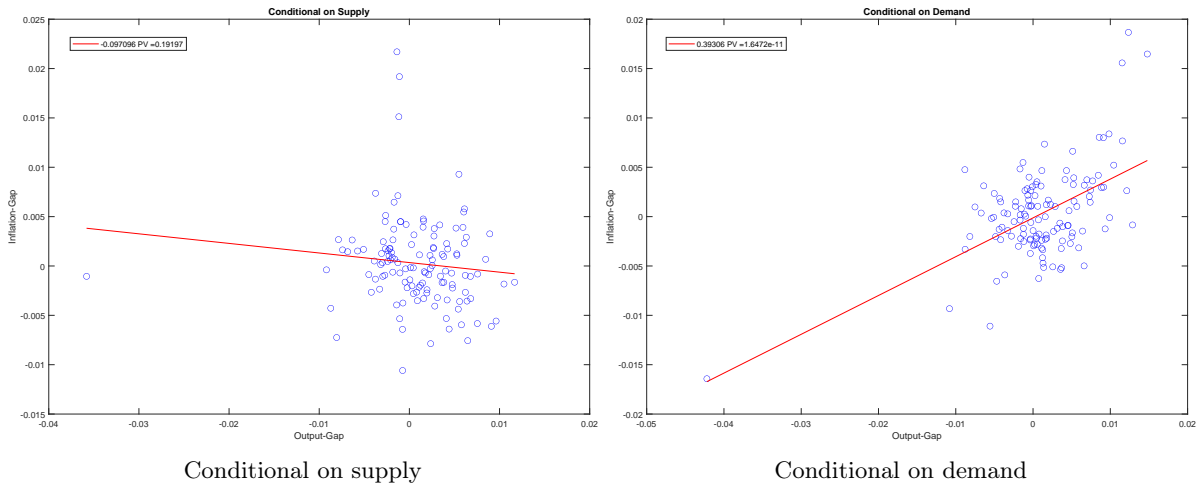


Figure 30. Purging supply-demand side shocks

Note: Priors governing the stochastic volatility of trends are 10 times larger. This implies that the current prior mean values exhibit reductions/increases by factors of 1.2 for GDP trends, 0.3 for inflation trends, and 0.12 for energy trends with respect to the prior mean imposed on the stochastic volatilities of the cycle part. Conditional data obtained from the estimated cycle model part. Supply shocks are calculated as the sum of domestic and global supply shocks. Demand shocks are calculated as the sum of domestic and global demand shocks. Corresponding supply (demand) slope estimate is -0.069 (0.33) with a P-value of 0.58 (0).

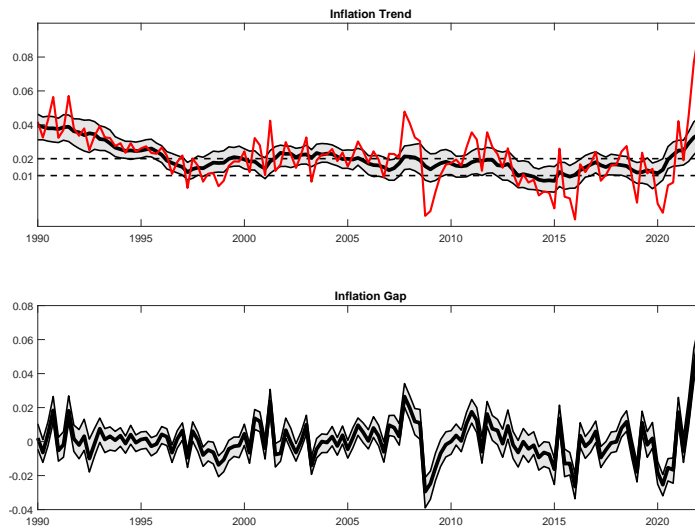


Figure 31. Actual data and estimated trends and cycles of HICP inflation

Note: Degrees of freedom equals to 50 for the priors governing the stochastic volatility of trends. Point-wise median (solid black line) with 68% credible bands. HICP is defined in annualized quarter-on-quarter terms.

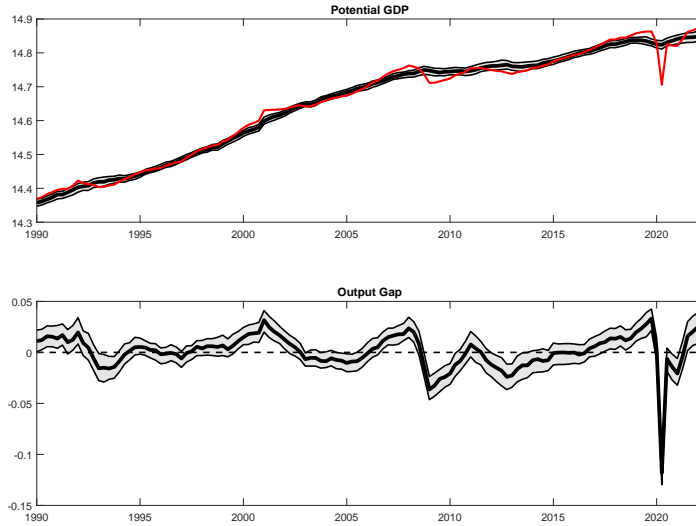


Figure 32. Actual data and estimated trends and cycles of real GDP

Note: Degrees of freedom equals to 50 for the priors governing the stochastic volatility of trends. Point-wise median (solid black line) with 68% credible bands. Real GDP is defined in log terms.

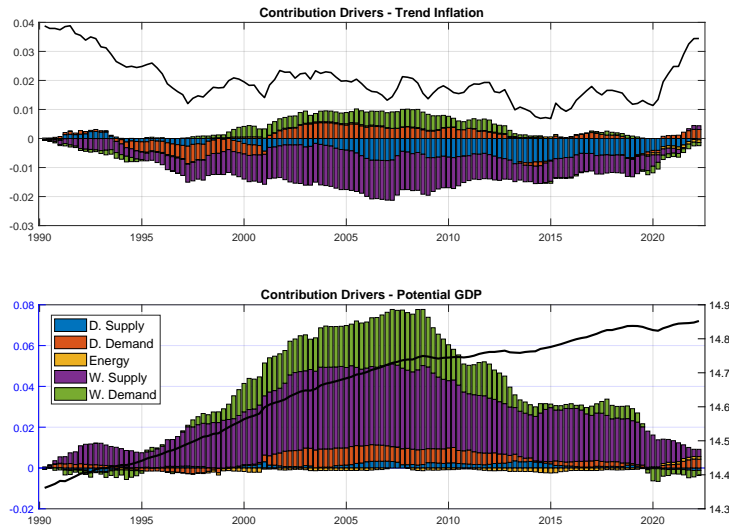


Figure 33. Estimated historical decomposition of the point-wise median of trend inflation (top) and potential GDP (bottom) from 1990.Q2 to 2022.Q2

Note: Degrees of freedom equals to 50 for the priors governing the stochastic volatility of trends. The black line is the point-wise median of trend inflation (top) and potential GDP (bottom). The colored bars represent the contribution of each structural shock - domestic (demand and supply-side), global (demand and supply-side) and energy supply - at time t .

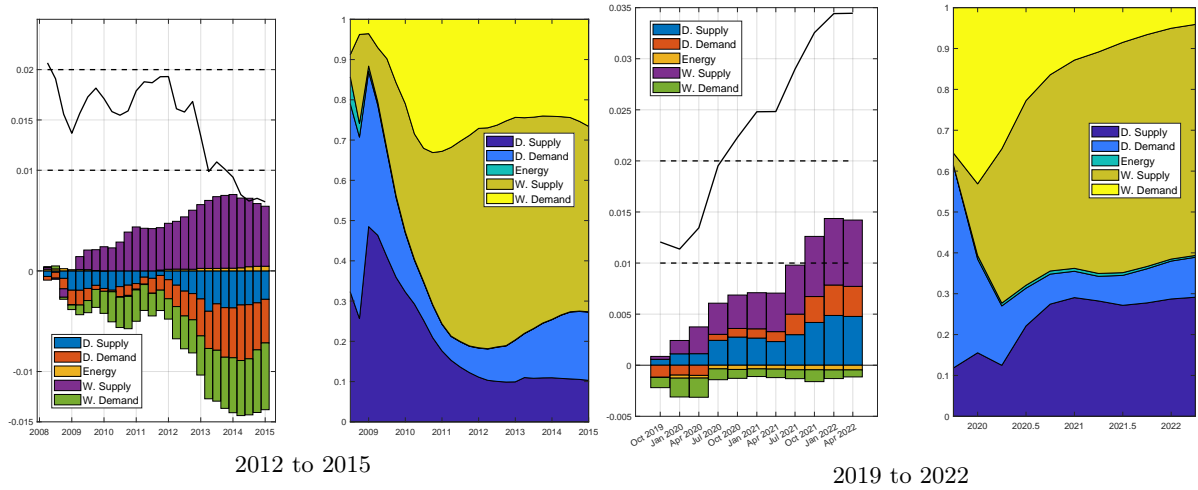


Figure 34. Estimated historical decomposition of median trend inflation

Note: Degrees of freedom equals to 50 for the priors governing the stochastic volatility of trends. The black line is the point-wise median of trend inflation. The colored bars (areas) represent the contribution (share of the variance decomposition) of each structural shock - domestic (demand and supply-side), global (demand and supply-side) and energy supply - at time t .

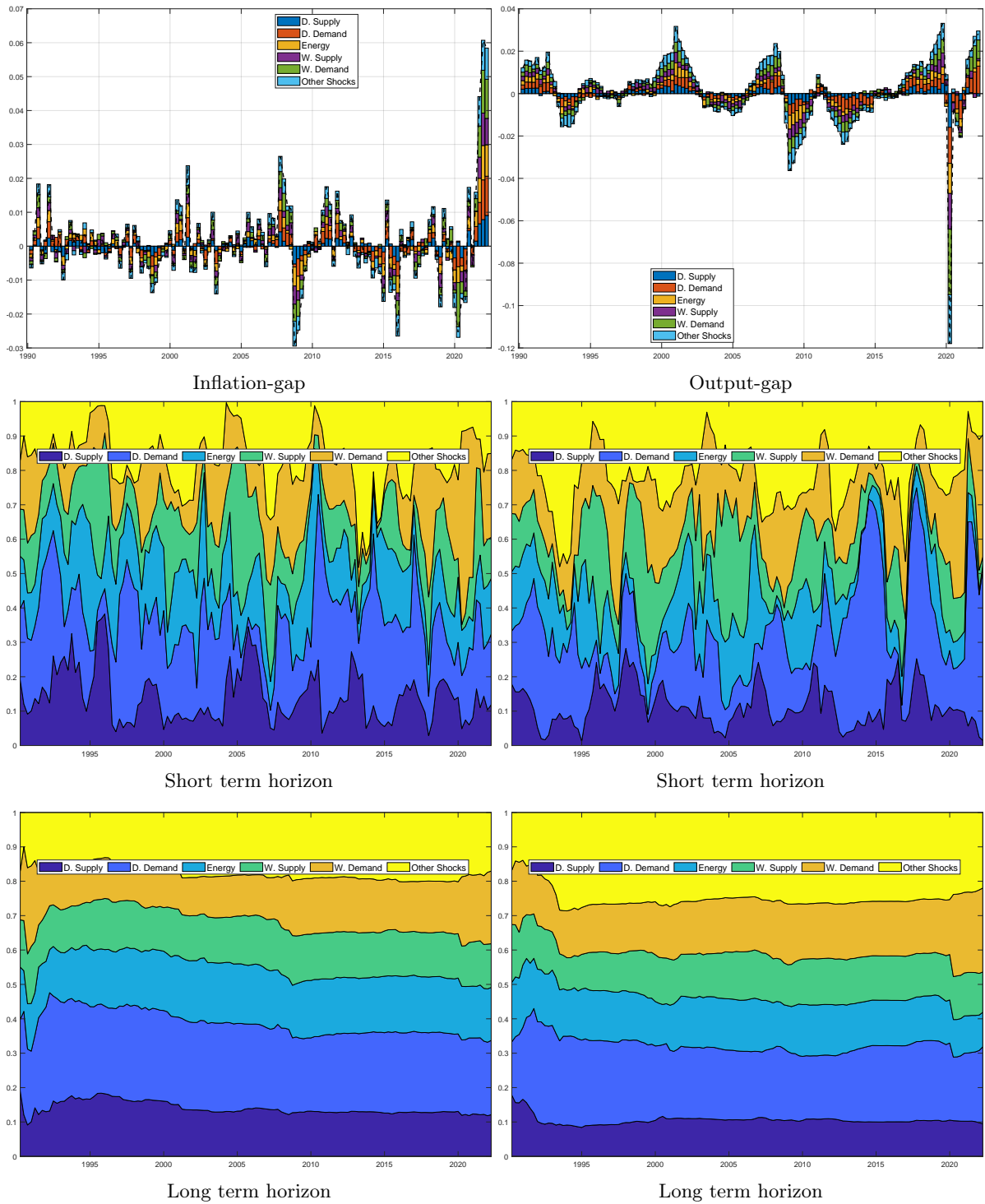


Figure 35. Estimated historical decomposition and variance decomposition

Note: Degrees of freedom equals to 50 for the priors governing the stochastic volatility of trends. The black line is the point-wise median of inflation (left) and output-gap (right). The colored bars (areas) represent the contribution (share of the variance decomposition) of each structural shock - domestic (demand and supply-side), global (demand and supply-side) and energy supply.

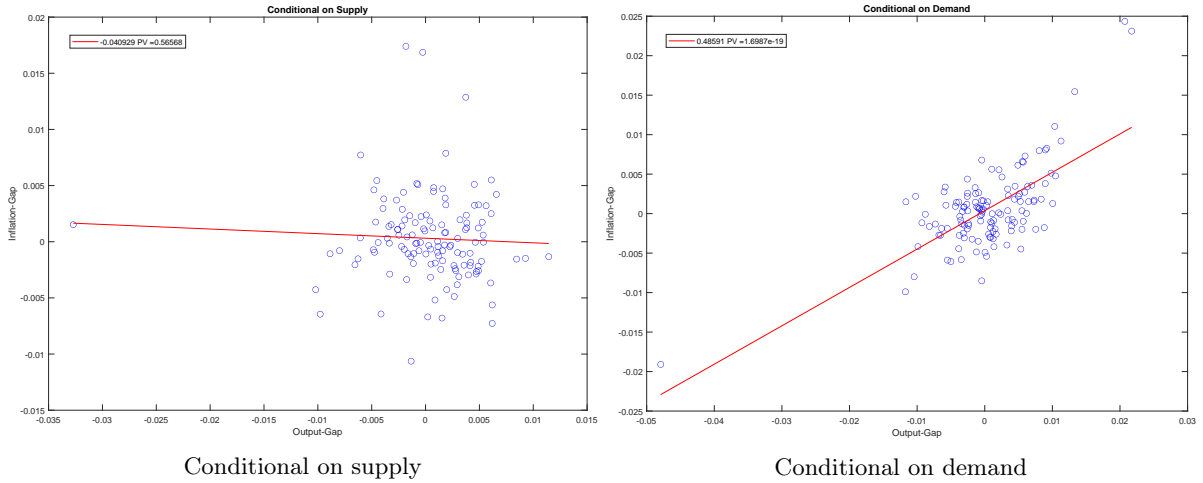


Figure 36. Purging supply-demand side shocks

Note: Degrees of freedom equals to 50 for the priors governing the stochastic volatility of trends. Conditional data obtained from the estimated cycle model part. Supply shocks are calculated as the sum of domestic and global supply shocks. Demand shocks are calculated as the sum of domestic and global demand shocks. Corresponding supply (demand) slope estimate is -0.0409 (0.4859) with a P-value of 0.56 (0).

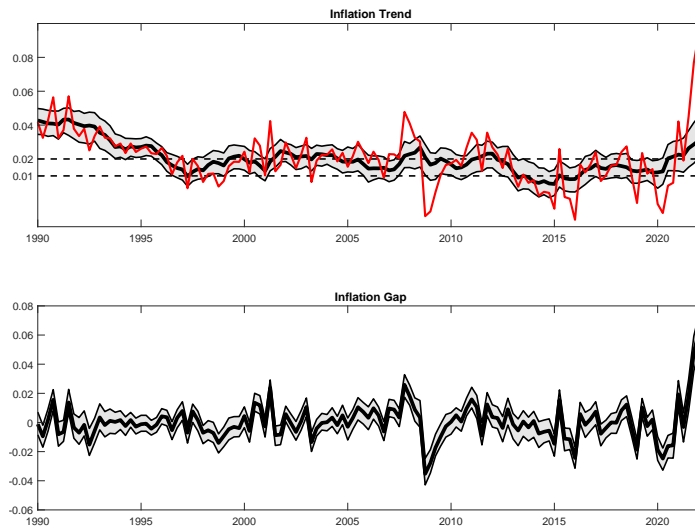


Figure 37. Actual data and estimated trends and cycles of HICP inflation

Note: Degrees of freedom equals to 25 for the priors governing the stochastic volatility of trends. Point-wise median (solid black line) with 68% credible bands. HICP is defined in annualized quarter-on-quarter terms.

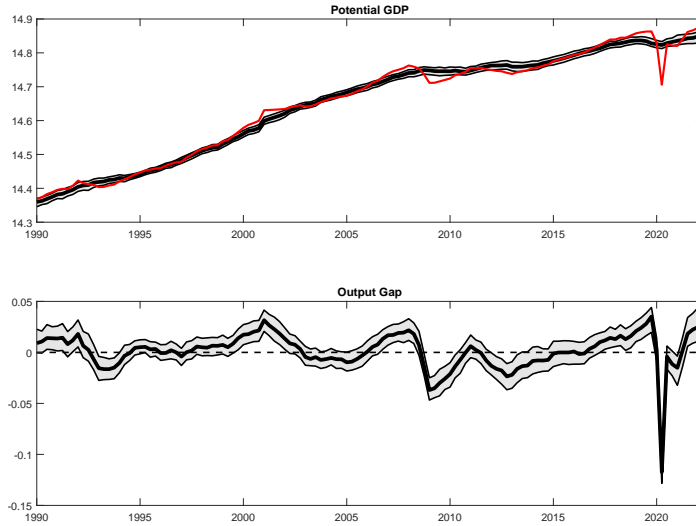


Figure 38. Actual data and estimated trends and cycles of real GDP

Note: Degrees of freedom equals to 25 for the priors governing the stochastic volatility of trends. Point-wise median (solid black line) with 68% credible bands. Real GDP is defined in log terms.

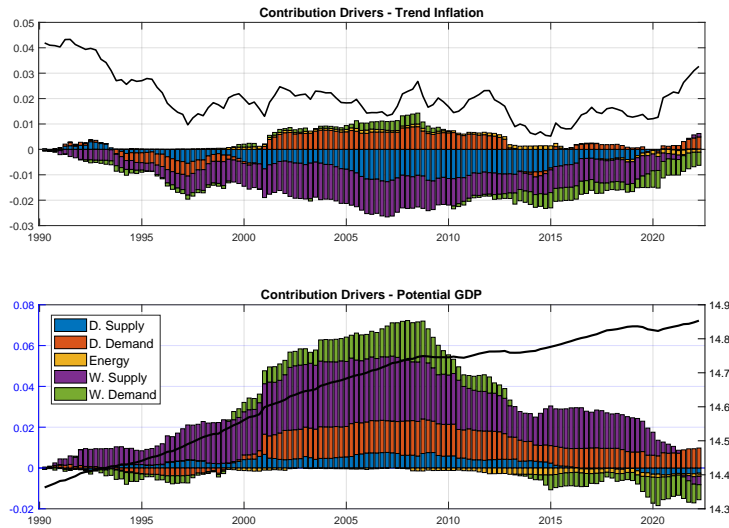


Figure 39. Estimated historical decomposition of the point-wise median of trend inflation (top) and potential GDP (bottom) from 1990.Q2 to 2022.Q2

Note: Degrees of freedom equals to 25 for the priors governing the stochastic volatility of trends. The black line is the point-wise median of trend inflation (top) and potential GDP (bottom). The colored bars represent the contribution of each structural shock - domestic (demand and supply-side), global (demand and supply-side) and energy supply - at time t .

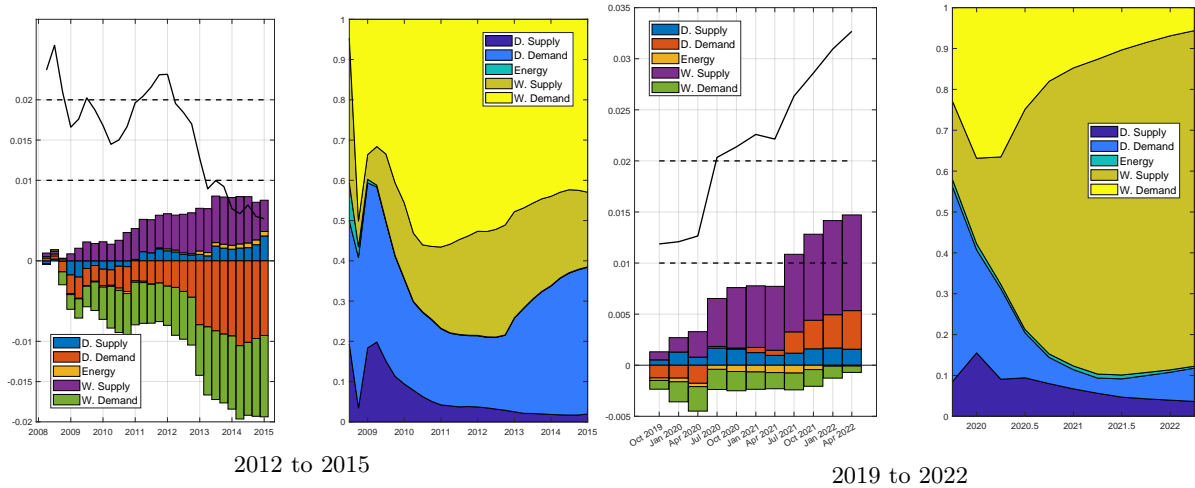


Figure 40. Estimated historical decomposition of median trend inflation

Note: Degrees of freedom equals to 25 for the priors governing the stochastic volatility of trends. The black line is the point-wise median of trend inflation. The colored bars (areas) represent the contribution (share of the variance decomposition) of each structural shock - domestic (demand and supply-side), global (demand and supply-side) and energy supply - at time t .

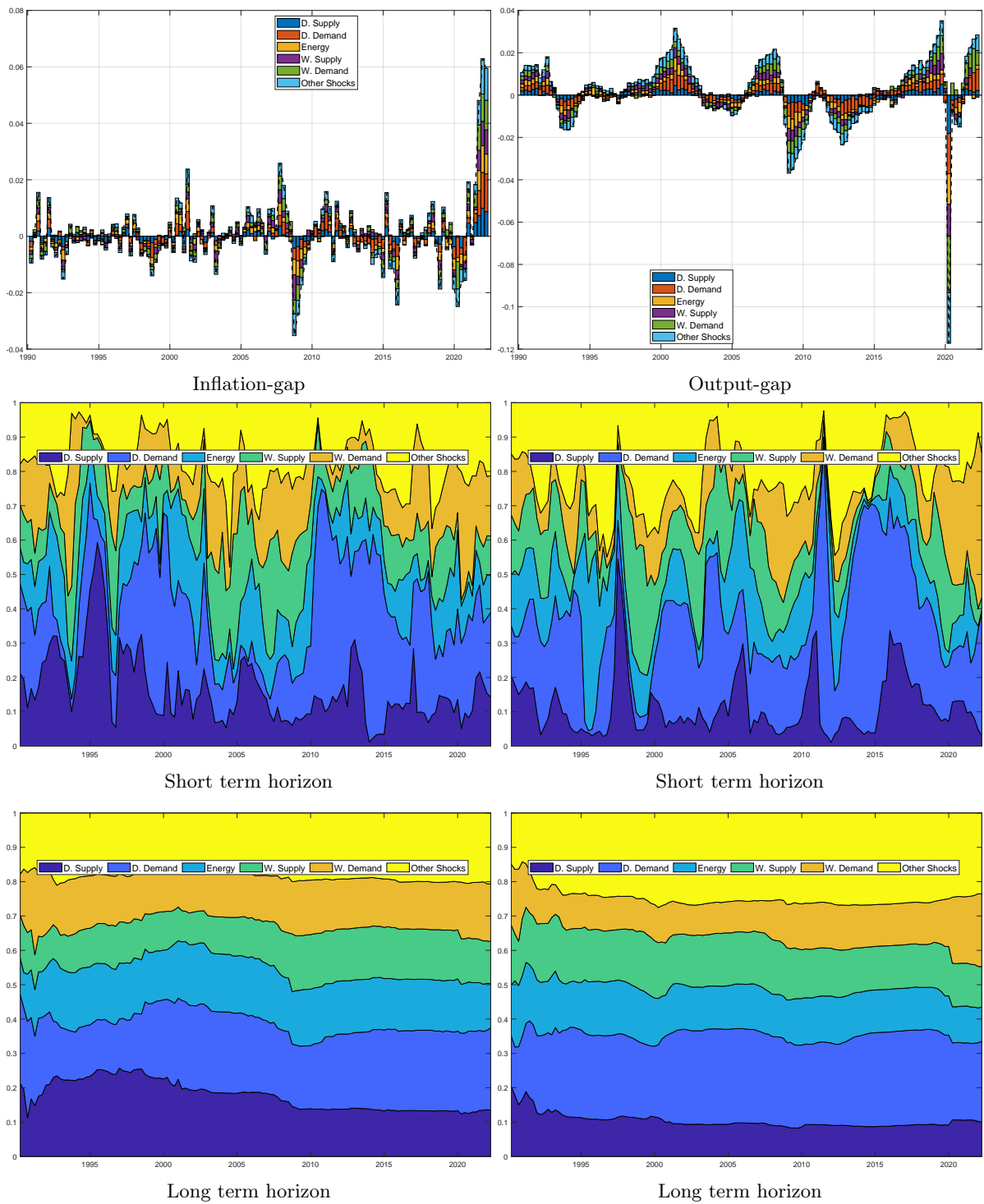


Figure 41. Estimated historical decomposition and variance decomposition

Note: Degrees of freedom equals to 25 for the priors governing the stochastic volatility of trends. The black line is the point-wise median of inflation (left) and output-gap (right). The colored bars (areas) represent the contribution (share of the variance decomposition) of each structural shock - domestic (demand and supply-side), global (demand and supply-side) and energy supply.

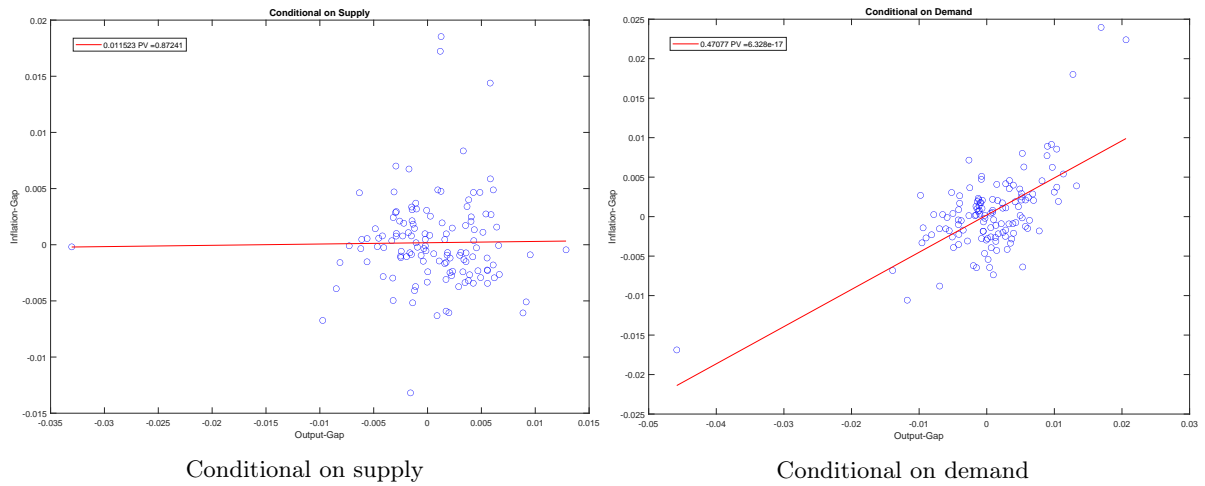


Figure 42. Purging supply-demand side shocks

Note: Degrees of freedom equals to 25 for the priors governing the stochastic volatility of trends. Conditional data obtained from the estimated cycle model part. Supply shocks are calculated as the sum of domestic and global supply shocks. Demand shocks are calculated as the sum of domestic and global demand shocks. Corresponding supply (demand) slope estimate is -0.0409 (0.4859) with a P-value of 0.56 (0).

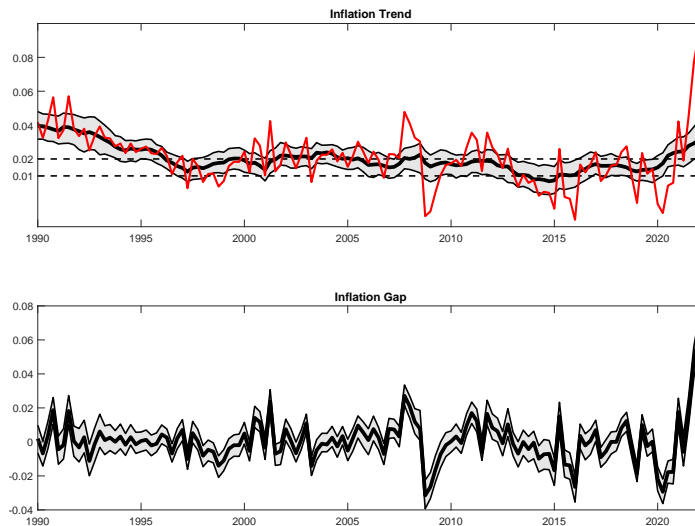


Figure 43. Actual data and estimated trends and cycles of HICP inflation

Note: Degrees of freedom equals to 15 for the priors governing the stochastic volatility of trends. Point-wise median (solid black line) with 68% credible bands. HICP is defined in annualized quarter-on-quarter terms.

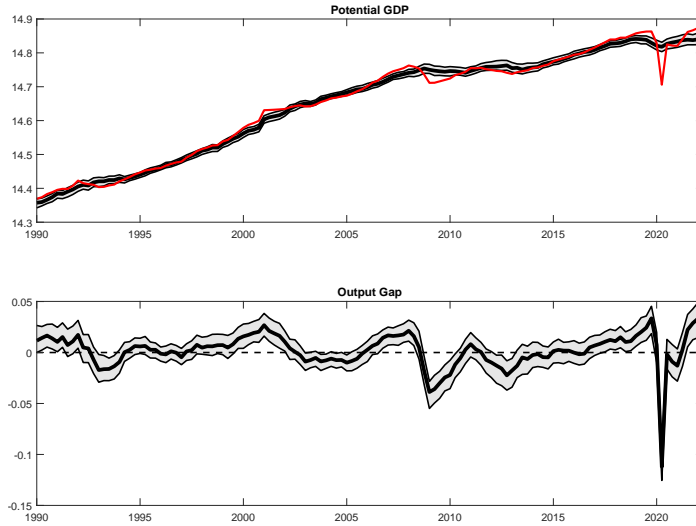


Figure 44. Actual data and estimated trends and cycles of real GDP

Note: Degrees of freedom equals to 15 for the priors governing the stochastic volatility of trends. Point-wise median (solid black line) with 68% credible bands. Real GDP is defined in log terms.

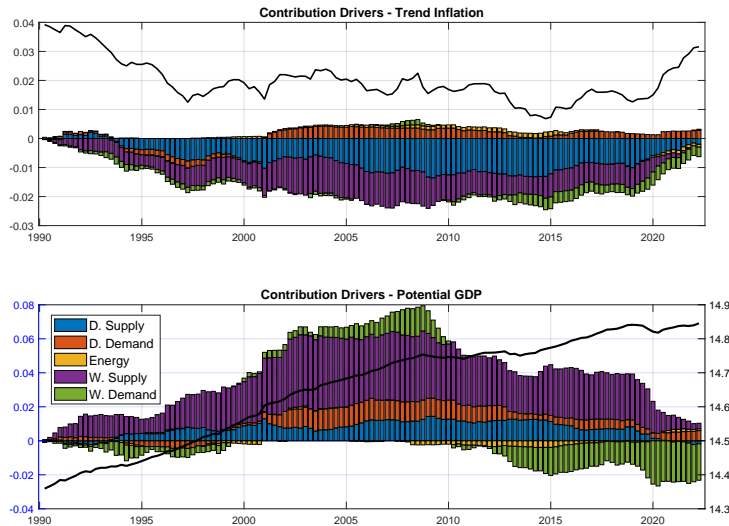


Figure 45. Estimated historical decomposition of the point-wise median of trend inflation (top) and potential GDP (bottom) from 1990.Q2 to 2022.Q2

Note: Degrees of freedom equals to 15 for the priors governing the stochastic volatility of trends. The black line is the point-wise median of trend inflation (top) and potential GDP (bottom). The colored bars represent the contribution of each structural shock - domestic (demand and supply-side), global (demand and supply-side) and energy supply - at time t .

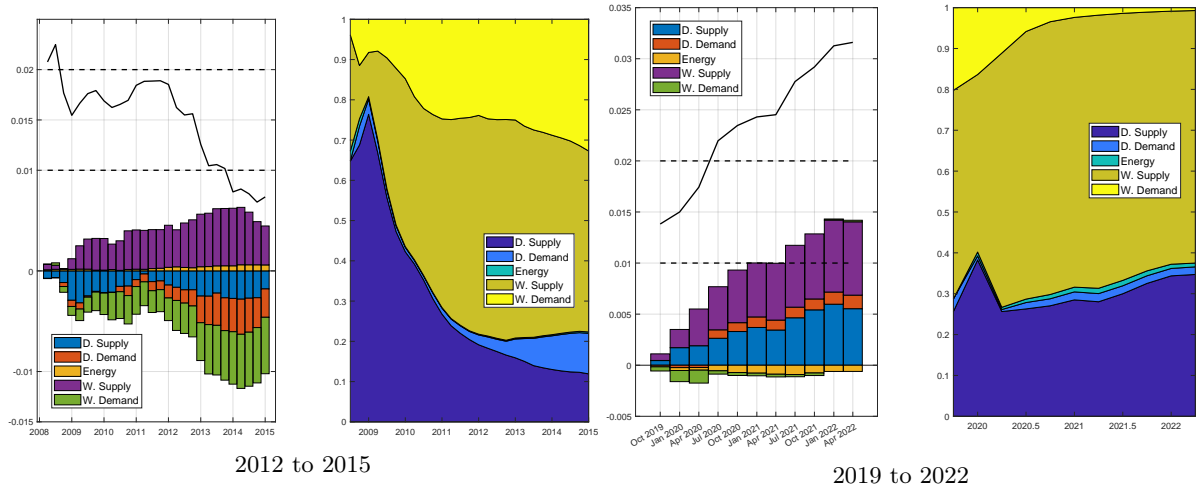


Figure 46. Estimated historical decomposition of median trend inflation

Note: Degrees of freedom equals to 15 for the priors governing the stochastic volatility of trends. The black line is the point-wise median of trend inflation. The colored bars (areas) represent the contribution (share of the variance decomposition) of each structural shock - domestic (demand and supply-side), global (demand and supply-side) and energy supply - at time t .

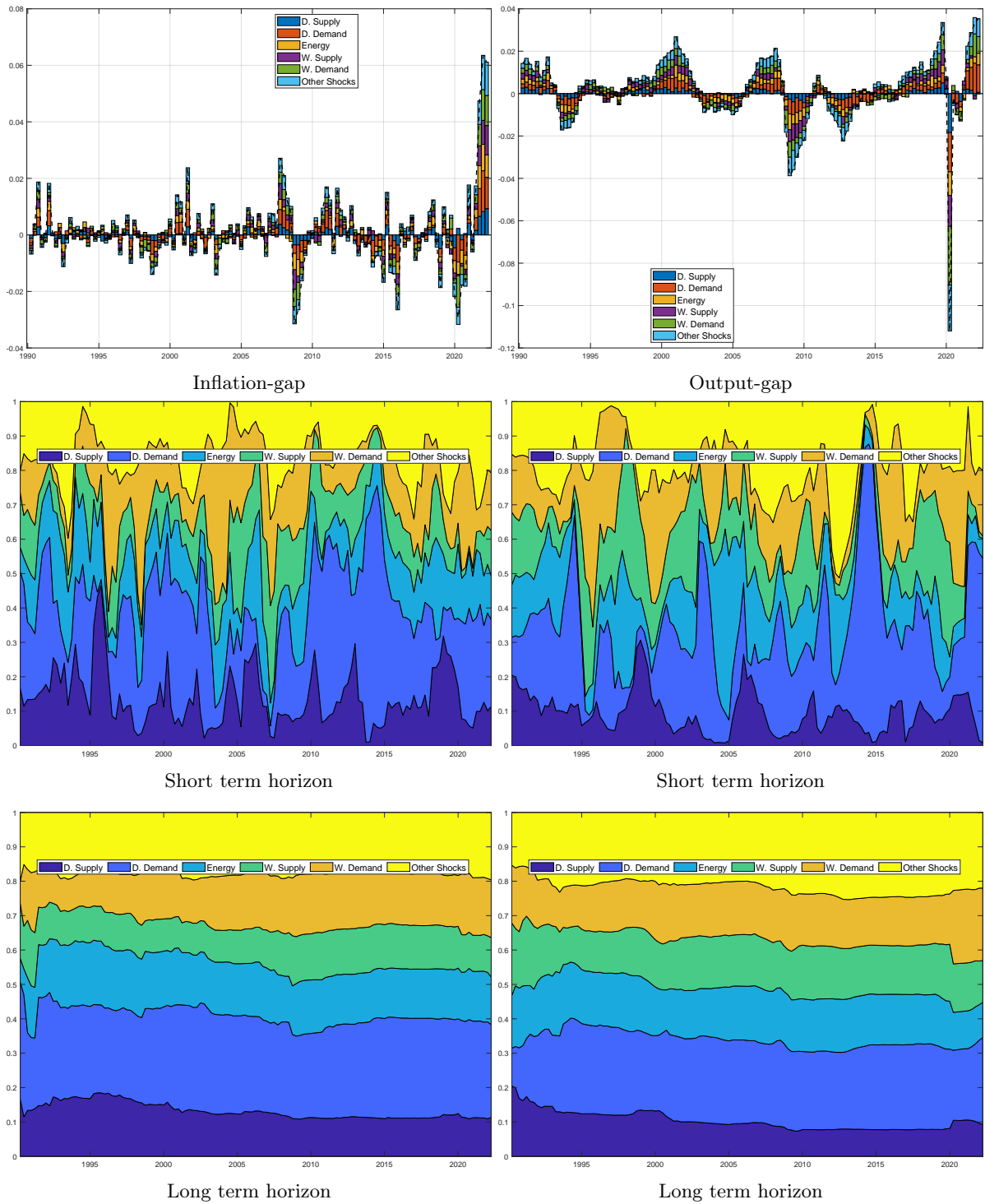


Figure 47. Estimated historical decomposition and variance decomposition

Note: Degrees of freedom equals to 15 for the priors governing the stochastic volatility of trends. The black line is the point-wise median of inflation (left) and output-gap (right). The colored bars (areas) represent the contribution (share of the variance decomposition) of each structural shock - domestic (demand and supply-side), global (demand and supply-side) and energy supply.

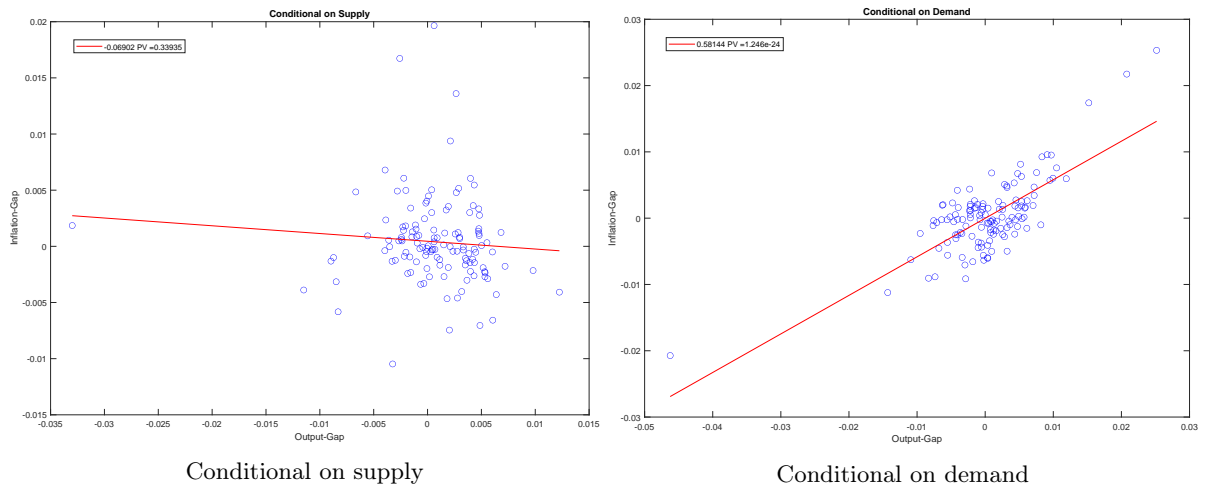


Figure 48. Purging supply-demand side shocks

Note: Degrees of freedom equals to 15 for the priors governing the stochastic volatility of trends. Conditional data obtained from the estimated cycle model part. Supply shocks are calculated as the sum of domestic and global supply shocks. Demand shocks are calculated as the sum of domestic and global demand shocks. Corresponding supply (demand) slope estimate is -0.069 (0.33) with a P-value of 0.58 (0).

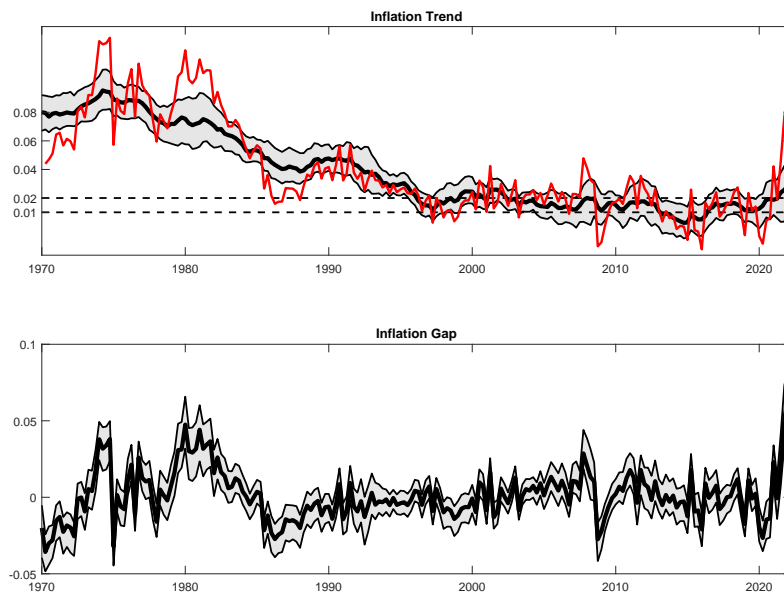


Figure 49. Actual data and estimated trends and cycles of HICP inflation

Note: Estimation sample 1970Q1 to 2022Q2. Point-wise median (solid black line) with 68% credible bands. HICP is defined in annualized quarter-on-quarter terms.

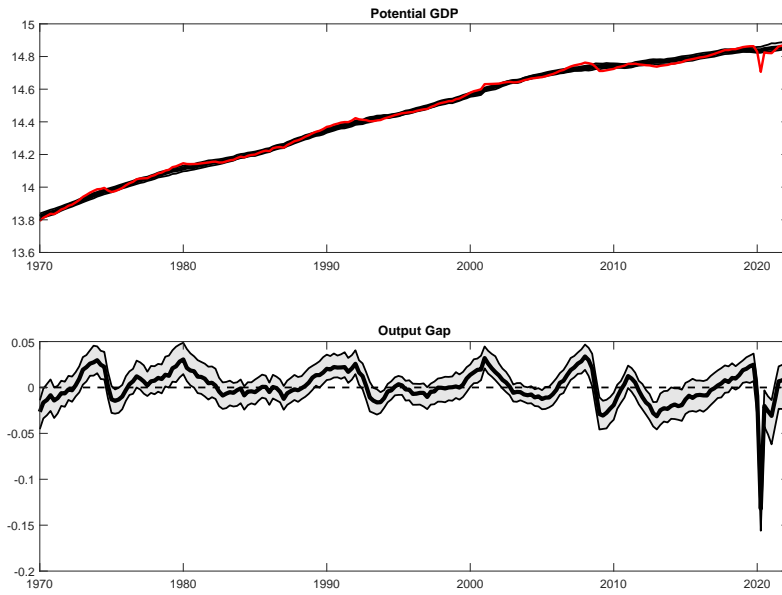


Figure 50. Actual data and estimated trends and cycles of real GDP

Note: Estimation sample 1970Q1 to 2022Q2. Point-wise median (solid black line) with 68% credible bands. Real GDP is defined in log terms.

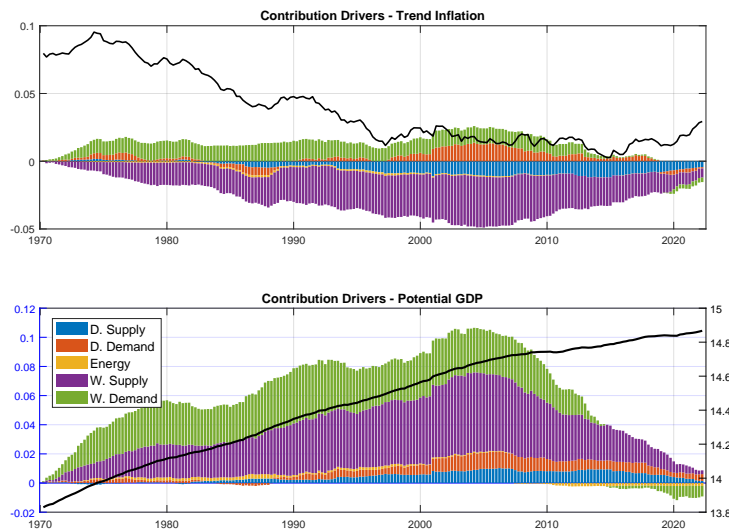


Figure 51. Estimated historical decomposition of the point-wise median of trend inflation (top) and potential GDP (bottom) from 1990.Q2 to 2022.Q2

Note: Estimation sample 1970Q1 to 2022Q2. The black line is the point-wise median of trend inflation (top) and potential GDP (bottom). The colored bars represent the contribution of each structural shock - domestic (demand and supply-side), global (demand and supply-side) and energy supply - at time t .

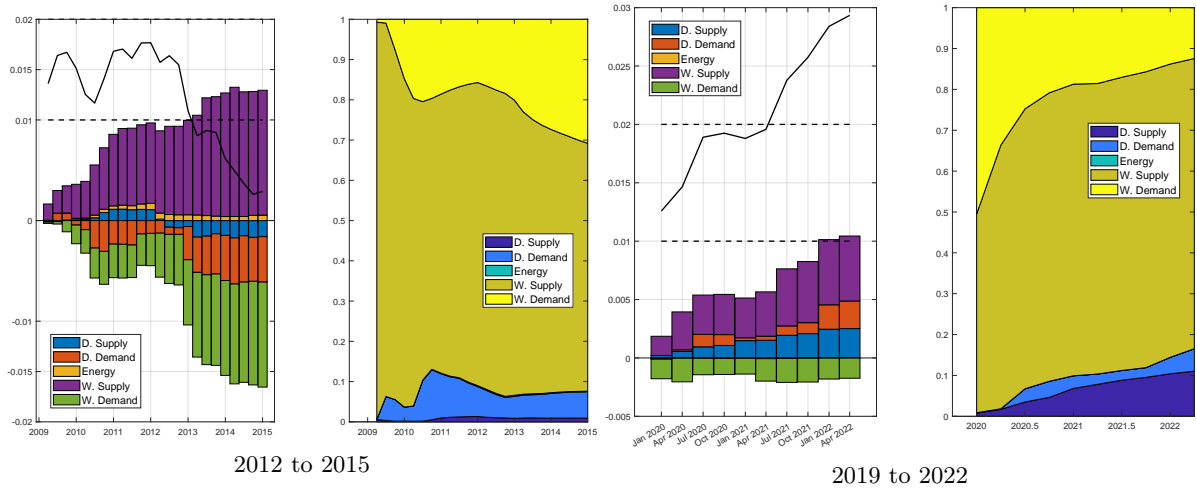


Figure 52. Estimated historical decomposition of median trend inflation

Note: Estimation sample 1970Q1 to 2022Q2. The black line is the point-wise median of trend inflation. The colored bars (areas) represent the contribution (share of the variance decomposition) of each structural shock - domestic (demand and supply-side), global (demand and supply-side) and energy supply - at time t .

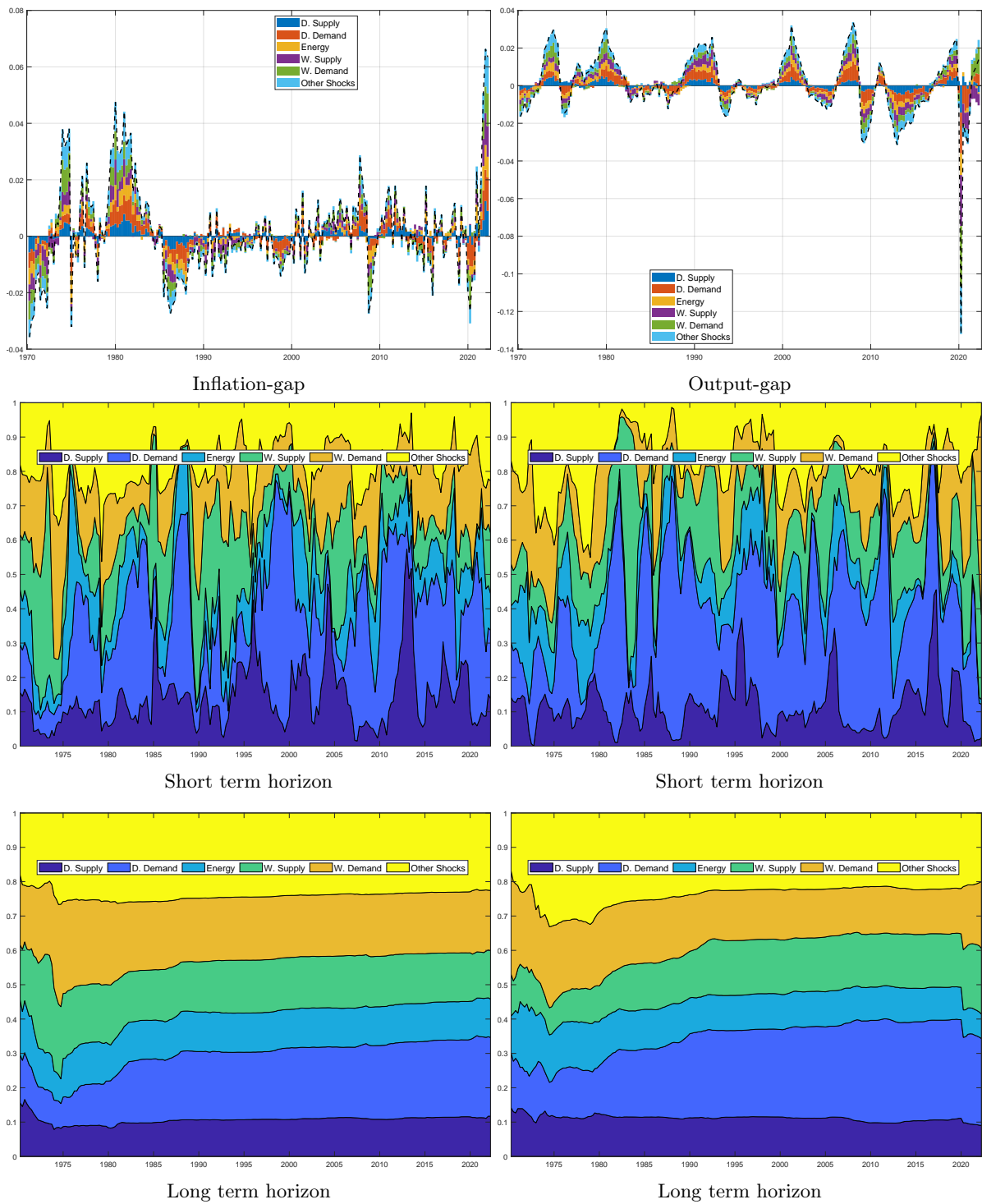


Figure 53. Estimated historical decomposition and variance decomposition

Note: Estimation sample 1970Q1 to 2022Q2. The black line is the point-wise median of inflation (left) and output-gap (right). The colored bars (areas) represent the contribution (share of the variance decomposition) of each structural shock - domestic (demand and supply-side), global (demand and supply-side) and energy supply.

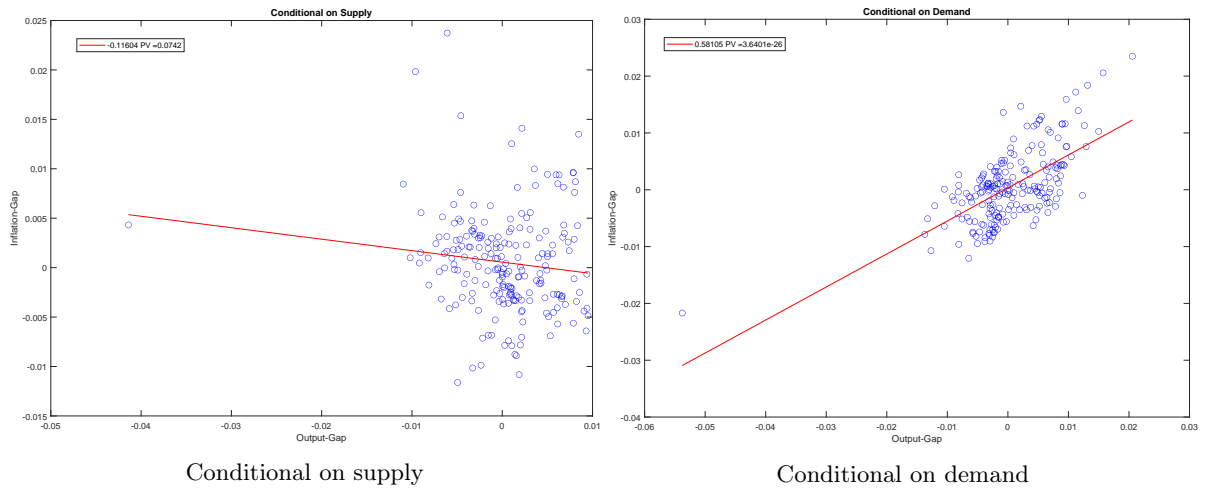


Figure 54. Purging supply-demand side shocks

Note: Estimation sample 1970Q1 to 2022Q2. Conditional data obtained from the estimated cycle model part. Supply shocks are calculated as the sum of domestic and global supply shocks. Demand shocks are calculated as the sum of domestic and global demand shocks. Corresponding supply (demand) slope estimate is -0.11 (0.58) with a P-value of 0.07 (0).

References

- Abiad, Abdul, Prachi Mishra, and Petia Topalova**, “How does trade evolve in the aftermath of financial crises?,” *IMF Economic Review*, 2014, 62 (2), 213–247.
- Altissimo, Filippo, Michael Ehrmann, and Frank Smets**, “Inflation persistence and price-setting behaviour in the Euro Area—a summary of the IPN evidence,” *ECB Occasional paper*, 2006, (46).
- Álvarez, Luis J and Mónica Correa-López**, “Inflation expectations in euro area Phillips curves,” *Economics Letters*, 2020, 195, 109449.
- Antolin-Diaz, Juan, Thomas Drechsel, and Ivan Petrella**, “Tracking the slowdown in long-run GDP growth,” *Review of Economics and Statistics*, 2017, 99 (2), 343–356.
- Ascari, Guido and Argia M Sbordone**, “The macroeconomics of trend inflation,” *Journal of Economic Literature*, 2014, 52 (3), 679–739.
- Baldwin, Richard and Daria Taglioni**, “The great trade collapse and trade imbalances,” *The Great Trade Collapse: Causes, Consequences and Prospects. Centre for Economic Policy Research and VoxEu.org*, 2009, 6, 47–58.
- Ball, Laurence, N Gregory Mankiw, David Romer, George A Akerlof, Andrew Rose, Janet Yellen, and Christopher A Sims**, “The new Keynesian economics and the output-inflation trade-off,” *Brookings papers on economic activity*, 1988, 1988 (1), 1–82.
- Bańkowski, Krzysztof, Othman Bouabdallah, Cristina Checherita-Westphal, Maximilian Freier, Pascal Jacquinot, and Philip Muggenthaler**, “Fiscal policy and high inflation,” *Economic Bulletin Articles*, 2023, 2.
- Barbarino, Alessandro, Travis J Berge, Han Chen, and Andrea Stella**, “Which output gap estimates are stable in real time and why?,” 2020.
- Benati, Luca and Haroon Mumtaz**, “US evolving macroeconomic dynamics: a structural investigation,” 2007.
- Bergholt, Drago, Francesco Furlanetto, and Etienne Vaccaro-Grange**, *Did monetary policy kill the Phillips curve? Some simple arithmetics*, Norges Bank, 2023.
- Beveridge, Stephen and Charles R Nelson**, “A new approach to decomposition of economic time series into permanent and transitory components with particular attention to measurement of the ‘business cycle’,” *Journal of Monetary economics*, 1981, 7 (2), 151–174.
- Bluedorn, Mr John C and Mr Daniel Leigh**, *Hysteresis in labor Markets? Evidence from professional long-term forecasts*, International Monetary Fund, 2019.
- Bobeica, Elena and Marek Jarociński**, “Missing disinflation and missing inflation: A VAR perspective,” *57th issue (March 2019) of the International Journal of Central Banking*, 2019.

- , **Matteo Ciccarelli**, and **Isabel Vansteenkiste**, “The link between labor cost and price inflation in the euro area,” 2019.
- Bodnár, Katalin, Julien Le Roux, Paloma Lopez-Garcia, Béla Szörfi et al.**, “The impact of Covid-19 on potential output in the euro area,” *Economic Bulletin Articles*, 2020, 7.
- Bowles, Carlos, Roberta Friz, Veronique Genre, Geoff Kenny, Aidan Meyler, and Tuomas Rautanen**, “The ECB survey of professional forecasters (SPF)-A review after eight years’ experience,” *ECB occasional paper*, 2007, (59).
- Candia, Bernardo, Olivier Coibion, and Yuriy Gorodnichenko**, “The Inflation Expectations of US Firms: Evidence from a new survey,” Technical Report, National Bureau of Economic Research 2021.
- Canova, Fabio and Gianni De Nicolò**, “Monetary disturbances matter for business fluctuations in the G-7,” *Journal of Monetary Economics*, 2002, 49 (6), 1131–1159.
- Carriero, Andrea, Todd E Clark, Massimiliano Giuseppe Marcellino, and Elmar Mertens**, “Addressing COVID-19 outliers in BVARs with stochastic volatility,” 2021.
- Carter, Chris K and Robert Kohn**, “On Gibbs sampling for state space models,” *Biometrika*, 1994, 81 (3), 541–553.
- Chen, Ms Wenjie, Mr Mico Mrkaic, and Mr Malhar S Nabar**, *The global economic recovery 10 years after the 2008 financial crisis*, International Monetary Fund, 2019.
- Ciccarelli, Matteo and Juan Angel García**, “Expectation spillovers and the return of inflation,” *Economics Letters*, 2021, 209, 110119.
- , **Chiara Osbat, Elena Bobeica, Caroline Jardet, Marek Jarocinski, Caterina Mendicino, Alessandro Notarpietro, Sergio Santoro, and Arnaud Stevens**, “Low inflation in the euro area: Causes and consequences,” *ECB occasional paper*, 2017, (181).
- Clark, Peter K**, “The cyclical component of US economic activity,” *The Quarterly Journal of Economics*, 1987, 102 (4), 797–814.
- Clark, Todd E and Troy Davig**, “The Relationship between Inflation and Inflation Expectations,” 2009.
- Cogley, Timothy and Thomas J Sargent**, “Evolving post-world war II US inflation dynamics,” *NBER macroeconomics annual*, 2001, 16, 331–373.
- and – , “Drifts and volatilities: monetary policies and outcomes in the post WWII US,” *Review of Economic dynamics*, 2005, 8 (2), 262–302.
- Coibion, Olivier and Yuriy Gorodnichenko**, “Is the Phillips curve alive and well after all? Inflation expectations and the missing disinflation,” *American Economic Journal: Macroeconomics*, 2015, 7 (1), 197–232.

- Conti, Antonio Maria, Stefano Neri, and Andrea Nobili**, “Low inflation and monetary policy in the euro area,” 2017.
- Corsello, Francesco, Stefano Neri, and Alex Tagliabracci**, “Anchored or de-anchored? That is the question,” *European Journal of Political Economy*, 2021, 69, 102031.
- Corsetti, Giancarlo, Luca Dedola, and Sylvain Leduc**, “The international dimension of productivity and demand shocks in the US economy,” *Journal of the European Economic Association*, 2014, 12 (1), 153–176.
- Dovern, Jonas, Geoff Kenny et al.**, “Anchoring inflation expectations in unconventional times: Micro evidence for the euro area,” *International Journal of Central Banking*, 2020, 16 (5), 309–347.
- Duncan, Roberto and Enrique Martínez-García**, “Forecasting inflation in open economies: What can a NOEM model do?,” *Journal of Forecasting*, 2023, 42 (3), 481–513.
- Durbin, James and Siem Jan Koopman**, “A simple and efficient simulation smoother for state space time series analysis,” *Biometrika*, 2002, 89 (3), 603–616.
- Fagan, Gabriel, Jerome Henry, and Ricardo Mestre**, “An area-wide model for the euro area,” *Economic Modelling*, 2005, 22 (1), 39–59.
- Ferroni, Filippo and Benoit Mojon**, “Domestic and global inflation,” *Mimeo. Federal Reserve Bank of Chicago*, 2014.
- Furlanetto, Francesco, Antoine Lepetit, Ørjan Robstad, Juan Rubio Ramírez, and Pål Ulvedal**, “Estimating hysteresis effects,” 2021.
- Galí, Jordi and Luca Gambetti**, “On the sources of the great moderation,” *American Economic Journal: Macroeconomics*, 2009, 1 (1), 26–57.
- Gemma, Yasufumi, Takushi Kurozumi, and Mototsugu Shintani**, “Trend Inflation and Evolving Inflation Dynamics: A Bayesian GMM Analysis,” *Review of Economic Dynamics*, 2023.
- Geweke, John**, “Interpretation and inference in mixture models: Simple MCMC works,” *Computational Statistics & Data Analysis*, 2007, 51 (7), 3529–3550.
- Geweke, John F et al.**, “Evaluating the accuracy of sampling-based approaches to the calculation of posterior moments,” Technical Report, Federal Reserve Bank of Minneapolis 1991.
- Giannone, Domenico, Michele Lenza, and Giorgio E Primiceri**, “Prior selection for vector autoregressions,” *Review of Economics and Statistics*, 2015, 97 (2), 436–451.
- Gimeno, Ricardo and Eva Ortega**, “The evolution of inflation expectations in euro area markets,” 2016.
- Giordani, Paolo, Michael Pitt, and Robert Kohn**, “Bayesian inference for time series state space models,” 2011.

- Gordon, Robert J**, “Inflation, flexible exchange rates, and the natural rate of unemployment,” Technical Report, National Bureau of Economic Research 1981.
- , “US inflation, labor’s share, and the natural rate of unemployment,” 1988.
- , “The turtle’s progress: Secular stagnation meets the headwinds,” *Secular stagnation: facts, causes and cures*, 2014, pp. 47–59.
- Gorter, Janko, Jan Jacobs, and Jakob De Haan**, “Taylor rules for the ECB using expectations data,” *Scandinavian Journal of Economics*, 2008, 110 (3), 473–488.
- Hamilton, James D**, “Why you should never use the Hodrick-Prescott filter,” *Review of Economics and Statistics*, 2018, 100 (5), 831–843.
- Harvey, Andrew C**, “Trends and cycles in macroeconomic time series,” *Journal of Business & Economic Statistics*, 1985, 3 (3), 216–227.
- Hasenzagl, Thomas, Filippo Pellegrino, Lucrezia Reichlin, and Giovanni Ricco**, “A Model of the Fed’s View on Inflation,” *The Review of Economics and Statistics*, 2018, pp. 1–45.
- Higgins, Matthew, Thomas Klitgaard et al.**, “How Much Have Consumers Spent on Imports during the Pandemic?,” Technical Report, Federal Reserve Bank of New York 2021.
- Hilscher, Jens, Alon Raviv, and Ricardo Reis**, “How likely is an inflation disaster?,” 2022.
- IMF**, “Global disinflation in an era of constrained monetary policy,” *World Economic Outlook*, 2016.
- , “Recent wage dynamics in advanced economies: Drivers and implications,” *World Economic Outlook, October 2017: Seeking sustainable growth: Short-term recovery, long-term challenges*, 2017, pp. 73–112.
- Jacquier, Eric, Nicholas G Polson, and Peter E Rossi**, “Bayesian analysis of stochastic volatility models with fat-tails and correlated errors,” *Journal of Econometrics*, 2004, 122 (1), 185–212.
- Jarociński, Marek and Michele Lenza**, “An inflation-predicting measure of the output gap in the euro area,” *Journal of Money, Credit and Banking*, 2018, 50 (6), 1189–1224.
- Kabukçuoğlu, Ayşe and Enrique Martínez-García**, “Inflation as a global phenomenon—Some implications for inflation modeling and forecasting,” *Journal of Economic Dynamics and Control*, 2018, 87, 46–73.
- Kamber, Güneş, James Morley, and Benjamin Wong**, “Intuitive and reliable estimates of the output gap from a Beveridge-Nelson filter,” *Review of Economics and Statistics*, 2018, 100 (3), 550–566.
- Kilian, Lutz**, “The economic effects of energy price shocks,” *Journal of economic literature*, 2008, 46 (4), 871–909.

- , “Not all oil price shocks are alike: Disentangling demand and supply shocks in the crude oil market,” *American Economic Review*, 2009, *99* (3), 1053–69.
- Koester, Gerrit, Jakob Nordeman, Michel Soudan et al.**, “Comparing recent inflation developments in the United States and the euro area,” *Economic Bulletin Boxes*, 2021, *6*.
- , **Sofia Cuquerella Ricarte, Ramon Gomez-Salvador et al.**, “Recent inflation developments in the United States and the euro area—an update,” *Economic Bulletin Boxes*, 2022, *1*.
- Laxton, Douglas and Robert Tetlow**, *A simple multivariate filter for the measurement of potential output*, Vol. 59, Bank of Canada Technical Report No. 59. Ottawa, 1992.
- Lenza, Michele and Giorgio E Primiceri**, “How to estimate a vector autoregression after march 2020,” *Journal of Applied Econometrics*, 2022.
- Łyziak, Tomasz and Maritta Paloviita**, “Anchoring of inflation expectations in the euro area: recent evidence based on survey data,” *European Journal of Political Economy*, 2017, *46*, 52–73.
- Maffei-Faccioli, Nicolò**, “Identifying the sources of the slowdown in growth: Demand vs. supply,” Technical Report, Working Paper 2021.
- Martínez-García, E and MA Wynne**, “The Global Slack Hypothesis. Federal Reserve Bank of Dallas Staff Papers, 10. September,” 2010.
- Mehra, Yash P**, “Wage growth and the inflation process: An empirical note,” *The American Economic Review*, 1991, *81* (4), 931–937.
- Negro, Marco Del, Domenico Giannone, Marc P Giannoni, and Andrea Tambalotti**, “Safety, liquidity, and the natural rate of interest,” *Brookings Papers on Economic Activity*, 2017, *2017* (1), 235–316.
- , – , – , and – , “Global trends in interest rates,” *Journal of International Economics*, 2019, *118*, 248–262.
- O’Brien, Derry, Clemence Dumoncel, Eduardo Goncalves et al.**, “The role of demand and supply factors in HICP inflation during the COVID-19 pandemic—a disaggregated perspective,” *Economic Bulletin Articles*, 2021, *1*.
- Primiceri, Giorgio E**, “Time varying structural vector autoregressions and monetary policy,” *The Review of Economic Studies*, 2005, *72* (3), 821–852.
- Reis, Ricardo**, “The burst of high inflation in 2021–22: how and why did we get here?,” 2022.
- Rubio-Ramirez, Juan F, Daniel F Waggoner, and Tao Zha**, “Structural vector autoregressions: Theory of identification and algorithms for inference,” *The Review of Economic Studies*, 2010, *77* (2), 665–696.

- Santis, Roberto A De and Grigor Stoevsky**, “The role of supply and demand in the post-pandemic recovery in the euro area,” *Economic Bulletin Articles*, 2023, 4.
- **et al.**, “Sources of supply chain disruptions and their impact on euro area manufacturing,” *Economic Bulletin Boxes*, 2022, 8.
- Schorfheide, Frank and Dongho Song**, “Real-time forecasting with a (standard) mixed-frequency VAR during a pandemic,” Technical Report, National Bureau of Economic Research 2021.
- Shirota, Toyochiro**, “Flattening of the Phillips curve under low trend inflation,” *Economics Letters*, 2015, 132, 87–90.
- Staff, ECB**, “Annual Report 2021,” 2021.
- , “Economic Bulletin Issue 8, 2022,” 2022.
- Stephens, Matthew**, “Dealing with label switching in mixture models,” *Journal of the Royal Statistical Society: Series B (Statistical Methodology)*, 2000, 62 (4), 795–809.
- Stock, James H and Mark W Watson**, “Median unbiased estimation of coefficient variance in a time-varying parameter model,” *Journal of the American Statistical Association*, 1998, 93 (441), 349–358.
- **and** – , “Why has US inflation become harder to forecast?,” *Journal of Money, Credit and banking*, 2007, 39, 3–33.
- Strohsal, Till and Lars Winkelmann**, “Assessing the anchoring of inflation expectations,” *Journal of International Money and Finance*, 2015, 50, 33–48.
- Uhlig, Harald**, “What are the effects of monetary policy on output? Results from an agnostic identification procedure,” *Journal of Monetary Economics*, 2005, 52 (2), 381–419.
- Watson, Mark W**, “Univariate detrending methods with stochastic trends,” *Journal of monetary economics*, 1986, 18 (1), 49–75.
- Yellen, Janet**, “Macroeconomic Research After the Crisis: a speech at \" The Elusive 'Great' Recovery: Causes and Implications for Future Business Cycle Dynamics\" 60th annual economic conference sponsored by the Federal Reserve Bank of Boston, Boston, Massachusetts, October 14, 2016,” Technical Report, Board of Governors of the Federal Reserve System (US) 2016.